

Adaptive beamforming and power allocation in multi-carrier multicast wireless networks

Vom Fachbereich 18
Elektrotechnik und Informationstechnik
der Technischen Universität Darmstadt
zur Erlangung der Würde eines
Doktor-Ingenieurs (Dr.-Ing.)
genehmigte Dissertation

von
M.Sc. Yuri Carvalho Barbosa Silva
geboren am 15.09.1978 in Fortaleza, Brasilien

Referent:	Prof. Dr.-Ing. Anja Klein
Korreferent:	Prof. Dr. Alex B. Gershman
Tag der Einreichung:	14. Januar 2008
Tag der mündlichen Prüfung:	18. März 2008

D 17
Darmstädter Dissertation
Darmstadt 2008

Acknowledgments

This thesis was prepared in the period of time between April 2005 and March 2008, during which I have been with the Communications Engineering Lab at the Institute of Telecommunications of the Technische Universität Darmstadt.

I would like to deeply thank Prof. Dr.-Ing. Anja Klein for her steady support, trust, and incentive during the supervision of my studies. The many fruitful discussions and her valuable suggestions and guidance have decisively contributed to the successful elaboration of this work.

I also thank Prof. Dr. Alex B. Gershman for the interest in my work and for taking the time to be on my dissertation committee. Moreover, I thank Prof. Dr.-Ing. habil. Dr.-Ing. E.h. Paul W. Baier from the Technische Universität Kaiserslautern for reviewing parts of this thesis.

My gratitude goes to all my colleagues at the Communications Engineering Lab, as well as to the technical and administrative staff, for the friendly atmosphere, the cooperation, and all the helpful discussions. I also thank all the students I had the chance to work with.

I would also like to acknowledge the scholarship support of CAPES-Brazil and the orientation of DAAD.

Finally, I would like to thank my family for their incentive and support. I especially thank my wife Linda, who stood by my side at all times and gave me all of her love and support. This work is dedicated to her.

Darmstadt, March 2008

Yuri C. B. Silva

Kurzfassung

Für Mobilfunksysteme der nächsten Generation ist zu erwarten, dass Massendienste, in denen dieselben Informationen an eine Gruppe von Teilnehmern (Multicast) oder an alle Teilnehmer (Broadcast) verbreitet werden, deutlich an Bedeutung gewinnen. Dies zeigt sich unter anderen auch an den verstärkten Standardisierungsaktivitäten für die Nutzung dieser Dienste in gegenwärtigen Mobilfunknetzen. Beispiele für solche Massendienste sind u.a. Audio-/Video-Streaming, Newsclips, Lokalisierungsdienste und Herunterladen.

Die vorliegende Arbeit behandelt das Problem der Strahlformung in Mehrantennensystemen für Multicast-Dienste. Sowohl Szenarien mit einer einzelnen Gruppe als auch mit mehreren Gruppen werden dabei berücksichtigt, wobei im ersten Fall nur eine einzige Multicast-Gruppe pro Ressource zugeteilt werden darf und im zweiten Fall mehrere Multicast-Gruppen pro Ressource erlaubt sind.

Es wird ein neues Systemmodell für Multicast-Szenarien vorgeschlagen, das die mathematische Grundlage für die Analyse der betrachteten Algorithmen bildet. Durch die entsprechende Wahl der Systemparameter können Sonderfälle wie z.B. der Mehrnutzer-, der Einzelnutzer- und der Einzelgruppen-Fall aus dem allgemeinen Modell abgeleitet werden.

Verschiedene Algorithmen zur Strahlformung, die aus Unicast-Szenarien bekannt sind, werden für Multicast-Szenarien formuliert. Desweiteren wird ein neuer Algorithmus namens User-Selective Matched Filter (USMF) vorgeschlagen, der speziell an die Anforderungen für Multicast-Szenarien angepasst ist. Dieser Algorithmus bildet einen guten Kompromiss zwischen Leistungsfähigkeit und Komplexität. Durch die gemeinsame Nutzung der Ressourcen für den Fall mehrere Gruppen entsteht Interferenz zwischen den Gruppen, die durch entsprechende Algorithmen zur Strahlformung unterdrückt werden soll. Zu diesem Zweck werden lineare und nichtlineare Algorithmen, die aus Unicast-Szenarien bekannt sind, an Multicast-Szenarien mit mehreren Gruppen angepasst. Durch zusätzliche Modifikationen der Algorithmen können bessere Ergebnisse für Multicast-Dienste erzielt werden. Die vorgestellten Algorithmen werden sowohl für den Fall einzelner als auch mehrerer Gruppen bezüglich ihrer Leistungsfähigkeit und Komplexität analysiert.

Schließlich wird die Zuweisung der Ressourcen zu den Multicast-Gruppen analysiert, die einen erheblichen Einfluss auf die Algorithmen zur Strahlformung hat. Es werden

mehrere Alternativen für die Aufteilung der Gesamtsendeleistung zwischen den einzelnen Trägern eines Mehrträgersystems mit einer einzelnen Gruppe in einem Multicast-Szenario vorgeschlagen und analysiert. Einer davon ist eine Erweiterung des traditionellen Waterfilling-Algorithmus für den Unicast-Fall. Zusätzlich werden einige Vorschläge für die Ressourcenzuweisung in Mehrträger-Mehrgruppen-Multicastsystemen gemacht.

Abstract

In the context of next-generation wireless systems, it is expected that services targeted at mass content distribution become widely popular, which is reflected for instance in the standardization activities for their implementation within current cellular networks. Examples of such services are audio/video streaming, mobile TV, messaging, news clips, localized services, download, among others. Their common characteristic is that the same information has to be transmitted to a group of users (multicast) or to all users (broadcast) within a certain coverage area.

This thesis deals with the problem of multicast beamforming for multi-antenna wireless cellular networks. Both single-group and multi-group scenarios are taken into account, with the former corresponding to a single multicast group per radio resource and the latter referring to multiple multicast groups per resource.

In order to provide the necessary mathematical framework for the analysis of the algorithms, a general system model is proposed for the multi-group multicast scenario. Particular cases, such as the multi-user, single-group, and single-user cases, can be derived from the general model by properly adjusting the system parameters.

Different beamforming algorithms known from the unicast case are formulated for the single-group multicast case. Moreover, a new algorithm termed User-Selective Matched Filter (USMF) specifically designed for the multicast case is proposed, which is shown to provide a good trade-off between performance and complexity. For the multi-group multicast case, the resource sharing results in inter-group interference, which needs to be suppressed by the beamforming algorithms. Linear and non-linear algorithms known from the unicast case are formulated for the multi-group multicast scenario. These algorithms are also further modified with the purpose of improving the performance of the multicast services. The strategies proposed for both single-group and multi-group cases are analyzed in terms of their performance and computational complexity.

Finally, since the allocation of resources among the multicast groups is expected to have a significant impact on the performance of the beamforming algorithms, this issue is addressed as well. The analysis focuses on the proposal and evaluation of different alternatives for allocating the power among the subcarriers of a multi-carrier single-group multicast system. One of these alternatives is an extension of the traditional unicast waterfilling algorithm for the multicast case. Additionally, some considerations are made with regard to the allocation of resources in multi-carrier multi-group multicast

scenarios. It is shown that, in spite of the inter-group interference, the sharing of resources among unicast and multicast users provides better performance than isolating them into different resources.

Contents

1	Introduction	1
1.1	Multicast services in wireless networks	1
1.1.1	Service characterization	1
1.1.2	Multicast scenario description	2
1.1.3	State-of-the-art	3
1.2	Problem statement	5
1.3	Contributions and thesis overview	6
2	System model	9
2.1	Introduction	9
2.2	System assumptions	9
2.3	General system model	10
2.4	Particular cases	18
2.4.1	Introduction	18
2.4.2	Single-group multicast	19
2.4.3	Multi-user unicast	20
2.4.4	Single-user unicast	21
2.5	Extension for multi-antenna terminals	22
3	Adaptive single-group multicast beamforming	25
3.1	Introduction	25
3.2	Problem formulation	25
3.3	State-of-the-art	26
3.4	Beamforming algorithms	28
3.4.1	Matched filter	28
3.4.2	Linear zero-forcing filter	30
3.4.3	Linear minimum mean square error filter	32
3.4.4	Tomlinson-Harashima precoding	34
3.4.5	Switched fixed beams	35
3.4.6	User-selective matched filter	37
3.5	Performance and complexity analysis	38
3.5.1	Analysis assumptions	38
3.5.2	Bit error rate analysis	40
3.5.3	Worst-user SNR analysis	46
3.5.4	Remarks on complexity	51
3.6	Conclusions	52

4	Adaptive multi-group multicast beamforming	53
4.1	Introduction	53
4.2	Problem formulation	53
4.3	State-of-the-art	55
4.4	Linear algorithms	57
4.4.1	Matched filter	57
4.4.2	Zero-forcing based algorithms	58
4.4.2.1	Zero-forcing	58
4.4.2.2	Multicast-aware zero-forcing	59
4.4.3	Minimum mean square error based algorithms	61
4.4.3.1	Minimum mean square error	61
4.4.3.2	Multicast-aware minimum mean square error	62
4.4.4	SINR balancing based algorithms	63
4.4.4.1	SINR balancing	63
4.4.4.2	Multicast-aware SINR balancing	66
4.5	Non-linear algorithms	70
4.5.1	Tomlinson-Harashima precoding based algorithms	70
4.5.1.1	Tomlinson-Harashima precoding	70
4.5.1.2	Multicast-aware Tomlinson-Harashima precoding	71
4.5.2	Vector precoding based algorithms	75
4.5.2.1	Vector precoding	75
4.5.2.2	Multicast-aware vector precoding	77
4.5.3	Hybrid linear and non-linear precoding	78
4.6	Performance and complexity analysis	80
4.6.1	Analysis assumptions	80
4.6.2	Performance of linear algorithms	82
4.6.3	Performance of non-linear algorithms	87
4.6.4	Remarks on complexity	92
4.7	Conclusions	95
5	Resource allocation in multi-carrier multicast systems	97
5.1	Introduction	97
5.2	Overview of resource allocation	97
5.3	Power allocation	99
5.3.1	System assumptions	99
5.3.2	Sum throughput maximization	99
5.3.3	Sum throughput maximization based on group criterion	103
5.3.4	Fair power allocation	104
5.4	Performance and complexity analysis	105

5.4.1	Analysis assumptions	105
5.4.2	Performance of the power allocation algorithms	106
5.4.3	Remarks on complexity	109
5.5	Considerations for SDMA scenarios	112
5.6	Conclusions	114
6	Conclusions	117
	Appendix	119
A.1	Considerations on the variance of THP-precoded symbols	119
A.2	Complexity of mathematical operations and decompositions	121
	List of Acronyms	123
	List of Symbols	127
	Bibliography	135
	Lebenslauf	145

Chapter 1

Introduction

1.1 Multicast services in wireless networks

1.1.1 Service characterization

In the context of next-generation wireless systems, it is expected that services targeted at mass content distribution become widely popular. Examples of such services are audio/video streaming, mobile TV, messaging, news clips, localized services, download, among others.

Multicast services have the characteristic that the same information has to be transmitted to a group of recipients. Broadcast services can be seen as a particular case of multicast services, in which there is not a specific target group, i.e., *all* users belong to the same group. Such services can be implemented through Point-to-Multipoint (P2M) connections, in which a single source transmits the data to all users belonging to the intended group. In information theory, the multicast concept is usually understood as the downlink [Sha48, BB99], i.e., different data streams are transmitted to the users, but in this work the strict definition of multicast is adopted, i.e., the same information is transmitted to the users.

The support of multicast services in cellular networks has been introduced by both the Global System for Mobile communications (GSM) and Universal Mobile Telecommunications System (UMTS) networks in the form of the Multimedia Broadcast/Multicast Service (MBMS) [3GP06a, BH05, OM03]. More recently, a multicast architecture based on MBMS has been proposed in [JXCN07] for Worldwide interoperability for Microwave Access (WiMAX) networks.

The MBMS specification introduces additional functionalities and procedures, which have a certain impact on the network architecture. The support of P2M connections is one of the main features, since it avoids the establishment of individual Point-to-Point (P2P) connections for each member of the multicast group. This has the benefit of reducing the data traffic within the core network, due to the elimination of redundant connections, as well as reducing the number of radio resources required at the base stations for multicast transmission. For other types of networks, such as multi-hop

systems, the establishment of the P2M connections may encompass several network hops. The problem of determining the best routes for the distribution of the multicast data has been approached by several previous works [Mir01, Var02].

In this work, a single wireless hop between source and recipients is taken into account. More specifically, it is here assumed that the P2M connection is realized over the radio link between base station and users within a cell of a wireless cellular network.

1.1.2 Multicast scenario description

In this section, the multicast scenario is described when taking into account a single-cell of the cellular system. Fig. 1.1 illustrates the considered scenario, in which there is a base station at the corner and the mobile stations are uniformly distributed within the cell. Representing a sectorized cell environment, the figure shows the connections between the base station and mobile stations, which can be either P2P or P2M. The former allocates one radio resource per user, whereas the latter allocates a single radio resource for all users of a multicast group.

P2M connections present the advantage of higher resource efficiency than P2P, since less resources are required in order to serve the multicast users. In spite of this advantage, the sharing of radio resources by the users of a same multicast group presents some drawbacks as well. By having the users grouped together, it is no longer possible to fully adapt to the individual radio link conditions of each user. This limited adaptivity may have a negative impact on the quality perceived by the users. As a consequence, the choice between P2M and P2P depends on the trade-off between resource efficiency and user quality, which can be summarized as follows:

- P2P: resource inefficient vs. fully adaptive (increased user quality),
- P2M: resource efficient vs. partially adaptive (reduced user quality).

In order to take advantage of the resource efficiency of P2M, the problem with regard to the user quality can be mitigated by applying adaptive techniques specifically designed for the multicast case. Examples of such techniques are: power control [Löf98a, Löf98b], error control mechanisms [RZF04, JLSX05], non-uniform modulation [PS99, Lar03, IGAG05], macrodiversity [BH05, OKKK05], among others. Besides these techniques, the introduction of adaptive antenna arrays at the base station may also contribute to the performance improvement of multicast services. The multicast

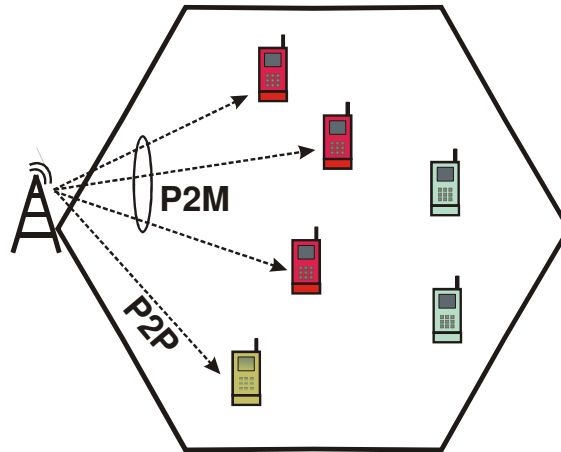


Figure 1.1. Single-cell multicast scenario with P2P and P2M connections.

beamforming problem consists of determining suitable antenna weight vectors, assuming that knowledge of the radio link of all multicast users is available at the transmitter. The following two different types of multicast beamforming techniques are regarded:

- Single-group: Each multicast group is assigned to a different radio resource. The single-group multicast beamforming corresponds to an extension of the single-user unicast beamforming to the multicast case.
- Multi-group: Multiple multicast groups can share the same radio resource. This sharing of resources among groups leads to the problem of intra-cell co-channel interference, which needs to be addressed by the multicast beamforming. Due to this characteristic of separating streams through spatial processing, this case can also be regarded as Spatial Division Multiple Access (SDMA). The multi-group multicast beamforming corresponds to an extension of the multi-user unicast beamforming to the multicast case.

1.1.3 State-of-the-art

A summary of the state-of-the-art of multicast beamforming is presented in Table 1.1. Table 1.1 is organized according to the type of multicast beamforming and the optimization criterion considered by the algorithms. Note that a more detailed review of the state-of-the-art is presented at the beginning of each chapter of this thesis.

For the single-group case, two different optimization criteria have been considered by previous works, which aim at maximizing either the average or the minimum Signal-to-Noise Ratio (SNR) perceived by the multicast users, while subject to transmit power

Table 1.1. Summary of previous contributions to multicast beamforming.

Grouping	Criterion	Reference	Remarks
Single-group	Maxim. of avg. SNR	[NLTW98, Lop02]	Drawback of unbalanced SNR values among the users.
	Maxim. of min. SNR	[ZSV02, ZSV04]	Iterative algorithms for multicast CDMA systems.
		[SL04]	Solution through Sequential Quadratic Programming (SQP).
		[SD04, SDL06]	Simplification through Semi-Definite Relaxation (SDR).
		[HSJ ⁺ 07]	Iterative SNR-increasing update algorithm.
Multi-group	Interference suppression	[Lop02]	Suggestion of a null-space-based approach.
		[Khi04]	DPC-based precoding for sum rate maximization.
	SINR target provision	[KSL05, KSL06]	Simplification through Semi-Definite Relaxation (SDR).
		[GS05a]	DPC-based precoding with single-group SDR.
	Maxim. of min. SINR	[GS06, KSL07]	Bisection method.

constraints. Note that the power minimization problem subject to the provision of a certain SNR target has been considered as well [SD04, SDL06], but it was shown to be equivalent to the max-min SNR problem up to a real scaling factor [SD04, SDL06]. The maximization of the average SNR is not quite a suitable criterion, since it may lead to unbalanced SNR values among the users [NLTW98, Lop02]. The maximization of the minimum SNR, on the other hand, is a fair criterion, which has been more extensively investigated. Nevertheless, the max-min problem was shown to be NP-hard [SDL06], thus requiring efficient suboptimal algorithms in order to allow for a feasible practical implementation. Previous works have proposed solutions based on the computationally intensive Sequential Quadratic Programming (SQP) [SL04], the simplification of the problem through Semi-Definite Relaxation (SDR) [SD04, SDL06], as well as specific iterative algorithms [ZSV02, ZSV04, HSJ⁺07].

The multi-group case has so far been investigated taking the following criteria into account: the complete suppression of inter-group interference, the minimization of the transmit power subject to providing a certain target Signal-to-Interference plus Noise

Ratio (SINR), and the maximization of the minimum SINR. The first criterion is briefly suggested in [Lop02], while in [Khi04] it aims at the sum rate maximization, which is highly unfair. The second criterion is the subject of [KSL05, KSL06, GS05a], for which SDR-based algorithms are proposed. In [GS06, KSL07], it is shown that the solution of the third criterion can be obtained from the solution of the second criterion by means of a bisection method.

1.2 Problem statement

In the previous section it has been shown that multicast beamforming stands out as one of the most promising adaptive techniques for improving the quality of the multicast services, still with a number of open problems to be investigated. In this section, the main problems and goals approached by this thesis are discussed.

First, with multicast beamforming being the main focus of the thesis, a general mathematical model of the system is required, which must be valid for all possible configurations, i.e., single-user/single-group and multi-user/multi-group. Next, efficient multicast beamforming algorithms need to be proposed and analyzed for both single-group and multi-group scenarios. Finally, since the performance of the multicast beamforming algorithms depends to a certain extent on how the radio resources are allocated to the users, this issue needs to be addressed as well. These topics can be detailed in the following list of problems to be solved:

1. How can a general system model be formulated for the multi-group multicast case?
2. How can adaptive beamforming be performed for the single-group multicast scenario? Is it possible to design efficient algorithms specifically for the multicast case?
3. How can linear SDMA precoding schemes be efficiently extended to the multi-group multicast scenario?
4. How can non-linear SDMA precoding schemes be efficiently extended to the multi-group multicast scenario?
5. How best can the resources be allocated, in terms of throughput maximization and user fairness, for multi-carrier systems with multiple multicast groups?
6. How can this resource allocation be efficiently extended to the SDMA scenario, in which different multicast groups can share the same channel?

1.3 Contributions and thesis overview

This section discusses the main contributions of the thesis and how the thesis is organized. In the following, the contents of each chapter are briefly described, along with the contributions presented by each one of them.

In Chapter 2, with the purpose of solving problem 1 of the problem statement, a new general system model is developed for the multi-group multicast scenario. The proposed model specifies the transmission/reception chain, the system parameters, and both complete and reduced representations. It is shown that particular cases, such as the multi-user, single-group, and single-user cases, can be derived from the general model by properly adjusting the system parameters.

Chapter 3 presents a formulation of beamforming algorithms for the single-group multicast case as an extension of algorithms known for the unicast case. The algorithms are the Matched Filter (MF), Zero-Forcing (ZF), Minimum Mean Square Error (MMSE), Tomlinson-Harashima Precoding (THP), and Switched Fixed Beams (SFB). The formulation of these algorithms answers the first question of problem 2. Additionally, a new suboptimal algorithm called USMF, which is specifically designed for the multicast case, is proposed in order to address the second question of problem 2. In Section 3.5, an analysis of the algorithms' performance in terms of the uncoded Bit Error Rate (BER) and worst-user SNR is presented. The analysis also takes into account the impact of different channel models and different multicast group sizes, as well as the complexity order of the algorithms.

The multi-group multicast case is approached by Chapter 4. New linear and non-linear beamforming algorithms are formulated as an extension of algorithms known for the unicast case. The algorithms are the MF, ZF, MMSE, SINR Balancing (SB), THP, and Vector Precoding (VP). Additionally, with the purpose of improving the performance of the multicast services, the algorithms are further enhanced, being called "multicast-aware" (MA). The linear and non-linear algorithms are presented in Sections 4.4 and 4.5, respectively, which refer to problems 3 and 4. A performance and complexity analysis is presented in Section 4.6. For both linear and non-linear algorithms it is investigated which gains the multicast awareness is capable of providing with regard to the non-multicast-aware algorithms.

In Chapter 5, the theme of resource allocation in multi-carrier multicast systems is approached. The term "resources" refers to both the available subcarriers and the available transmit power. The main contribution of the chapter is the proposal and

analysis of different power allocation schemes, which is presented in Section 5.3. The algorithms take into account different optimization criteria, such as throughput maximization and user fairness, thus addressing problem 5. One of these algorithms is an extension of the traditional unicast waterfilling algorithm for the multicast case. Some new approaches for the allocation of resources in SDMA scenarios are proposed in Section 5.5, which refers to problem 6.

Finally, a summary of the main conclusions of the thesis is presented in Chapter 6.

Chapter 2

System model

2.1 Introduction

This chapter presents a detailed description of the considered radio system. A general system model is derived for the multi-group multicast scenario with multiple antennas at the base station and single-antenna terminals. This model is a generalization of the unicast-only models, e.g. [PNG03, GS05b], as well as of the single-group multicast models, e.g. [SL04, SDL06]. It is also a further development of the multi-group multicast models presented in [KSL05, GS05a]. The proposed model provides details on the transmission/reception chain and introduces two possible representations of the system. Moreover, the system parameters are flexible enough, so that they can be adjusted to represent particular cases of the general model.

This chapter is organized as follows. In Section 2.2, some general system assumptions are discussed. Section 2.3 describes the proposed general multi-group multicast system model. In Section 2.4, it is shown that in the situation of other user scenarios, such as the single-group multicast or single-user/multi-user unicast, particular cases of the general model can be derived. Finally, Section 2.5 presents how the model can be extended to the case of multi-antenna user terminals.

2.2 System assumptions

This section describes the main characteristics of the system, which are considered throughout the thesis unless otherwise stated. The system corresponds to the downlink of a multicast, multi-carrier, multi-antenna, SDMA radio communication system. A more detailed description of these concepts follows:

- Multicast: There is a total of N users in the system, which are divided into K multicast groups, i.e., groups of users expecting the same data stream. A unicast user can be seen as a multicast group of size 1.

- Multi-carrier: “Modern” wireless communications systems, e.g. Wireless Local Area Network (WLAN) [ANS03], WiMAX [IEE04], and the 4G long term evolution of UMTS Terrestrial Radio Access Network (UTRAN) [3GP06b], employ multi-carrier modulation schemes in the downlink, such as Orthogonal Frequency Division Multiplexing (OFDM). For this reason, a multi-carrier system containing F available subcarriers is considered. Each subcarrier is assumed to have a tight enough bandwidth, i.e., less than the coherence bandwidth of the channel, to ensure flat fading and negligible inter-symbol interference [Pro95, Skl97].
- Multi-antenna: Adaptive antenna arrays are a key technology for enhancing the performance of wireless communications systems. An L -element adaptive antenna array is assumed to be installed at the base station, while the users have single-antenna devices. Since there are multiple antennas at the transmitter and multiple distributed receive antennas, this can also be called a Multiple Input Multiple Output (MIMO) system. Due to the orthogonality of the subcarriers, it is assumed that the antenna array can independently perform beamforming for the signals transmitted at each subcarrier (see Section 9.3 of [PNG03]).
- SDMA: In order to further improve the spectral efficiency of the system, the antenna array can be employed to perform SDMA. This technique separates the signals in the space dimension and allows that multiple streams be transmitted simultaneously on the same channel. Several works, e.g. [SSH04, Qiu05], employ the expression MIMO Multi User (MIMO-MU) as a synonym to SDMA, where the “multi-user” term refers to multiple unicast users being served simultaneously. Similarly, the term “multi-group” multicast has been employed, e.g. in [GS06], to refer to an SDMA scenario in which multiple multicast groups share the same channel. Throughout the thesis the terms multi-user/multi-group refer to SDMA scenarios, while the terms single-user/single-group refer to non-SDMA scenarios.

2.3 General system model

In this section, the general system model is presented. Initially, in order to simplify the notation, the unicast-only case is considered, in which each user expects a different data stream. Later in this section, however, the scenario is extended to the multicast case.

Let N denote the total number of data streams, F the number of subcarriers, N_f the number of streams per subcarrier, and L the number of antenna elements at the base

station. The variables $f \in \{1, \dots, F\}$, $n \in \{1, \dots, N_f\}$, and $l \in \{1, \dots, L\}$ represent the index of subcarriers, users, and antenna elements, respectively.

Fig. 2.1 illustrates the multi-carrier multi-antenna transmission chain. The low-pass frequency domain is considered [Kes07]. The variables depicted in the figure are defined as follows: $\{s_1, \dots, s_N\}$ represents the set of all input data symbols; $s_{n,f}$ denotes a data symbol mapped to user n on subcarrier f , $x_{l,f}$ corresponds to the output of the beamformer on antenna element l and subcarrier f , ν denotes the frequency, $x_l(\nu)$ is the spectral signal transmitted by antenna element l in the frequency domain, and $y_n(\nu)$ is the spectral signal received by user terminal n in the frequency domain.

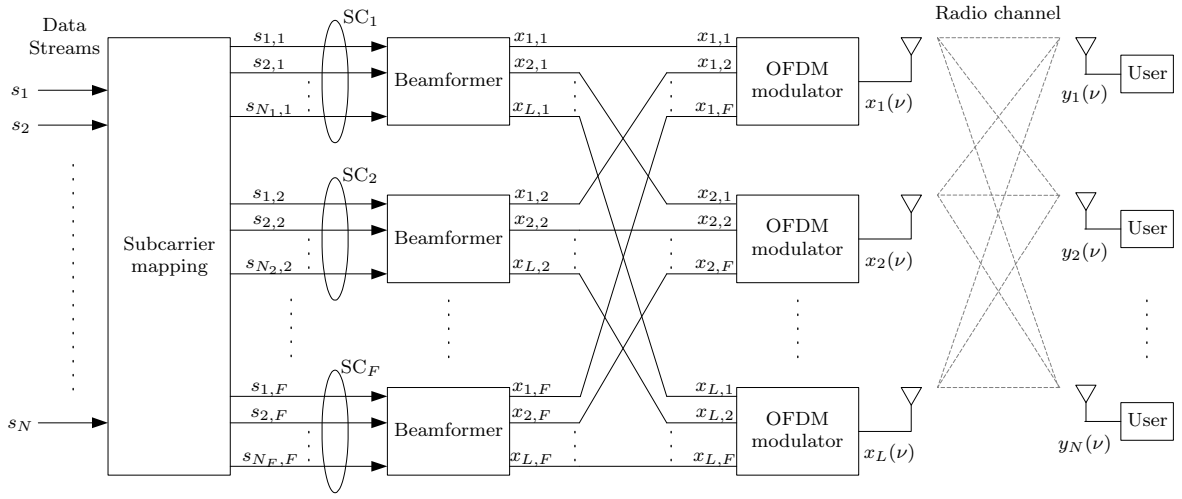


Figure 2.1. Overall illustration of the multi-carrier multi-antenna transmission chain.

The N data streams of all users are generated and then are mapped onto the F available subcarriers. It is here assumed that N_f streams are assigned per subcarrier. At each subcarrier, beamforming is performed and the resulting L spectral signals are provided to the L antenna elements for transmission. At each antenna branch L the spectral signals are fed into the OFDM modulator [HP03,SBM⁺04], which performs the Inverse Fast Fourier Transform (IFFT) and inserts the Cyclic Prefix (CP), and then are finally transmitted.

The spectral signal $x_l(\nu)$ of each antenna element l is transmitted over a linear radio channel and is received by user n . Note that each user has a different channel. It is assumed that the OFDM symbol time T_s is short enough so that the radio channel can be considered time-invariant during T_s . As a matter of fact, this assumption of time-invariance is assumed to be valid for a whole frame duration T_f , which corresponds to a number of consecutive OFDM symbols. The radio link between transmit antenna element l and user n has a transfer function denoted by $H_{n,l}(\nu)$.

The spectral signal $y_n(\nu)$ received by each user corresponds to the sum of the spectral signals $x_l(\nu)$ transmitted by each antenna element l multiplied by their respective transfer function $H_{n,l}(\nu)$. The received spectral signal is given by

$$y_n(\nu) = \sum_{l=1}^L x_l(\nu) H_{n,l}(\nu) + z_n(\nu), \quad (2.1)$$

where $z_n(\nu)$ corresponds to additive white Gaussian noise in the frequency domain.

Note that the considered OFDM system assumes a CP large enough to ensure flat fading per subcarrier. This implies that there is no inter-symbol interference, i.e., the channel coefficients for a certain time instant do not depend on previous samples. It is also assumed that the OFDM modulation guarantees the orthogonality among the subcarriers, so that they can be analyzed individually.

Let $H_{n,l,f}$ denote the sampled frequency response of the channel between user n and antenna l on subcarrier f . Due to the structure of the OFDM modulator/demodulator [PNG03], which includes the IFFT/FFT and the cyclic prefix operations, the expression of the spectral signal sample received by user n at subcarrier f can be reduced to

$$y_{n,f} = \sum_{l=1}^L x_{l,f} H_{n,l,f} + z_{n,f}. \quad (2.2)$$

For simplicity of notation, the subscript $(\cdot)_f$ is from now on dropped from the equations, resulting in

$$y_n = \sum_{l=1}^L x_l H_{n,l} + z_n, \quad (2.3)$$

for which a single subcarrier is considered in the following.

Now the precoding and decoding procedures, which complete the description of the transmission/reception chain, are explained. Let s_n denote the information symbol intended for transmission to user n , which may assume complex values drawn from the symbol constellation of the considered digital modulation scheme, e.g. M_o -Phase Shift Keying (PSK) or M_o -Quadrature Amplitude Modulation (QAM), where M_o denotes the modulation order. These N symbols are precoded before transmission, i.e., they pass through a linear filter which produces an equivalent symbol x_l for each transmit antenna element l . This transmit filter, which is also often called precoding or beamforming filter [PNG03, JUN05], can be designed based on channel knowledge available at the base station. Its optimization for different scenarios is the topic of Chapters 3 and 4. Each filter coefficient is denoted by $m_{l,n}$, which is associated to antenna element

l and user n . Each equivalent symbol x_l is a composition of all s_n symbols and the corresponding filter coefficients, as illustrated in Fig. 2.2, and is given by

$$x_l = \sum_{n=1}^N s_n m_{l,n}. \quad (2.4)$$

The decoding procedure is done after the OFDM demodulation at each user terminal. The sample of the received spectral signal y_n is passed through a receive filter with coefficient d_n . The receive filter design is discussed later in this section. The output of the filter corresponds to the estimate \hat{s}_n of data symbol s_n , which is illustrated in Fig. 2.3 and is given by

$$\hat{s}_n = y_n d_n = \left(\sum_{l=1}^L \left(\sum_{n=1}^N s_n m_{l,n} \right) H_{n,l} + z_n \right) d_n. \quad (2.5)$$

The system representation in (2.5) can also be expressed in terms of matrices and vectors. The data symbols s_n are grouped into vector $\mathbf{s} \in \mathbb{C}^N$. The coefficients $m_{l,n}$ of the transmit filter are stacked within matrix $\mathbf{M} \in \mathbb{C}^{L \times N}$, which is also called modulation matrix, such as in [SSH04]. Matrix $\mathbf{H} \in \mathbb{C}^{N \times L}$ contains the channel coefficients $H_{n,l}$ corresponding to all radio links between transmit antenna elements and user terminals. The noise components z_n are grouped into vector $\mathbf{z} \in \mathbb{C}^N$. The receive filter coefficients d_n of all user terminals are stacked into a diagonal matrix $\mathbf{D} \in \mathbb{C}^{N \times N}$, which is also usually called demodulation matrix. The elements outside the diagonal are zero since no receiver cooperation is assumed. The estimates of the data symbols are grouped into vector $\hat{\mathbf{s}} \in \mathbb{C}^N$, which is given by

$$\hat{\mathbf{s}} = \mathbf{DHMs} + \mathbf{Dz}. \quad (2.6)$$

Fig. 2.4 depicts the block diagram of the system. Note that the intermediate transmit and receive samples x_l and y_n are also grouped into vectors $\mathbf{x} \in \mathbb{C}^L$ and $\mathbf{y} \in \mathbb{C}^N$, respectively, where

$$\mathbf{x} = \mathbf{Ms}, \quad (2.7)$$

$$\mathbf{y} = \mathbf{HMs} + \mathbf{z}. \quad (2.8)$$

Since matrices \mathbf{M} and \mathbf{D} contain the transmit and receive filter coefficients, respectively, these matrices are often referred to as filters themselves in the following. Both \mathbf{M} and \mathbf{D} were so far assumed to be linear filters. In Chapter 4, however, non-linear versions of \mathbf{M} and \mathbf{D} are considered as well. The reason for the general system model to consider only linear transmit and receive filters is that, as shown in Chapter 4, the non-linear filters also have an equivalent linear representation.

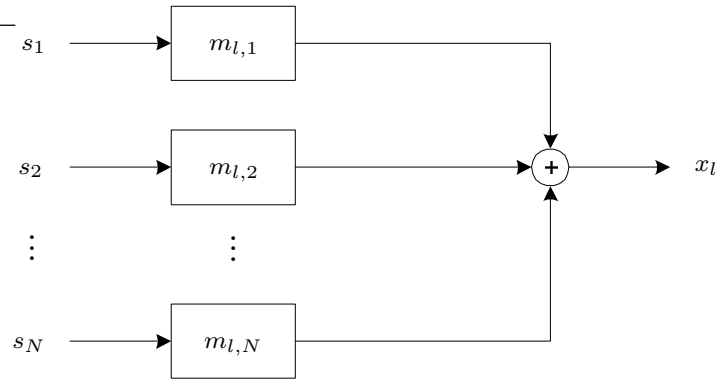


Figure 2.2. Illustration of symbol x_l composed at each antenna element l .

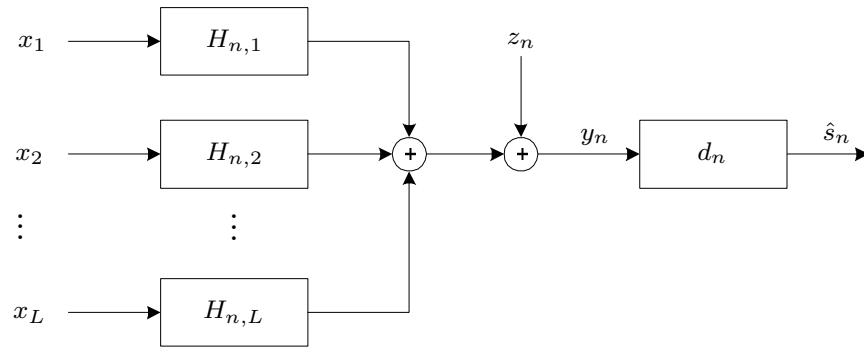


Figure 2.3. Illustration of the output \hat{s}_n for each user n .

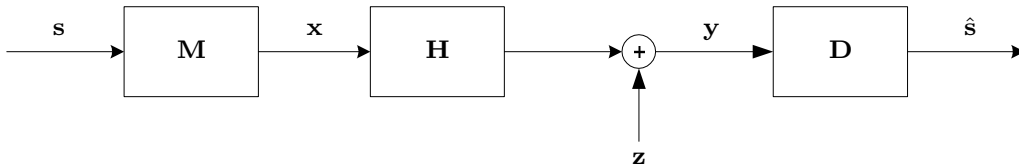


Figure 2.4. Block diagram of the general system model in the frequency domain.

The system model is not yet complete at this point, since the multicast characterization is still missing. For this purpose it is necessary to introduce a pair of auxiliary vectors and a set. Let K denote the total number of multicast groups. The number of users within each group is represented by vector $\mathbf{g} \in \mathbb{Z}^K$, whose k^{th} element $g_k \in \{1, \dots, N\}$ indicates the number of users within group $k \in \{1, \dots, K\}$. Note that the unicast users can be interpreted as multicast groups of unit size and that $\sum_{k=1}^K g_k = N$. In order to associate which users belong to which group, an index vector $\mathbf{b} \in \mathbb{Z}^N$ is also introduced, whose n^{th} element $b_n \in \{1, \dots, K\}$ indicates the group to which user

n belongs. Finally, the set \mathcal{N}_k is defined, which contains the indices of the users belonging to group k , i.e., for which $b_n = k$. For example, in a system with two unicast users and one multicast group composed of two users, we would have: $N = 4$, $K = 3$, $\mathbf{g} = [1, 1, 2]^T$, $\mathbf{b} = [1, 2, 3, 3]^T$, $\mathcal{N}_1 = \{1\}$, $\mathcal{N}_2 = \{2\}$, and $\mathcal{N}_3 = \{3, 4\}$. In order to better illustrate some concepts, in the following, this particular system configuration will be again used as an example, being referred to as the exemplary system.

An alternative representation for the system in (2.6), called reduced representation, is now presented. Since the users of a multicast group expect the same stream, the number K of multicast groups is also equivalent to the number of different data streams. For this reason there are $N - K$ repeated entries within vector $\mathbf{s} \in \mathbb{C}^N$. The removal of such repeated entries results in vector $\mathbf{s}' \in \mathbb{C}^K$. This operation can be mathematically expressed as

$$\mathbf{s}' = \mathbf{T}\mathbf{s}, \quad (2.9)$$

where $\mathbf{T} \in \mathbb{R}_+^{K \times N}$ is a transformation matrix with the n^{th} column given by $\mathbf{t}_n = g_{b_n}^{-1} \mathbf{e}_{b_n}$, for which \mathbf{e}_i corresponds to the i^{th} column of the identity matrix of dimension K . In the case of the exemplary system, matrix $\mathbf{T} \in \mathbb{R}^{3 \times 4}$ is given by

$$\mathbf{T} = \begin{bmatrix} 1 & 0 & 0 & 0 \\ 0 & 1 & 0 & 0 \\ 0 & 0 & 0.5 & 0.5 \end{bmatrix}. \quad (2.10)$$

Fig. 2.5 illustrates, for the exemplary scenario, the difference in terms of dimension between the complete and reduced representations, with the former containing 4 elements and the latter 3 elements. In the complete representation there is a direct correspondence between the indices of the actual and estimated data symbols. In the reduced representation, however, several user terminals may provide estimates to the same data symbol, e.g., \hat{s}_3 and \hat{s}_4 relate to data symbol s'_3 .

The reduced dimension of the data vector also leads to a reduced modulation matrix $\mathbf{M}' \in \mathbb{C}^{M \times K}$, i.e., instead of one beamforming vector per user there is now one beamforming vector per multicast group. Let \mathbf{m}_i and \mathbf{m}'_i represent the i^{th} column of matrices \mathbf{M} and \mathbf{M}' , respectively. They are related by

$$\mathbf{m}'_k = \sum_{n \in \mathcal{N}_k} \mathbf{m}_n, \quad \text{for } k = 1, \dots, K. \quad (2.11)$$

Matrix \mathbf{M}' can also be written as the following transformation of matrix \mathbf{M} :

$$\mathbf{M}' = \mathbf{M}\mathbf{T}^+, \quad (2.12)$$

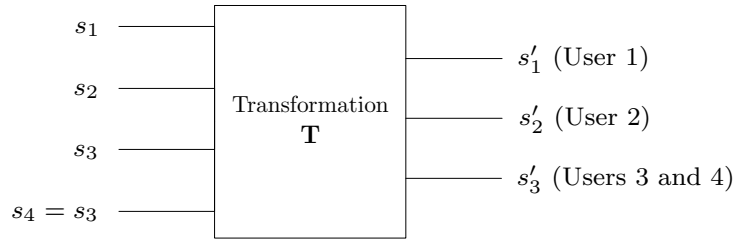


Figure 2.5. Complete (left) and reduced (right) representations for the exemplary scenario.

where $\mathbf{T}^+ \in \mathbb{R}^{N \times K}$ is the right pseudoinverse of matrix \mathbf{T} in (2.9). \mathbf{T}^+ has its n^{th} row given by $\mathbf{t}_n^+ = \mathbf{e}_{b_n}^T$, for which \mathbf{e}_i corresponds to the i^{th} column of the identity matrix of dimension K . In the case of the exemplary system, matrix $\mathbf{T}^+ \in \mathbb{R}^{4 \times 3}$ is given by

$$\mathbf{T}^+ = \begin{bmatrix} 1 & 0 & 0 \\ 0 & 1 & 0 \\ 0 & 0 & 1 \\ 0 & 0 & 1 \end{bmatrix}. \quad (2.13)$$

The complete and reduced representations have different symbol vectors and modulation matrices, nevertheless they still represent the same system. This can be confirmed by the following equation:

$$\mathbf{M}'\mathbf{s}' = \mathbf{M}\mathbf{T}^+\mathbf{T}\mathbf{s} = \mathbf{M}\mathbf{s}. \quad (2.14)$$

Note that, even though $\mathbf{T}^+\mathbf{T}$ is not an identity matrix, it can be shown that $\mathbf{T}^+\mathbf{T}\mathbf{s} = \mathbf{s}$, due to the repeated entries within \mathbf{s} . This same property can also be used to isolate \mathbf{s} in (2.9), which leads to

$$\mathbf{s} = \mathbf{T}^+\mathbf{s}'. \quad (2.15)$$

After substituting \mathbf{M}' and \mathbf{s}' in (2.6), the system equation can be rewritten in reduced form as

$$\hat{\mathbf{s}} = \mathbf{D}\mathbf{H}\mathbf{M}'\mathbf{s}' + \mathbf{D}\mathbf{z}. \quad (2.16)$$

From this system equation, the expression for the estimated data symbol of each user n can be written as

$$\hat{s}_n = d_n \mathbf{h}_n \mathbf{m}'_{b_n} s'_{b_n} + \sum_{k=1, k \neq b_n}^K d_n \mathbf{h}_n \mathbf{m}'_k s'_k + d_n z_n, \quad (2.17)$$

where \mathbf{h}_n corresponds to the n^{th} row of matrix \mathbf{H} . The three summands correspond, respectively, to the signal, interference, and noise parts of \hat{s}_n .

The design of the transmit filter is the topic of Chapters 3 and 4. The receive filter, on the other hand, can already be determined at this point. This independent receive filter determination does not necessarily lead to the optimal solution in terms of joint transmit/receive design, but it represents a simple approach that can be implemented regardless of the transmit filter. As it has been previously mentioned, there is an independent receive filter $d_n \in \mathbb{C}$ at each user terminal. It is assumed that each user terminal n knows the equivalent radio channel to the base station, which is given by $\mathbf{h}_n \mathbf{m}'_{b_n} \in \mathbb{C}$. This information can be obtained, for example, if the base station transmits pilot symbols at the beginning of each OFDM frame, so that the user terminal can estimate the equivalent channel. It is here assumed that the receive filter satisfies the constraint that, in the absence of noise and interference, the estimated symbols are exactly the same as the original data symbols. This leads to

$$d_n \mathbf{h}_n \mathbf{m}'_{b_n} s'_{b_n} = s'_{b_n} \implies d_n \mathbf{h}_n \mathbf{m}'_{b_n} = 1 \implies d_n = (\mathbf{h}_n \mathbf{m}'_{b_n})^{-1}, \quad (2.18)$$

and the filter expression in matrix form is given by

$$\mathbf{D} = \text{diag}(\mathbf{h}_1 \mathbf{m}'_{b_1}, \dots, \mathbf{h}_N \mathbf{m}'_{b_N})^{-1}, \quad (2.19)$$

where the $\text{diag}(\cdot)$ operator returns a diagonal matrix when the argument is a vector or it returns a vector with the main diagonal elements when the argument is a matrix.

Next, the system is further characterized by defining the downlink SINR, the transmit power constraints, and the signal covariance matrices.

The expression for the average downlink SINR γ_n , measured at each user terminal n , corresponds to the average of the SINR measurements performed at each OFDM symbol time over the whole OFDM frame duration T_f . As previously mentioned, it is assumed that during the period of time T_f , the channel as well as the transmit and receive filters are time-invariant. The random variables correspond to the data symbols and noise. The SINR is calculated for a given channel realization, and a large enough number of symbols is considered, such that the symbol and noise powers converge to their average values. Taking (2.17) into account, the SINR γ_n is given by

$$\begin{aligned} \gamma_n &= \frac{\text{E}\{|d_n \mathbf{h}_n \mathbf{m}'_{b_n} s'_{b_n}|^2\}}{\text{E}\left\{\sum_{k=1, k \neq b_n}^K |d_n \mathbf{h}_n \mathbf{m}'_k s'_k|^2\right\} + \text{E}\{|d_n z_n|^2\}} = \\ &= \frac{|d_n|^2 \text{E}\{|s'_{b_n}|^2\} |\mathbf{h}_n \mathbf{m}'_{b_n}|^2}{|d_n|^2 \sum_{k=1, k \neq b_n}^K \text{E}\{|s'_k|^2\} |\mathbf{h}_n \mathbf{m}'_k|^2 + |d_n|^2 \text{E}\{|z_n|^2\}} = \\ &= \frac{\sigma_s^2 |\mathbf{h}_n \mathbf{m}'_{b_n}|^2}{\sum_{k=1, k \neq b_n}^K \sigma_s^2 |\mathbf{h}_n \mathbf{m}'_k|^2 + \sigma_z^2}, \quad \text{for } n = 1, \dots, N, \end{aligned} \quad (2.20)$$

where σ_s^2 and σ_z^2 correspond, respectively, to the average symbol and noise power.

It is assumed that the maximum power available for transmission is denoted by P . As a consequence, the design of matrix \mathbf{M} must satisfy the following power constraint:

$$\mathbb{E}\{|\mathbf{M}\mathbf{s}|^2\} = \mathbb{E}\{\mathbf{s}^H \mathbf{M}^H \mathbf{M} \mathbf{s}\} = \text{tr}(\mathbf{M}^H \mathbf{M} \mathbb{E}\{\mathbf{s}\mathbf{s}^H\}) = \text{tr}(\mathbf{M}^H \mathbf{M} \mathbf{R}_s) \leq P, \quad (2.21)$$

where $\text{tr}(\cdot)$ denotes the trace of a matrix and $\mathbf{R}_s = \mathbb{E}\{\mathbf{s}\mathbf{s}^H\} \in \mathbb{C}^{N \times N}$ is the signal covariance matrix. Note that, in the case of uncorrelated and equiprobable symbols, \mathbf{R}_s corresponds to a block diagonal matrix, with each block k equal to $\sigma_s^2 \mathbf{J} \in \mathbb{R}^{g_k \times g_k}$, where \mathbf{J} corresponds to a matrix of ones. Equivalently, with \mathbf{M}' given by (2.11), the constraint may also be expressed as:

$$\text{tr}(\mathbf{M}'^H \mathbf{M}' \mathbf{R}'_s) \leq P, \quad (2.22)$$

for which $\mathbf{R}'_s = \mathbb{E}\{\mathbf{s}'\mathbf{s}'^H\} \in \mathbb{C}^{K \times K}$. Considering the assumption of uncorrelated and equiprobable symbols, $\mathbf{R}'_s = \sigma_s^2 \mathbf{I} \in \mathbb{R}^{K \times K}$, where \mathbf{I} corresponds to the identity matrix. An example of matrices \mathbf{R}_s and \mathbf{R}'_s , considering the exemplary system, follows:

$$\mathbf{R}_s = \begin{bmatrix} \sigma_s^2 & 0 & 0 & 0 \\ 0 & \sigma_s^2 & 0 & 0 \\ 0 & 0 & \sigma_s^2 & \sigma_s^2 \\ 0 & 0 & \sigma_s^2 & \sigma_s^2 \end{bmatrix}, \quad \mathbf{R}'_s = \begin{bmatrix} \sigma_s^2 & 0 & 0 \\ 0 & \sigma_s^2 & 0 \\ 0 & 0 & \sigma_s^2 \end{bmatrix}. \quad (2.23)$$

2.4 Particular cases

2.4.1 Introduction

In this section, particular cases of the general system model are derived. These particular cases are obtained through a proper adjustment of the system parameters. All particular cases represent multi-carrier multi-antenna systems. They differ with regard to whether or not they employ SDMA and whether unicast or multicast users are considered. The following particular system model cases are considered: the single-group multicast in Section 2.4.2, the multi-user unicast in Section 2.4.3, and the single-user unicast in Section 2.4.4.

The single-group multicast model corresponds to the case in which only one multicast group is allowed per subcarrier, and it is considered in Chapter 3. The other two unicast models are presented for illustration and comparison purposes. The multi-user unicast model corresponds to an SDMA scenario with only unicast users, whereas the single-user unicast model represents the case in which only a single unicast user is allowed per subcarrier.

2.4.2 Single-group multicast

The single-group multicast scenario corresponds to a situation in which only users of the same multicast group share the same subcarrier. In this case, the number of multicast groups K and the auxiliary vectors \mathbf{g} and \mathbf{b} assume the following values:

$$K = 1, \quad (2.24a)$$

$$\mathbf{g} \in \mathbb{Z} \quad | \quad g = N, \quad (2.24b)$$

$$\mathbf{b} \in \mathbb{Z}^N \quad | \quad \mathbf{b} = \mathbf{1}. \quad (2.24c)$$

When applying these parameters to the general model, it is verified that the complete form of the system equation remains the same as (2.6), whereas the reduced form is simplified. In the reduced form, the transmit filter is expressed by vector $\mathbf{m} \in \mathbb{C}^M$ and a single data symbol $s \in \mathbb{C}$ is considered. Note that, in order to simplify the reduced form notation, the $(\cdot)'$ symbol has been dropped, since both forms can now be identified by their corresponding dimensions.

The transformation matrix \mathbf{T} is in this case a vector \mathbf{t} . The values of \mathbf{t} and \mathbf{t}^+ are

$$\mathbf{t} = \frac{1}{N} \mathbf{1}^T \quad \text{and} \quad \mathbf{t}^+ = \mathbf{1}, \quad (2.25)$$

which leads to the following relationship between the complete and reduced forms:

$$s = \frac{1}{N} \mathbf{1}^T \mathbf{s} \quad \text{and} \quad \mathbf{m} = \mathbf{M} \mathbf{1}. \quad (2.26)$$

From (2.15) and (2.25), it also follows that

$$\mathbf{s} = s \mathbf{1}. \quad (2.27)$$

The single-group multicast system block diagram is shown in Fig. 2.6 and (2.16) can be written as:

$$\hat{\mathbf{s}} = \mathbf{D} \mathbf{H} \mathbf{m} s + \mathbf{D} \mathbf{z}. \quad (2.28)$$

Since there is no interference among the users of a same group, the SINR in (2.20) becomes:

$$\gamma_n = \frac{\sigma_s^2 |\mathbf{h}_n \mathbf{m}|^2}{\sigma_z^2}, \quad \text{for } n = 1, \dots, N. \quad (2.29)$$

The signal covariance matrix is expressed as $\mathbf{R}_s = \sigma_s^2 \mathbf{J} \in \mathbb{R}^{N \times N}$ in the complete form, while in the reduced form it becomes a scalar $R_s = \sigma_d^2$. The corresponding power



Figure 2.6. System block diagram of the single-group multicast scenario.

constraints of the complete and reduced forms, given in (2.21) and (2.22), respectively, may be rewritten as:

$$\sigma_s^2 \text{tr}(\mathbf{M}^H \mathbf{M} \mathbf{J}) \leq P, \quad (2.30)$$

$$\sigma_s^2 \|\mathbf{m}\|^2 \leq P. \quad (2.31)$$

And since there is only one multicast group, the receive filter in (2.19) can also be expressed as:

$$\mathbf{D} = \text{diag}(\mathbf{H}\mathbf{m})^{-1}. \quad (2.32)$$

2.4.3 Multi-user unicast

In the multi-user unicast scenario, there are several unicast users sharing the same resource. Descriptions of the multi-user unicast scenario can be found in works such as [SSH04, JUN05]. In this case, the number of multicast groups K and the auxiliary vectors \mathbf{g} and \mathbf{b} assume the following values:

$$K = N, \quad (2.33a)$$

$$\mathbf{g} \in \mathbb{Z}^N \quad | \quad \mathbf{g} = \mathbf{1}, \quad (2.33b)$$

$$\mathbf{b} \in \mathbb{Z}^N \quad | \quad \mathbf{b} = [1, 2, \dots, N]^T. \quad (2.33c)$$

For this configuration of the auxiliary vectors, the transformation matrix \mathbf{T} is an identity, i.e., $\mathbf{T} = \mathbf{T}^+ = \mathbf{I}$. This results in the reduced form being equal to the complete form, i.e., $\mathbf{M}' = \mathbf{M}$ and $\mathbf{s}' = \mathbf{s}$. The system equation is therefore the same as (2.6) for both forms. The same is valid for the system block diagram, which is identical to that of Fig. 2.4.

From (2.33c) it can be seen that $b_n = n$, for $n = 1, \dots, N$. By substituting this expression in (2.20), the SINR can be rewritten as:

$$\gamma_n = \frac{\sigma_s^2 |\mathbf{h}_n \mathbf{m}_n|^2}{\sum_{k=1, k \neq n}^N \sigma_s^2 |\mathbf{h}_n \mathbf{m}_k|^2 + \sigma_z^2}, \quad \text{for } n = 1, \dots, N. \quad (2.34)$$

The signal covariance matrix is expressed as $\mathbf{R}_s = \sigma_s^2 \mathbf{I} \in \mathbb{R}^{N \times N}$, and the power constraint is given by

$$\sigma_s^2 \text{tr}(\mathbf{M}^H \mathbf{M}) \leq P. \quad (2.35)$$

The receive filter becomes:

$$\mathbf{D} = \text{diag}(\text{diag}(\mathbf{H}\mathbf{M}))^{-1}. \quad (2.36)$$

2.4.4 Single-user unicast

The single-user unicast scenario is the simplest case, in which only one unicast user is considered. In this case, the number of multicast groups K and the auxiliary vectors \mathbf{g} and \mathbf{b} assume the following values:

$$K = N = 1, \quad (2.37a)$$

$$\mathbf{g} \in \mathbb{Z} \quad | \quad g = 1, \quad (2.37b)$$

$$\mathbf{b} \in \mathbb{Z} \quad | \quad b = 1. \quad (2.37c)$$

In this case, the transformation matrix \mathbf{T} becomes a scalar t , with $t = t^+ = 1$. For this reason, similarly to the multi-user unicast case, the complete form is also identical to the reduced form. The channel and modulation matrices are replaced by a row vector $\mathbf{h} \in \mathbb{C}^M$ and a column vector $\mathbf{m} \in \mathbb{C}^M$, respectively. The data symbol vector \mathbf{s} , the estimated symbol vector $\hat{\mathbf{s}}$, the noise vector \mathbf{z} , and the demodulation matrix \mathbf{D} , are reduced to the scalars $s \in \mathbb{C}$, $\hat{s} \in \mathbb{C}$, $z \in \mathbb{C}$, and $d \in \mathbb{C}$, respectively. The system block diagram is shown in Fig. 2.7, and the system equation is rewritten as

$$\hat{s} = d\mathbf{h}\mathbf{m}s + dz. \quad (2.38)$$

Since there is only a single unicast user, the index n is dropped and the SINR is

$$\gamma = \frac{\sigma_s^2 |\mathbf{h}\mathbf{m}|^2}{\sigma_z^2}. \quad (2.39)$$

The signal covariance matrix \mathbf{R}_s becomes a scalar $R_s = \sigma_s^2 \in \mathbb{R}$ and the transmit power constraint becomes

$$\sigma_s^2 \|\mathbf{m}\|^2 \leq P. \quad (2.40)$$

The receive filter is given by

$$d = (\mathbf{h}\mathbf{m})^{-1}. \quad (2.41)$$

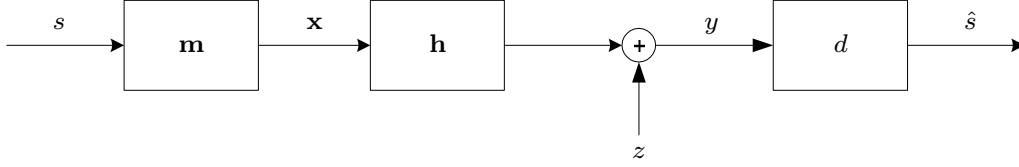


Figure 2.7. System block diagram of the single-user unicast scenario.

Descriptions of the unicast system model can be found in works such as [PNG03, KBB⁺05]. The general system model presented in this chapter is in accordance with the aforementioned literature, since the single-user unicast model can be derived from the general model as a particular case.

2.5 Extension for multi-antenna terminals

Multi-antenna terminals have been the focus of several recent studies, such as [KBB⁺05], which investigate the performance of different MIMO techniques. The number of antenna elements at each terminal, however, is not expected to be very large, due to the usually small dimensions of mobile devices [AH04]. Throughout this work, only single-antenna terminals are considered, but it is shown in this section that the extension of the model for multi-antenna terminals is straightforward.

Let L_t and L_r denote the total amount of transmit and receive antenna elements, respectively. The number of antenna elements at each user terminal n is denoted by $L_r^{(n)}$ and the sum of all receive antenna elements results in the total amount L_r , i.e., $\sum_{n=1}^N L_r^{(n)} = L_r$. The system equation is the same as (2.6), but the system variables are defined as follows:

$$\mathbf{s} = [s_1, \dots, s_N]^T \in \mathbb{C}^N, \quad (2.42a)$$

$$\mathbf{M} = [\mathbf{m}_1, \dots, \mathbf{m}_N] \in \mathbb{C}^{L_t \times N}, \quad (2.42b)$$

$$\mathbf{H} = [\mathbf{H}_1^T, \dots, \mathbf{H}_N^T]^T \in \mathbb{C}^{L_r \times L_t}, \quad (2.42c)$$

$$\mathbf{z} = [\mathbf{z}_1^T, \dots, \mathbf{z}_N^T]^T \in \mathbb{C}^{L_r}, \quad (2.42d)$$

$$\mathbf{D} = \text{diag}(\mathbf{d}_1^T, \dots, \mathbf{d}_N^T) \in \mathbb{C}^{N \times L_r}, \quad (2.42e)$$

$$\hat{\mathbf{s}} = [\hat{s}_1, \dots, \hat{s}_N]^T \in \mathbb{C}^N, \quad (2.42f)$$

where $\mathbf{H}_n \in \mathbb{C}^{L_r^{(n)} \times L_t}$, $\mathbf{z}_n \in \mathbb{C}^{L_r^{(n)}}$, and $\mathbf{d}_n \in \mathbb{C}^{L_r^{(n)}}$. This is equivalent to stacking together the components associated to the group of receive antenna elements of each

user terminal. Note that it has been assumed that the number of data streams is equal to the number of users N , and not to the total number of receive antenna elements L_r .

The reduced representation of the system equation is obtained similarly to Section 2.3, with the reduced data vector denoted by $\mathbf{s}' \in \mathbb{C}^K$ and the reduced modulation matrix denoted by $\mathbf{M}' \in \mathbb{C}^{L_t \times K}$. The average SINR γ_n measured at each user terminal n is given by

$$\begin{aligned}
\gamma_n &= \frac{\mathbb{E}\{|\mathbf{d}_n^T \mathbf{H}_n \mathbf{m}'_{b_n} s'_{b_n}|^2\}}{\mathbb{E}\left\{\sum_{k=1, k \neq b_n}^K |\mathbf{d}_n^T \mathbf{H}_n \mathbf{m}'_k s'_k|^2\right\} + \mathbb{E}\{|\mathbf{d}_n^T \mathbf{z}_n|^2\}} = \\
&= \frac{\mathbb{E}\{|s'_{b_n}|^2\} |\mathbf{d}_n^T \mathbf{H}_n \mathbf{m}'_{b_n}|^2}{\sum_{k=1, k \neq b_n}^K \mathbb{E}\{|s'_k|^2\} |\mathbf{d}_n^T \mathbf{H}_n \mathbf{m}'_k|^2 + \mathbb{E}\{\mathbf{z}_n^H \mathbf{d}_n^* \mathbf{d}_n^T \mathbf{z}_n\}} = \\
&= \frac{\sigma_s^2 |\mathbf{d}_n^T \mathbf{H}_n \mathbf{m}'_{b_n}|^2}{\sum_{k=1, k \neq b_n}^K \sigma_s^2 |\mathbf{d}_n^T \mathbf{H}_n \mathbf{m}'_k|^2 + \sigma_z^2 \mathbf{d}_n^T \mathbf{d}_n^*}, \quad \text{for } n = 1, \dots, N.
\end{aligned} \tag{2.43}$$

Regarding the receive filter design, instead of a single scalar d_n per user, there is now a vector \mathbf{d}_n . A possible optimization criterion for determining \mathbf{D} consists of maximizing the received SNR. Assuming the constraint that, in the absence of noise and interference, the estimated symbols are exactly the same as the original data symbols, the optimization problem for each user n can be written as:

$$\begin{aligned}
\mathbf{d}_{n,\text{opt}} &= \underset{\mathbf{d}_n}{\operatorname{argmax}} \gamma_n \\
&\text{subject to: } \mathbf{d}_n^T \mathbf{H}_n \mathbf{m}'_{b_n} = 1.
\end{aligned} \tag{2.44}$$

Furthermore, if there are multiple streams per user and cooperation among the receive antenna elements of a same user terminal is assumed, then the receive filter of user n becomes a matrix \mathbf{D}_n , and the global receive filter expression in (2.42e) becomes a block diagonal matrix. For this case, different receive filters may be applied [JUN05], such as the zero-forcing, the minimum mean square error, and the matched filter. Nevertheless, the further investigation and design of different receive filters for multi-antenna terminals is not within the scope of this thesis, and is left as a topic for further studies.

Chapter 3

Adaptive single-group multicast beamforming

3.1 Introduction

The theme of this chapter is beamforming for the single-group multicast scenario. The typical multicast beamforming problem of maximizing the worst-user SNR is formulated in Section 3.2. This problem has been considered by several works, such as [SL04, ZSV04, SDL06, HSJ⁺07], and different solutions have been proposed. A review of the state-of-the-art and recent advances on multicast beamforming algorithms is presented in Section 3.3. Nevertheless, algorithms based on other optimization criteria known from the unicast case, such as the Matched Filter (MF), linear Zero-Forcing (ZF) filter, linear Minimum Mean Square Error (MMSE) filter, Tomlinson-Harashima Precoding (THP), and Switched Fixed Beams (SFB), are also of interest for the multicast case. Only a few works have dealt with this issue in the multicast context [SK06a, SK06b, SK06c]. In Section 3.4, these algorithms are formulated for the multicast case. Additionally, a new suboptimal algorithm, called User-Selective Matched Filter (USMF), is proposed for dealing with the problem of maximizing the worst-user SNR. It is shown that it achieves good results, especially for scenarios with a strong Line-Of-Sight (LOS). The performance of the algorithms is analyzed in Section 3.5 through simulations. Finally, the main conclusions are drawn in Section 3.6.

3.2 Problem formulation

The single-group multicast beamforming optimization problem can be specified in different ways, which depend on the cost function and constraints that are considered. A reasonable optimization objective corresponds to the maximization of the minimum SNR among the users of the multicast group [SL04,SDL06]. Such an approach promotes fairness among the users and is adequate to the context of reliable multicast services. Taking into account the single-group multicast system model presented in Section 2.4.2, the optimization problem of determining the beamforming vector $\mathbf{m} \in \mathbb{C}^L$ that maximizes the minimum SNR γ_n can be expressed as

$$\begin{aligned} \mathbf{m}_{\text{opt}} &= \underset{\mathbf{m}}{\operatorname{argmax}} \min_n \gamma_n, \quad n = 1, \dots, N \\ \text{subject to: } & \sigma_s^2 \|\mathbf{m}\|^2 \leq P, \end{aligned} \tag{3.1}$$

where γ_n is given by

$$\gamma_n = \frac{\mathbb{E}\{|\mathbf{h}_n \mathbf{m}_s|^2\}}{\mathbb{E}\{|z_n|^2\}} = \frac{\sigma_s^2 |\mathbf{h}_n \mathbf{m}|^2}{\sigma_z^2}. \quad (3.2)$$

This optimization problem is a quadratically constrained quadratic programming problem [BV04]. It has been shown in [SDL06] that this problem is NP-hard (Nondeterministic Polynomial time hard), i.e., it is at least as hard to solve as an NP (Non-Polynomial time) problem [GJ79]. For this reason, lower-complexity suboptimal algorithms capable of providing solutions in an acceptable amount of time are required.

Another possible optimization problem corresponds to the minimization of the transmit power subject to individual user quality constraints. It can be written as

$$\begin{aligned} \mathbf{m}_{\text{opt}} &= \underset{\mathbf{m}}{\text{argmin}} \|\mathbf{m}\|^2, \\ \text{subject to: } &\gamma_n \geq \gamma_{\text{tgt}} \quad n = 1, \dots, N, \end{aligned} \quad (3.3)$$

where γ_n is defined in (3.2) and γ_{tgt} corresponds to the target SNR required by the users. It has been shown in [SDL06] that this problem is equivalent to the maximization of the minimum SNR and is also NP-hard. Given a feasible γ_{tgt} , the solution can be scaled according to the power constraint in order to reach the same solution as (3.1).

3.3 State-of-the-art

The single-group multicast beamforming problem has been first approached by Narula et al. in [NLTW98]. The beamforming optimization aimed at maximizing the average SNR perceived by the users within the multicast group. Lopez further developed this algorithm by showing capacity bounds in [Lop02]. Nevertheless, the drawback of maximizing the average SNR is that it can be rather unfair to the users. For this reason, other works have proposed different optimization criteria, such as the maximization of the minimum SNR. These works, which were introduced by Table 1.1 of Chapter 1, are discussed in the following, according to their order of appearance in the literature.

Zhang et al. have proposed numerical methods for solving the problem of maximizing the minimum SNR. In [ZSV02], transmit signature codes and receive filters are designed for multicast Code Division Multiple Access (CDMA) systems. An Iterative Least Distance Programming (ILDLP) algorithm is proposed, as well as a lower complexity solution based on Linear Programming (LP). In [ZSV04] these algorithms are extended to the space-time and space-only cases, which take beamforming into account. An

Iterative Spatial Diagonalization (ISD) algorithm is proposed for the space-only case, which has the restriction that the number of users has to be less than or equal to the number of antennas at the base station. The ISD algorithm requires a Least Squares with Inequality constraint (LSI) algorithm in order to calculate the beamforming vector at each iteration, and the convergence is achieved by employing a steepest descent algorithm.

Sun and Liu expressed the optimization problem of maximizing the minimum SNR in its dual form, such as in (3.3), which corresponds to the minimization of the transmit power subject to SNR constraints [SL04]. The problem was solved by employing Sequential Quadratic Programming (SQP) methods, whose performance was shown to be much superior to the maximization of the average SNR. Nevertheless, existing SQP solvers are rather time-consuming, and they require the selection of good starting points in order to avoid falling into local minima. For this reason, the performance of the algorithm solved through SQP was compared in [SL04] to that of diversity techniques, such as space-time coding, applied to the multicast case, which have lower complexity and do not require channel knowledge at the transmitter. It was shown that there are specific cases in which each of these techniques is most adequate. Diversity techniques are particularly more efficient for reasonably large group sizes.

A more efficient solution to the maximization of the minimum SNR problem, as well as its dual form, was proposed by Sidiropoulos et al. in [SD04,SDL06]. They have demonstrated that the problem is NP-hard and have proposed a suboptimum solution based on Semi-Definite Relaxation (SDR). The optimization problem is rewritten in an equivalent form, in which the non-convex term is expressed by a rank-one constraint, which is given by

$$\begin{aligned} \mathbf{X}_{\text{opt}} &= \underset{\mathbf{X}}{\operatorname{argmax}} \min_n \operatorname{tr}(\mathbf{X}\mathbf{G}_n), \quad n = 1, \dots, N, \\ \text{subject to: } &\begin{cases} \operatorname{tr}(\mathbf{X}) = P/\sigma_s^2 \\ \mathbf{X} \succeq \mathbf{0} \\ \operatorname{rank}(\mathbf{X}) = 1 \end{cases}, \end{aligned} \quad (3.4)$$

where $\mathbf{X} \in \mathbb{C}^{L \times L}$ is the new variable to be optimized, $\mathbf{G}_n = \mathbf{h}_n^H \mathbf{h}_n / \sigma_z^2 \in \mathbb{C}^{L \times L}$, and $\mathbf{X} \succeq \mathbf{0}$ means that matrix \mathbf{X} is semi-definite positive. The idea is to drop the rank-one constraint and solve the problem through Semi-Definite Programming (SDP), for which there exist very efficient numerical methods, such as those implemented by the SeDuMi Matlab toolbox [Stu99]. If it happens that \mathbf{X} has in fact rank one, then the optimal solution has been achieved and is given by the principal eigenvector of \mathbf{X} , otherwise randomization methods are employed in order to provide an approximation of the optimal solution. In [SDL06], some different randomization methods are proposed,

such as *randA*, *randB*, and *randC*, which differ in how the candidate beamforming vector solutions are obtained from matrix \mathbf{X} . The *randB* method, for example, assumes that each element l of vector \mathbf{m} is given by $m_l = \sqrt{X_{l,l}} e^{j\theta}$, where θ is uniformly distributed within $[0, 2\pi]$.

More recently, some numerical optimization alternatives to the SDR approach have been proposed by Hunger et al. in [HSJ⁺07]. They derived a successive beamforming-filter computation algorithm, which is suitable for the case in which the number of users is lower than the number of transmit antennas. For the opposite case, an iterative SNR-increasing update algorithm is proposed, which iteratively improves the worst-user SNR and has a complexity lower than that of SDR. In [HSJ⁺07] it was shown that, for large group sizes, this iterative algorithm achieves better results than the SeDuMi SDR approach with a randomization process limited to 100 random vectors.

None of these previous works, however, has approached the application of traditional unicast beamforming techniques, such as the matched filter or zero-forcing, to the multicast case. In the next section, these traditional beamforming techniques, which have different optimization criteria, are derived for the multicast context. Moreover, the design of efficient suboptimal algorithms for maximizing the minimum SNR for varied radio propagation scenarios is still a relevant issue. For this reason, a new low-complexity algorithm is also proposed in the next section, which is shown to provide a good trade-off between complexity and performance for both Non-Line-Of-Sight (NLOS) and Line-Of-Sight (LOS) scenarios.

3.4 Beamforming algorithms

3.4.1 Matched filter

The Matched Filter (MF) optimization has been extensively studied for unicast scenarios. The initial focus was on the receive matched filter, which does not require channel knowledge at the transmitter, but later the idea was extended to transmit processing. In [EN93,BF99,CLM01] the prerake filter has been studied, which was shown in [JUN01] to be equivalent to the transmit matched filter. In [Joh04,JUN05] it was shown that both the receive and transmit filters are based on similar optimizations. In this section, the matched filter expression is derived for the multicast single-group scenario. The optimization problem can be written as

$$\mathbf{m}_{\text{MF}} = \underset{\mathbf{m}}{\operatorname{argmax}} \frac{|\mathbf{E}\{\mathbf{s}^H \mathbf{y}\}|^2}{\mathbf{E}\{|\mathbf{s}|^2\} \mathbf{E}\{|\mathbf{z}|^2\}}, \quad \text{subject to: } \sigma_s^2 \|\mathbf{m}\|^2 \leq P. \quad (3.5)$$

From Section 2.4.2 it is seen that the signal vector \mathbf{s} is also given by $\mathbf{s} = s\mathbf{1}$. The cost function of the optimization problem corresponds to an equivalent group SNR γ_{eq} , which can be further expressed as

$$\gamma_{\text{eq}} = \frac{|\mathbf{E}\{(s\mathbf{1})^H \mathbf{y}\}|^2}{\mathbf{E}\{||s\mathbf{1}||^2\}\mathbf{E}\{||\mathbf{z}||^2\}} = \frac{|\mathbf{E}\{s^* \mathbf{1}^T (\mathbf{H}\mathbf{m}s + \mathbf{z})\}|^2}{(\sigma_s^2 \mathbf{1}^T \mathbf{1})(N\sigma_z^2)} = \frac{\sigma_s^2}{N^2 \sigma_z^2} |\mathbf{1}^T \mathbf{H}\mathbf{m}|^2. \quad (3.6)$$

The problem can be solved through Lagrange optimization. The expression of the Lagrangian function L is given by

$$L(\mathbf{m}, \mu) = -\frac{\sigma_s^2}{N^2 \sigma_z^2} \mathbf{m}^H \mathbf{H}^H \mathbf{1} \mathbf{1}^T \mathbf{H}\mathbf{m} + \mu(\sigma_s^2 \mathbf{m}^H \mathbf{m} - P), \quad (3.7)$$

where $\mu \in \mathbb{R}$ is a Lagrange multiplier. The Karush-Kuhn-Tucker (KKT) conditions for optimality are

$$\sigma_s^2 ||\mathbf{m}||^2 \leq P, \quad \mu \geq 0, \quad \mu(P - \sigma_s^2 \mathbf{m}^H \mathbf{m}) = 0, \quad \frac{\partial L(\mathbf{m}, \mu)}{\partial \mathbf{m}} = \mathbf{0}. \quad (3.8)$$

From the last condition it follows that

$$\begin{aligned} \frac{\partial L(\mathbf{m}, \mu)}{\partial \mathbf{m}} &= -\frac{\sigma_s^2}{N^2 \sigma_z^2} \mathbf{H}^T \mathbf{1} \mathbf{1}^T \mathbf{H}^* \mathbf{m}^* + \mu \sigma_s^2 \mathbf{m}^* = \mathbf{0}, \\ \mathbf{H}^H \mathbf{1} \mathbf{1}^T \mathbf{H}\mathbf{m} &= \mu N^2 \sigma_z^2 \mathbf{m}. \end{aligned} \quad (3.9)$$

In order to avoid the trivial solution, i.e., $\mathbf{m} = \mathbf{0}$, and according to the second KKT condition, then $\mu > 0$. Additionally, the third KKT condition implies that the power constraint is an equality, i.e., $\sigma_s^2 \mathbf{m}^H \mathbf{m} = P$. Note that (3.9) corresponds to an eigenvalue problem of the form $\mathbf{A}\mathbf{m} = \lambda\mathbf{m}$, for which $\mathbf{A} = \mathbf{H}^H \mathbf{1} \mathbf{1}^T \mathbf{H}$ and $\lambda = \mu N^2 \sigma_z^2$. The solution is given by a scaled version of the eigenvector associated to the largest eigenvalue of \mathbf{A} . In this particular case, matrix \mathbf{A} results from the product of two vectors, having therefore rank 1. Assuming that $\mathbf{A} = \mathbf{v}\mathbf{v}^H$, where $\mathbf{v} = \mathbf{H}^H \mathbf{1}$, rank 1 matrices present the following properties [Osn05]: \mathbf{A} has at most one non-zero eigenvalue, this eigenvalue is given by $\mathbf{v}^H \mathbf{v}$, and \mathbf{v} is the associated eigenvector. This leads to

$$\mathbf{m} = \beta \mathbf{H}^H \mathbf{1}, \quad (3.10)$$

where $\beta \in \mathbb{R}$ can be found by substituting (3.10) into the power constraint:

$$\sigma_d^2 ||\beta \mathbf{H}^H \mathbf{1}||^2 = P \implies \beta^2 = \frac{P}{\sigma_s^2 \mathbf{1}^T \mathbf{H} \mathbf{H}^H \mathbf{1}} \implies \beta = \sqrt{\frac{P}{\sigma_s^2 \text{tr}(\mathbf{H} \mathbf{H}^H \mathbf{J})}}. \quad (3.11)$$

The final solution is given by

$$\mathbf{m}_{\text{MF}} = \sqrt{\frac{P}{\sigma_s^2 \text{tr}(\mathbf{H} \mathbf{H}^H \mathbf{J})}} \mathbf{H}^H \mathbf{1}. \quad (3.12)$$

The expression of the receive filter, when substituting (3.12) into (2.32), becomes:

$$\mathbf{D}_{\text{MF}} = \sqrt{\frac{\sigma_s^2 \text{tr}(\mathbf{H}\mathbf{H}^H\mathbf{J})}{P}} \text{diag}(\mathbf{H}\mathbf{H}^H\mathbf{1})^{-1}. \quad (3.13)$$

Another possible optimization procedure, which can also be considered a variant of the matched filter in the multicast single-group context, has been investigated by previous works [NLTW98, Lop02, SL04]. It presents a different cost function and aims at maximizing the average user SNR. The solution is given by the eigenvector associated to the largest eigenvalue of $\mathbf{H}^H\mathbf{H}$, and its performance is also analyzed later in Section 3.5. The filter expression is given by

$$\mathbf{m}_{\text{AVG}} = \sqrt{\frac{P}{\sigma_s^2}} \text{eigv}(\mathbf{H}^H\mathbf{H}), \quad (3.14)$$

where the $\text{eigv}(\cdot)$ function returns the unit-norm principal eigenvector of a matrix. The receive filter can be written as

$$\mathbf{D}_{\text{AVG}} = \sqrt{\frac{\sigma_s^2}{P}} \text{diag}(\mathbf{H} \text{eigv}(\mathbf{H}^H\mathbf{H}))^{-1}. \quad (3.15)$$

3.4.2 Linear zero-forcing filter

The transmit linear Zero-Forcing (ZF) filter has been originally proposed for unicast scenarios with the purpose of removing interference among different data streams. Even though there is no interference in the single-group multicast scenario, the zero-forcing concept can still be applied. It has been shown in [Joh04] that the transmit zero-forcing filter minimizes the Mean Square Error (MSE) subject to certain constraints. For a multicast scenario, the MSE relates to the squared norm of the difference between the estimated symbol vector $\hat{\mathbf{s}}$ and the actual data symbol vector $\mathbf{s} = s\mathbf{1}$. The multicast zero-forcing optimization can be written as

$$\mathbf{m}_{\text{ZF}} = \underset{\mathbf{m}}{\text{argmin}} E\{\|\hat{\mathbf{s}} - s\mathbf{1}\|^2\}, \quad \text{subject to: } \begin{cases} \sigma_s^2 \|\mathbf{m}\|^2 \leq P \\ \hat{\mathbf{s}}|_{\mathbf{z}=\mathbf{0}} = s\mathbf{1} \end{cases}, \quad (3.16)$$

where the second constraint corresponds to the zero-forcing constraint, which means that in the absence of noise the estimated symbol vector $\hat{\mathbf{s}}$ must be equal to the actual symbol vector $s\mathbf{1}$. It is here assumed that the receive filter at each user is given by a scalar $\beta \in \mathbb{C}$, i.e., $\mathbf{D} = \beta\mathbf{I}$. The second constraint can be further expressed as

$$\hat{\mathbf{s}}|_{\mathbf{z}=\mathbf{0}} = s\mathbf{1} \implies \beta\mathbf{H}\mathbf{m}s = s\mathbf{1} \implies \beta\mathbf{H}\mathbf{m} = \mathbf{1}. \quad (3.17)$$

The MSE cost function, substituting $\hat{\mathbf{s}}$ and taking into account the zero-forcing constraint, is given by

$$\mathbb{E}\{|\beta\mathbf{H}\mathbf{m}s + \mathbf{z} - s\mathbf{1}|^2\} = \mathbb{E}\{|\mathbf{z}|^2\} = N\sigma_z^2. \quad (3.18)$$

The Lagrangian function can be expressed as

$$\mathbf{L}(\mathbf{m}, \mu, \boldsymbol{\nu}) = N\sigma_z^2 + \mu(\sigma_s^2 \mathbf{m}^H \mathbf{m} - P) + \boldsymbol{\nu}^T (\mathbf{1} - \beta\mathbf{H}\mathbf{m}), \quad (3.19)$$

where $\mu \in \mathbb{R}$ and $\boldsymbol{\nu} \in \mathbb{C}^N$ are Lagrange multipliers. The KKT conditions are:

$$\sigma_s^2 \|\mathbf{m}\|^2 \leq P, \quad \beta\mathbf{H}\mathbf{m} = \mathbf{1}, \quad \mu \geq 0, \quad \mu(P - \sigma_s^2 \mathbf{m}^H \mathbf{m}) = 0, \quad \frac{\partial \mathbf{L}(\mathbf{m}, \mu, \boldsymbol{\nu})}{\partial \mathbf{m}} = \mathbf{0}. \quad (3.20)$$

From the last condition it follows that

$$\begin{aligned} \frac{\partial \mathbf{L}(\mathbf{m}, \mu, \boldsymbol{\nu})}{\partial \mathbf{m}} &= \mu\sigma_s^2 \mathbf{m}^* - \beta\mathbf{H}^T \boldsymbol{\nu} = \mathbf{0}, \\ \mathbf{m} &= \frac{\beta}{\mu\sigma_s^2} \mathbf{H}^H \boldsymbol{\nu}^*. \end{aligned} \quad (3.21)$$

The Lagrange multiplier $\boldsymbol{\nu}$ can be determined by substituting (3.21) into the zero-forcing constraint:

$$\beta\mathbf{H}\mathbf{m} = \mathbf{1} \implies \frac{\beta^2}{\mu\sigma_s^2} \mathbf{H}\mathbf{H}^H \boldsymbol{\nu}^* = \mathbf{1} \implies \boldsymbol{\nu}^* = \frac{\mu\sigma_s^2}{\beta^2} (\mathbf{H}\mathbf{H}^H)^{-1} \mathbf{1}. \quad (3.22)$$

Substituting (3.22) back into (3.21) leads to

$$\mathbf{m} = \beta^{-1} \mathbf{H}^H (\mathbf{H}\mathbf{H}^H)^{-1} \mathbf{1}. \quad (3.23)$$

From (3.21) and the third KKT condition it follows that $\mu > 0$, since $\mu = 0$ results in an unfeasible beamforming vector. From the fourth KKT condition, a positive μ implies that the power constraint has to be an equality. The parameter β can be found by substituting (3.22) into the power constraint:

$$\sigma_s^2 \|\beta^{-1} \mathbf{H} (\mathbf{H}\mathbf{H}^H)^{-1} \mathbf{1}\|^2 = P \implies \beta = \sqrt{\frac{\sigma_s^2 \text{tr}((\mathbf{H}\mathbf{H}^H)^{-1} \mathbf{J})}{P}}, \quad (3.24)$$

where, in order to avoid multiple solutions, it has been assumed that β is positive real.

The zero-forcing solution is given by

$$\mathbf{m}_{\text{ZF}} = \sqrt{\frac{P}{\sigma_s^2 \text{tr}((\mathbf{H}\mathbf{H}^H)^{-1} \mathbf{J})}} \mathbf{H}^H (\mathbf{H}\mathbf{H}^H)^{-1} \mathbf{1}. \quad (3.25)$$

The substitution of (3.25) into the general receive filter expression (2.32) results in:

$$\mathbf{D}_{\text{ZF}} = \sqrt{\frac{\sigma_s^2 \text{tr}((\mathbf{H}\mathbf{H}^H)^{-1} \mathbf{J})}{P}} \mathbf{I}, \quad (3.26)$$

which confirms the assumption that the receive filter at each user is given by a scalar β . Note that, due to the channel inversion in (3.25), this algorithm has the limitation that the number of users cannot exceed the number of transmit antennas.

3.4.3 Linear minimum mean square error filter

The transmit linear Minimum Mean Square Error (MMSE) filter, as the name already indicates, aims at the minimization of the Mean Square Error (MSE). Different optimization procedures have been proposed for unicast scenarios. Some works have proposed an unconstrained optimization, such as [VJ98, BPD00], which has the drawback of not always providing feasible results, i.e., requiring more power than there is actually available. In [BF03], a constrained optimization with inequality constraint has been presented in order to overcome this problem. A more general result called Wiener filter, which considers the design of a scalar receive filter within the optimization procedure, has been proposed in [JBU04, Joh04]. In this section, an optimization procedure similar to the Wiener filter [JBU04, Joh04] is considered and the optimization problem is solved through Lagrange optimization for the multicast case.

It is assumed that each receiver implements a scalar filter $\beta \in \mathbb{C}$, and that β is part of the optimization. The problem is similar to that of zero-forcing, but without the zero-forcing constraint, and it is expressed as

$$\{\mathbf{m}_{\text{MMSE}}, \beta_{\text{MMSE}}\} = \underset{\{\mathbf{m}, \beta\}}{\operatorname{argmin}} \mathbb{E}\{|\hat{\mathbf{s}} - s\mathbf{1}|^2\}, \quad \text{subject to: } \sigma_s^2 \|\mathbf{m}\|^2 \leq P, \quad (3.27)$$

The MSE cost function can be further expressed as

$$\begin{aligned} \mathbb{E}\{|\hat{\mathbf{s}} - s\mathbf{1}|^2\} &= \mathbb{E}\{|\beta\mathbf{H}\mathbf{m} - \mathbf{1}\}s + \beta\mathbf{z}|^2\} \\ &= \sigma_s^2(\beta\mathbf{H}\mathbf{m} - \mathbf{1})^H(\beta\mathbf{H}\mathbf{m} - \mathbf{1}) + |\beta|^2 N\sigma_z^2 \\ &= \sigma_s^2|\beta|^2 \mathbf{m}^H \mathbf{H}^H \mathbf{H} \mathbf{m} - \sigma_s^2 \beta^* \mathbf{m}^H \mathbf{H}^H \mathbf{1} - \sigma_s^2 \beta \mathbf{1}^T \mathbf{H} \mathbf{m} + N\sigma_s^2 + |\beta|^2 N\sigma_z^2. \end{aligned} \quad (3.28)$$

The Lagrangian function is given by

$$\begin{aligned} \mathcal{L}(\mathbf{m}, \beta, \mu) &= \sigma_s^2|\beta|^2 \mathbf{m}^H \mathbf{H}^H \mathbf{H} \mathbf{m} - \sigma_s^2 \beta^* \mathbf{m}^H \mathbf{H}^H \mathbf{1} - \sigma_s^2 \beta \mathbf{1}^T \mathbf{H} \mathbf{m} \\ &\quad + N\sigma_s^2 + |\beta|^2 N\sigma_z^2 + \mu(\sigma_s^2 \mathbf{m}^H \mathbf{m} - P), \end{aligned} \quad (3.29)$$

where $\mu \in \mathbb{R}$ is a Lagrange multiplier. The KKT conditions are the following:

$$\sigma_s^2 \|\mathbf{m}\|^2 \leq P, \quad \mu \geq 0, \quad \mu(P - \sigma_s^2 \mathbf{m}^H \mathbf{m}) = 0, \quad \frac{\partial \mathcal{L}(\mathbf{m}, \beta, \mu)}{\partial \mathbf{m}} = \mathbf{0}, \quad \frac{\partial \mathcal{L}(\mathbf{m}, \beta, \mu)}{\partial \beta} = 0. \quad (3.30)$$

The partial derivatives with regard to \mathbf{m} and β , respectively, are given by

$$\frac{\partial \mathcal{L}(\mathbf{m}, \beta, \mu)}{\partial \mathbf{m}} = |\beta|^2 \mathbf{H}^H \mathbf{H} \mathbf{m} - \beta^* \mathbf{H}^H \mathbf{1} + \mu \mathbf{m} = \mathbf{0}, \quad (3.31)$$

and

$$\frac{\partial \mathcal{L}(\mathbf{m}, \beta, \mu)}{\partial \beta} = \sigma_s^2 \beta^* \mathbf{m}^H \mathbf{H}^H \mathbf{H} \mathbf{m} - \sigma_s^2 \mathbf{1}^T \mathbf{H} \mathbf{m} + \beta^* N\sigma_z^2 = 0. \quad (3.32)$$

The expression for the beamforming vector \mathbf{m} can be obtained from (3.31):

$$\mathbf{m} = \beta^{-1} \left(\mathbf{H}^H \mathbf{H} + \frac{\mu}{|\beta|^2} \mathbf{I} \right)^{-1} \mathbf{H}^H \mathbf{1} \quad (3.33)$$

The variable μ can be determined by first isolating β in (3.32)

$$\beta^* = \frac{\sigma_s^2 \mathbf{1}^T \mathbf{H} \mathbf{m}}{\sigma_s^2 |\mathbf{H} \mathbf{m}|^2 + N \sigma_z^2}, \quad (3.34)$$

and then substituting in (3.31) left-multiplied by \mathbf{m}^H

$$\begin{aligned} \mu \mathbf{m}^H \mathbf{m} &= \beta^* \mathbf{m}^H \mathbf{H}^H \mathbf{1} - |\beta|^2 \mathbf{m}^H \mathbf{H}^H \mathbf{H} \mathbf{m} \\ &= \frac{\sigma_s^2 |\mathbf{1}^T \mathbf{H} \mathbf{m}|^2}{\sigma_s^2 |\mathbf{H} \mathbf{m}|^2 + N \sigma_z^2} - \frac{\sigma_s^4 |\mathbf{1}^T \mathbf{H} \mathbf{m}|^2 |\mathbf{H} \mathbf{m}|^2}{(\sigma_s^2 |\mathbf{H} \mathbf{m}|^2 + N \sigma_z^2)^2} \\ &= \frac{N \sigma_s^2 \sigma_z^2 |\mathbf{1}^T \mathbf{H} \mathbf{m}|^2}{(\sigma_s^2 |\mathbf{H} \mathbf{m}|^2 + N \sigma_z^2)^2}. \end{aligned} \quad (3.35)$$

From (3.35), it can be concluded that $\mu > 0$. This implies, due to the third KKT condition, that the power constraint is an equality. When substituting $\mathbf{m}^H \mathbf{m} = P/\sigma_s^2$ and β in (3.35), μ is given by

$$\mu = \frac{N \sigma_z^2}{P} |\beta|^2. \quad (3.36)$$

This leads to the following expression for the transmit filter

$$\mathbf{m} = \beta^{-1} \left(\mathbf{H}^H \mathbf{H} + \frac{N \sigma_z^2}{P} \mathbf{I} \right)^{-1} \mathbf{H}^H \mathbf{1}, \quad (3.37)$$

where β can be found through the power constraint

$$\begin{aligned} \sigma_s^2 \mathbf{m}^H \mathbf{m} &= \sigma_s^2 \beta^{-2} \mathbf{1}^T \mathbf{H} \left(\mathbf{H}^H \mathbf{H} + \frac{N \sigma_z^2}{P} \mathbf{I} \right)^{-1} \left(\mathbf{H}^H \mathbf{H} + \frac{N \sigma_z^2}{P} \mathbf{I} \right)^{-1} \mathbf{H}^H \mathbf{1} = P \implies \\ \beta_{\text{MMSE}} &= \sqrt{\frac{\sigma_s^2 \text{tr} \left(\mathbf{H} \left(\mathbf{H}^H \mathbf{H} + \frac{N \sigma_z^2}{P} \mathbf{I} \right)^{-2} \mathbf{H}^H \mathbf{J} \right)}{P}}. \end{aligned} \quad (3.38)$$

In order to avoid multiple solutions, it has been assumed that β is positive real. The MMSE transmit and receive filters, respectively, are given by:

$$\mathbf{m}_{\text{MMSE}} = \sqrt{\frac{P}{\sigma_s^2 \text{tr} \left(\mathbf{H} \left(\mathbf{H}^H \mathbf{H} + \frac{N \sigma_z^2}{P} \mathbf{I} \right)^{-2} \mathbf{H}^H \mathbf{J} \right)}} \left(\mathbf{H}^H \mathbf{H} + \frac{N \sigma_z^2}{P} \mathbf{I} \right)^{-1} \mathbf{H}^H \mathbf{1}, \quad (3.39)$$

$$\mathbf{D}_{\text{MMSE}} = \sqrt{\frac{\sigma_s^2 \text{tr} \left(\mathbf{H} \left(\mathbf{H}^H \mathbf{H} + \frac{N \sigma_z^2}{P} \mathbf{I} \right)^{-2} \mathbf{H}^H \mathbf{J} \right)}{P}} \mathbf{I}. \quad (3.40)$$

Note that, since the receive filter has been determined as part of the optimization problem, the resulting receive filter expression in (3.40) is considered instead of the general receive filter in (2.32). Another important remark is that, similar to the zero-forcing algorithm, it is also required that the number of transmit antennas be greater than or equal to the number of receive antennas.

3.4.4 Tomlinson-Harashima precoding

The Tomlinson-Harashima Precoding (THP) was originally proposed in [Tom71, HM72] for mitigating intersymbol interference in the time domain. Later it was extended to the spatial domain [FWLH02], with the purpose of suppressing the interference among the multiple streams transmitted simultaneously by an antenna array. In this section, the THP concept is first presented for the unicast case, and then a discussion on how it can be applied to the single-group multicast case follows.

The THP algorithm introduces a feedback filter $\mathbf{F} \in \mathbb{C}^{N \times N}$ at the transmitter and a modulo operator at both transmitter and receivers [WFBVH04, Joh04]. The THP transmission chain is depicted in Fig. 3.1. Its linear representation [Joh04] is also shown in the figure, which is obtained by expressing the modulo operator as the addition of auxiliary signals $\mathbf{a} \in \mathbb{C}^N$ and $\hat{\mathbf{a}} \in \mathbb{C}^N$ at both transmitter and receiver, respectively.

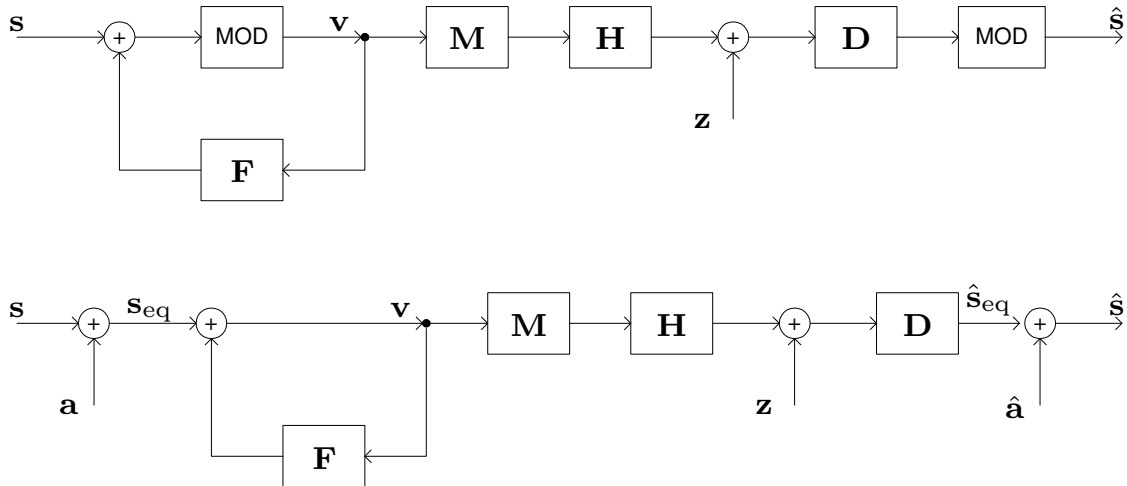


Figure 3.1. THP transmission chain and its linear representation.

The system equation is given by

$$\hat{\mathbf{s}}_{\text{eq}} = \mathbf{D}\mathbf{H}\mathbf{M}\mathbf{v} + \mathbf{D}\mathbf{z}, \quad (3.41\text{a})$$

$$\mathbf{v} = (\mathbf{I} - \mathbf{F})^{-1}\mathbf{s}_{\text{eq}}, \quad (3.41\text{b})$$

where $\mathbf{v} \in \mathbb{C}^N$ is the data vector after the feedback filter. The vectors $\mathbf{s}_{\text{eq}} \in \mathbb{C}^N$ and $\hat{\mathbf{s}}_{\text{eq}} \in \mathbb{C}^N$ correspond to the equivalent transmitted data vector and the estimated data vector, respectively, and are given by

$$\mathbf{s}_{\text{eq}} = \mathbf{s} + \mathbf{a}, \quad (3.42a)$$

$$\hat{\mathbf{s}}_{\text{eq}} = \hat{\mathbf{s}} - \hat{\mathbf{a}}. \quad (3.42b)$$

The optimization problem for the unicast zero-forcing THP filter is similar to that in (3.16), with the additional constraint that \mathbf{F} has to be spatially causal, i.e., it is a lower triangular matrix with zero main diagonal [WVH04, Joh04]. The solution of the unicast optimization, according to [Joh04], is

$$\mathbf{M}_{\text{THP}} = \sqrt{\frac{P}{\text{tr}(\mathbf{R}_v \mathbf{L}_d^{-2})}} \mathbf{H}^H \mathbf{L}^{H,-1} \mathbf{L}_d^{-1}, \quad (3.43a)$$

$$\mathbf{F} = \mathbf{I} - \mathbf{L} \mathbf{L}_d^{-1}, \quad (3.43b)$$

where $\mathbf{L} \in \mathbb{C}^{N \times N}$ is a lower triangular matrix that comes from the Cholesky factorization of the channel ($\mathbf{H}\mathbf{H}^H = \mathbf{L}\mathbf{L}^H$) [GL96], $(\cdot)^{X,Y}$ corresponds to the sequential application of matrix operators X and Y , $\mathbf{L}_d \in \mathbb{R}^{N \times N}$ is a diagonal matrix containing the elements of the main diagonal of \mathbf{L} , and $\mathbf{R}_v \in \mathbb{C}^{N \times N}$ is the covariance matrix of the precoded data vector \mathbf{v} . The receive filter, according to [Joh04], is given by

$$\mathbf{D}_{\text{THP}} = \sqrt{\frac{\text{tr}(\mathbf{R}_v \mathbf{L}_d^{-2})}{P}} \mathbf{I}. \quad (3.44)$$

Note that it is usually assumed that the elements of vector \mathbf{v} are uniformly distributed within the area of the complex plane delimited by the τ parameter [Joh04], which is a parameter employed by the modulo operator and that depends on the modulation alphabet. This assumption leads to a variance $\sigma_v^2 = \tau^2/6$. Assuming that the elements of \mathbf{v} are uncorrelated, then the covariance matrix is given by $\mathbf{R}_v = \sigma_v^2 \mathbf{I}$

In the case of multicast, even though the same symbol is transmitted to all users, the data vector \mathbf{v} contains different elements, due to the different channel profiles perceived by each user. Therefore, the THP procedure presented here is the same for both unicast and multicast. Similarly to zero-forcing, the THP algorithm is subject to the limitation that the number of users cannot be larger than the number of transmit antennas.

3.4.5 Switched fixed beams

Besides the fully-adaptive algorithms presented in the previous sections, another option for deploying antenna arrays in cellular networks is the use of Switched Fixed Beams

(SFB). They represent a low-cost solution which can be implemented, among other methods, through a Butler matrix [BL61]. The fixed set of weight vectors is designed so that beams spanning the whole cell area are made available.

In the case of unicast users, the beam providing the highest SNR, which can be identified through feedback on the uplink, is selected. For multicast, however, all users within the group need to be taken into account. The solution herein considered is to activate all those beams which are currently being requested by the users. The result is then a normalized linear combination of the selected weight vectors.

Let \mathcal{B} represent the set of indices of the available beams and $\mathcal{B}_g \subset \mathcal{B}$ the set of indices corresponding to the beams requested by the group of users. The resulting beamforming vector can be expressed as

$$\mathbf{m}_{\text{SFB}} = \sqrt{\frac{P}{\sigma_s^2} \left\| \sum_{i \in \mathcal{B}_g} \mathbf{w}_i \right\|^{-2}} \sum_{i \in \mathcal{B}_g} \mathbf{w}_i, \quad (3.45)$$

where $\mathbf{w}_i \in \mathbb{C}^M$ denotes the i^{th} beamforming vector of the set of fixed beamformers. The receive filter is given by

$$\mathbf{D}_{\text{SFB}} = \sqrt{\frac{\sigma_s^2}{P} \left\| \sum_{i \in \mathcal{B}_g} \mathbf{w}_i \right\|^2} \text{diag} \left(\mathbf{H} \sum_{i \in \mathcal{B}_g} \mathbf{w}_i \right)^{-1}. \quad (3.46)$$

Fig. 3.2 illustrates the concept of switched fixed beams. The example shows four beams covering the area of a hexagonal cell sector. The users depicted with an X request the two central beams, which are combined according to (3.45) in order to generate the resulting beam. The right-hand side of Fig. 3.2 shows the antenna pattern of each beam (dashed), as well as the combined pattern of the two activated beams (solid).

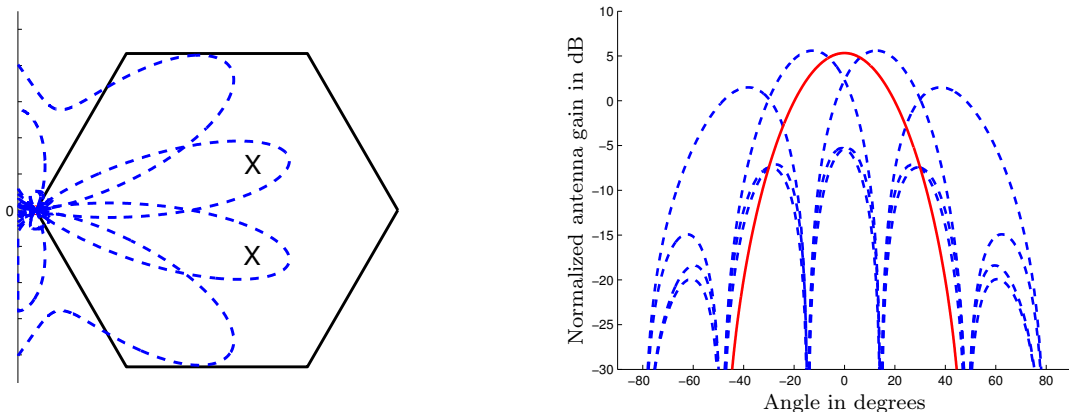


Figure 3.2. Illustration of 4 fixed switched beams and beam selection.

3.4.6 User-selective matched filter

In this section, a heuristic algorithm called User-Selective Matched Filter (USMF) is proposed, which does not claim to provide the optimum for (3.1), but which improves the performance of the matched filter in terms of fairness among the multicast users. By fairness it is here meant that the users should perceive similar quality levels, i.e., max-min fairness [SPC05]. The USMF aims at achieving a trade-off between the provision of user fairness and the low complexity of the matched filter.

If it were assumed that there is a point-to-point connection for each user n , the ideal solution in the sense of maximizing the SNR would be to employ a transmit matched filter, i.e., $\mathbf{m} = \mathbf{h}_n^H$. As it has been previously shown, the matched filter for the multicast case is given by $\mathbf{H}^H \mathbf{1}$. This results in a beamforming vector which corresponds to the sum of all individual single-user matched filter vectors, which are stacked within matrix \mathbf{H}^H . The idea of USMF is, instead of combining all of these vectors, to take a subset of them, such that the resulting weight vector be the one that maximizes the worst-user SNR. This can be done by introducing a diagonal selection matrix that postmultiplies \mathbf{H}^H . The filter expression may be written as

$$\mathbf{m}_{\text{USMF}} = \sqrt{\frac{P}{\sigma_s^2 \text{tr}(\mathbf{C}^T \mathbf{H} \mathbf{H}^H \mathbf{C} \mathbf{J})}} \mathbf{H}^H \mathbf{C} \mathbf{1}, \quad (3.47)$$

where $\mathbf{C} \in \mathbb{Z}^{N \times N}$ is a non-zero diagonal matrix, with elements $c_{i,i} \in \{0, 1\}$, for $i = 1, \dots, N$. Note that the matched filter of Section 3.4.1 corresponds to a special case of USMF when $\mathbf{C} = \mathbf{I}$. The receive filter expression is given by

$$\mathbf{D}_{\text{USMF}} = \sqrt{\frac{\sigma_s^2 \text{tr}(\mathbf{C}^T \mathbf{H} \mathbf{H}^H \mathbf{C} \mathbf{J})}{P}} \text{diag}(\mathbf{H} \mathbf{H}^H \mathbf{C} \mathbf{1})^{-1}. \quad (3.48)$$

Since there are N users, and the diagonal elements of \mathbf{C} are restricted to binary values, there exists a total of $2^N - 1$ possible matrices. Due to this exponential complexity, the exhaustive search procedure of testing each possible matrix and selecting the one which maximizes the minimum SNR is only feasible for small group sizes. For larger groups a more efficient methodology is required. Next, a correlation-based algorithm for determining \mathbf{C} is proposed.

Let $\rho_{i,j} \in \mathbb{R}$ denote the correlation between the vector channels of users i and j , which is given by the normalized scalar product [FN96]:

$$\rho_{i,j} = \frac{|\mathbf{h}_i \mathbf{h}_j^H|}{\|\mathbf{h}_i\| \|\mathbf{h}_j\|}, \quad (3.49)$$

for which $\rho_{i,i} = 1$ and $\rho_{i,j} = \rho_{j,i}$. All pairs of channels are sorted in their decreasing order of correlation and it is assumed initially that $\mathbf{C} = \mathbf{I}$. For each pair of channels $\{i, j\}$, the elements $\{c_{ii}, c_{jj}\}$ are iteratively updated. They either maintain the same values or one of them is set to zero. Among these possibilities, the one resulting in the highest worst-user SNR within the multicast group is selected. The algorithm is illustrated in Table 3.1, for which $\gamma_{\min}(\mathbf{C}) \in \mathbb{R}$ represents the worst-user SNR:

$$\gamma_{\min}(\mathbf{C}) = \min(\text{diag}(\mathbf{H}\mathbf{m}\mathbf{m}^H\mathbf{H}^H)) = \frac{1}{\|\mathbf{H}^H\mathbf{C}\mathbf{1}\|^2} \min(\text{diag}(\mathbf{H}\mathbf{H}^H\mathbf{C}\mathbf{J}\mathbf{C}\mathbf{H}\mathbf{H}^H)). \quad (3.50)$$

The number of times $\gamma_{\min}(\mathbf{C})$ is calculated is reduced from $2^N - 1$ in case of the exhaustive search to at most $N^2 - N + 1$ in case of the correlation-based algorithm.

Table 3.1. Pseudo-code of the correlation-based USMF algorithm.

```

Initialize  $\mathbf{C}^* \leftarrow \mathbf{I}$  and  $\gamma^* \leftarrow \gamma_{\min}(\mathbf{I})$ 
Calculate  $\rho_{i,j} \forall i, j \mid i < j$ 
Sort the pairs  $\{i, j\}$  in the decreasing order of  $\rho_{i,j}$ 
For each pair  $\{i, j\}$  do:
    Set  $\gamma^{(1)} \leftarrow 0$  and  $\gamma^{(2)} \leftarrow 0$ 
    If  $c_{i,i}^* \neq 0$ , set  $\mathbf{C}^{(1)} \leftarrow \mathbf{C}^*$ ,  $c_{i,i}^{(1)} \leftarrow 0$ , and  $\gamma^{(1)} \leftarrow \gamma_{\min}(\mathbf{C}^{(1)})$ 
    If  $c_{j,j}^* \neq 0$ , set  $\mathbf{C}^{(2)} \leftarrow \mathbf{C}^*$ ,  $c_{j,j}^{(2)} \leftarrow 0$ , and  $\gamma^{(2)} \leftarrow \gamma_{\min}(\mathbf{C}^{(2)})$ 
    If  $\max(\gamma^{(1)}, \gamma^{(2)}, \gamma^*) = \gamma^{(1)}$ 
        Set  $\mathbf{C}^* \leftarrow \mathbf{C}^{(1)}$  and  $\gamma^* \leftarrow \gamma^{(1)}$ 
    else if  $\max(\gamma^{(1)}, \gamma^{(2)}, \gamma^*) = \gamma^{(2)}$ 
        Set  $\mathbf{C}^* \leftarrow \mathbf{C}^{(2)}$  and  $\gamma^* \leftarrow \gamma^{(2)}$ 
    else
         $\mathbf{C}^*$  and  $\gamma^*$  remain unaltered
    end if
end loop
Calculate  $\mathbf{m}_{\text{USMF}}$  for  $\mathbf{C}^*$  according to (3.47)

```

3.5 Performance and complexity analysis

3.5.1 Analysis assumptions

The scenario considered for the performance evaluation of the algorithms from Section 3.4 consists of a single cell equipped with an L -element uniform linear antenna array

and N single antenna mobile terminals belonging to the same multicast group. The cell area is assumed to be hexagonal and the base station is located at the cell corner, representing a sector cell. The radio link between base station and mobile stations takes into account the effect of fast fading as well as the distance-based path-loss attenuation.

The implemented fast fading model [FLFV00, PNG03] regards both Line-Of-Sight (LOS) and Non-Line-Of-Sight (NLOS) components, and can be written as

$$\mathbf{H} = \sqrt{\kappa/(1+\kappa)} \bar{\mathbf{H}} + \sqrt{1/(1+\kappa)} \check{\mathbf{H}}, \quad (3.51)$$

where $\kappa \in \mathbb{R}$ is the Rician factor which determines the ratio of deterministic-to-scattered power, $\check{\mathbf{H}} \in \mathbb{C}^{N \times L}$ is composed of zero mean circularly symmetric complex Gaussian random variables with unit variance, and $\bar{\mathbf{H}} \in \mathbb{C}^{N \times L}$ models the LOS component, which has each row $\bar{\mathbf{h}}_n$ given by

$$\bar{\mathbf{h}}_n = [1, e^{j2\pi\delta\cos(\theta)}, \dots, e^{j2\pi\delta(L-1)\cos(\theta)}], \quad (3.52)$$

where δ is the antenna spacing in wavelengths and θ is the angular direction of the user, which is assumed to be uniformly distributed within $[0, 2\pi/3]$ (base station at the corner).

A simple distance-based path-loss model with exponent $\alpha = 3.5$ is considered. The model assumes that the distance r_n between each user and the base station is much larger than the antenna spacing. For this reason only one path-loss value is associated to each radio link n . The channel matrix including the effects of path-loss is given by

$$\mathbf{H}_{\text{PL}} = \text{diag}(\mathbf{r})^{-\alpha/2} \mathbf{H}, \quad (3.53)$$

where the vector $\mathbf{r} \in \mathbb{R}^N$ contains the distances of all users to the base station.

The following two different user scenarios are considered:

- Scenario S1: The users are assumed to be at a same distance from the base station. For this scenario, it has been chosen that $\mathbf{r} = \mathbf{1}$, which leads to $\mathbf{H}_{\text{PL}} = \mathbf{H}$. This particular \mathbf{r} was chosen in order to match the situation in which no path-loss is considered. The analysis of this scenario is mainly motivated by the fact that several other works found in the literature on multicast beamforming, such as [ZSV04, SDL06, HSJ⁺07], also disregard the path-loss in their evaluations. In the case of unicast, the usual argument for disregarding the path-loss is that the different path-loss of the users could be compensated by power control. In the case of multicast, however, this argument does not directly apply, since the power assigned to the multicast transmission affects all users within the multicast group. This scenario may correspond to a situation in which the users are close to each other, such as in the case of localized multicast services.

- Scenario S2: The users are assumed to be uniformly distributed over the whole cell area. For this scenario, the area over which the users are distributed is a hexagon with a distance of 1.5 between the base station at one corner and the cell border at the other. This distance of 1.5 has been chosen in order to provide results within the same range as those for scenario S1. This specific value leads, in average, to a situation in which roughly half of the channel realizations present users with $r_n < 1$, and the other half with $r_n > 1$. Note that the absolute value of the cell border distance is not expected to have a significant impact on the relative performance of the algorithms.

The following algorithms of Section 3.4 are considered in the simulations: the Matched Filter (MF), the algorithm that maximizes the average SNR (MaxAvg), the Zero-Forcing (ZF), the Minimum Mean Square Error (MMSE), the Tomlinson-Harashima Precoding (THP), the Switched Fixed Beams (SFB), and the User-Selective Matched Filter (USMF). Additionally, for comparison purposes, the algorithm based on Semi-Definite Relaxation (SDR) [SD04,SDL06] is considered as well.

The THP algorithm is implemented taking into account the suboptimal ordering procedure proposed in [Joh04]. The SDR algorithm makes use of the SeDuMi optimization library [Stu99] and considers a number of 1000 iterations for the *randB* randomization procedure [SDL06], which is employed when the solution has rank higher than 1.

3.5.2 Bit error rate analysis

In this section, the uncoded BER of the beamforming algorithms is analyzed and compared. The BER is an adequate measure for comparison, since it is strongly influenced by the users in bad conditions, thus reflecting in the results which algorithms better equilibrate the quality among the users. A four-antenna base station ($L = 4$) and a multicast group composed of four users ($N = 4$) are considered. The simulations take into account both QPSK and 16-QAM modulation schemes, and the constellation is normalized such that the average symbol power is $\sigma_s^2 = 1$. The total transmit power is assumed to be equal to the symbol power, i.e., $P = \sigma_s^2 = 1$. The τ parameter of THP, presented in Section 3.4.4, is set to $2\sqrt{2}$ for QPSK and $8/\sqrt{10}$ for 16-QAM [Joh04].

For each channel realization i , $S = 100$ symbols are transmitted and the average bit error rate \overline{BER}_i is calculated as follows:

$$\overline{BER}_i = \frac{E}{NS \log_2(M_o)}, \quad (3.54)$$

where E denotes the number of bit errors and M_o the modulation order. Note that, even though only S symbols are transmitted, a total of NS symbols are received by the users, since this is a multicast scenario. The numerator of (3.54) corresponds to the total number of bits erroneously detected by the receivers, while the denominator represents the total number of received bits, i.e., the total number of received symbols NS times the number of bits per symbol, which is given by $\log_2(M_o)$. In order to achieve statistically accurate results, the total number of channel realizations is adjusted individually for each simulated point, such that at least 100 errors are measured in average by each simulation [JBS00].

Figs. 3.3 and 3.4 show the average BER performance of the different algorithms for a QPSK modulation scheme in NLOS and LOS scenarios, respectively. Scenario S1 is considered, i.e., the users are assumed to be at the same distance from the base station. The BER is depicted as a function of the E_s/N_0 , which represents the ratio of the symbol power to the spectral noise density.

In Fig. 3.3, the worst performance is achieved by the ZF algorithm, which is due to the fact that it spends a considerable amount of energy trying to suppress interference among the data streams, which in the case of multicast is not necessary. The MMSE algorithm, as expected, outperforms ZF, since it introduces a regularization factor for avoiding the inversion of ill-conditioned matrices. The THP algorithm, similarly to the unicast case in [Joh04], presents better results for high E_s/N_0 values, outperforming both ZF and MMSE, which is mainly due to its non-linearity. It should be noticed that these three algorithms – ZF, MMSE, and THP – achieve the worst performance in comparison to the other algorithms due to the channel inversion implemented by them. The SFB algorithm comes next, but it does not perform particularly well, since it employs fixed beams in a scenario without LOS component. Both the MF and Max-Avg algorithms outperform SFB, since they are not constrained to fixed beamforming vectors. The USMF algorithm presents a significant performance gain over the previous algorithms, requiring roughly 10dB less E_b/N_0 than MaxAvg for providing a BER of 10^{-3} , which is due to the fact that it was specifically designed for the multicast case. The SDR algorithm outperforms USMF by approximately 3dB for a BER of 10^{-3} , but at the cost of a much higher computational complexity, as it will be shown later by the complexity analysis.

When we compare the results obtained for an NLOS scenario in Fig. 3.3 to those obtained for a purely LOS situation in Fig. 3.4, it becomes clear that the channel profile has a considerable impact on the performance of the algorithms.

In Fig. 3.4, the worst performance is achieved by the MaxAvg algorithm. Its poor performance is due to the fact that the objective of the algorithm is to maximize the

average and not the minimum SNR. Differently from the NLOS channel, the eigen-decomposition of $\mathbf{H}^H\mathbf{H}$ for the LOS channel results in a large ratio of the largest to smallest singular values (ill-conditioned matrix), which means that more energy is concentrated on the principal eigenmode. This has a positive effect on the average, but leads to a more uneven energy distribution within the group, i.e., some users achieve very high SNR at the expense of others with very low quality. The THP and ZF algorithms come next, with ZF presenting slightly lower bit error rates. The similar shapes of ZF and THP, as well as the degradation of THP with regard to ZF, are a consequence of the inversion of ill-conditioned channel matrices. The further ordering of the algorithms, in terms of increasing performance, is given by: SFB, MF, MMSE, USMF, and SDR. Some explanations are given in the following.

The USMF gets much closer to SDR, with an E_s/N_0 difference of less than 1dB, and the MF and SFB have their performance greatly improved in the presence of LOS. The increased spatial correlation of this scenario has a positive effect on USMF, which can be explained due to the fact that it increases the probability that the rows of \mathbf{H}^H be correlated, resulting in more zero entries within \mathbf{C} of (3.47), which brings it closer to the single-user beamforming case. Analogously, this higher correlation has a positive effect on MF as well, which was previously shown in Section 3.4.6 to be a particular case of USMF. For SFB the reason is similar, with an increased probability that less beams be requested by the users, and therefore allowing more energy to be concentrated in certain directions. The performance of MMSE in the LOS scenario is much better than in the NLOS scenario, approaching that of USMF and surpassing both the MF and SFB algorithms. It is known that the regularization factor introduced by MMSE improves the energy efficiency in comparison to ZF, and in the LOS scenario this regularization has a larger impact, which is due to the ill-conditioned $\mathbf{H}^H\mathbf{H}$ matrix. For this reason, ZF ends up requiring a large amount of energy to diagonalize the channel, whereas the MMSE regularization results in a much better conditioned matrix. It should be noticed that channel inversion methods, such as MMSE and ZF, provide roughly the same quality to all users, which is not the case of the MF and SFB algorithms. Usually this balancing effect comes at the cost of a high energy inefficiency, as shown for the NLOS case. For the LOS case, however, the regularization of MMSE largely compensates this inefficiency, and therefore it outperforms both MF and SFB.

It should be mentioned that the results obtained with the THP algorithm for the LOS scenario correspond to an ideal case, in which the precoding matrix is normalized at each symbol period, instead of on a per-frame basis. The reason for this procedure is that the assumption that the precoded THP symbols are uniformly distributed over the area of the complex plane bounded by the τ parameter is no longer valid for the LOS scenario. More details on this subject are provided in Appendix A.1.

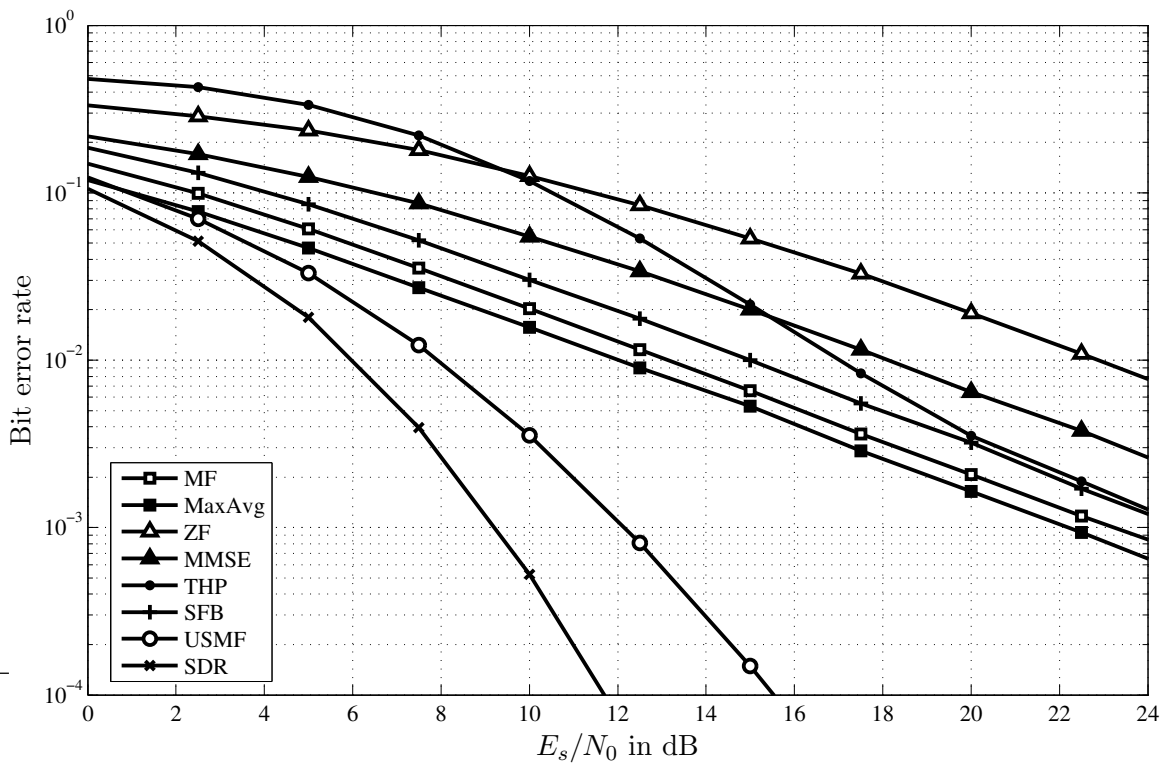


Figure 3.3. BER performance of multicast beamforming: QPSK, NLOS, and S1.

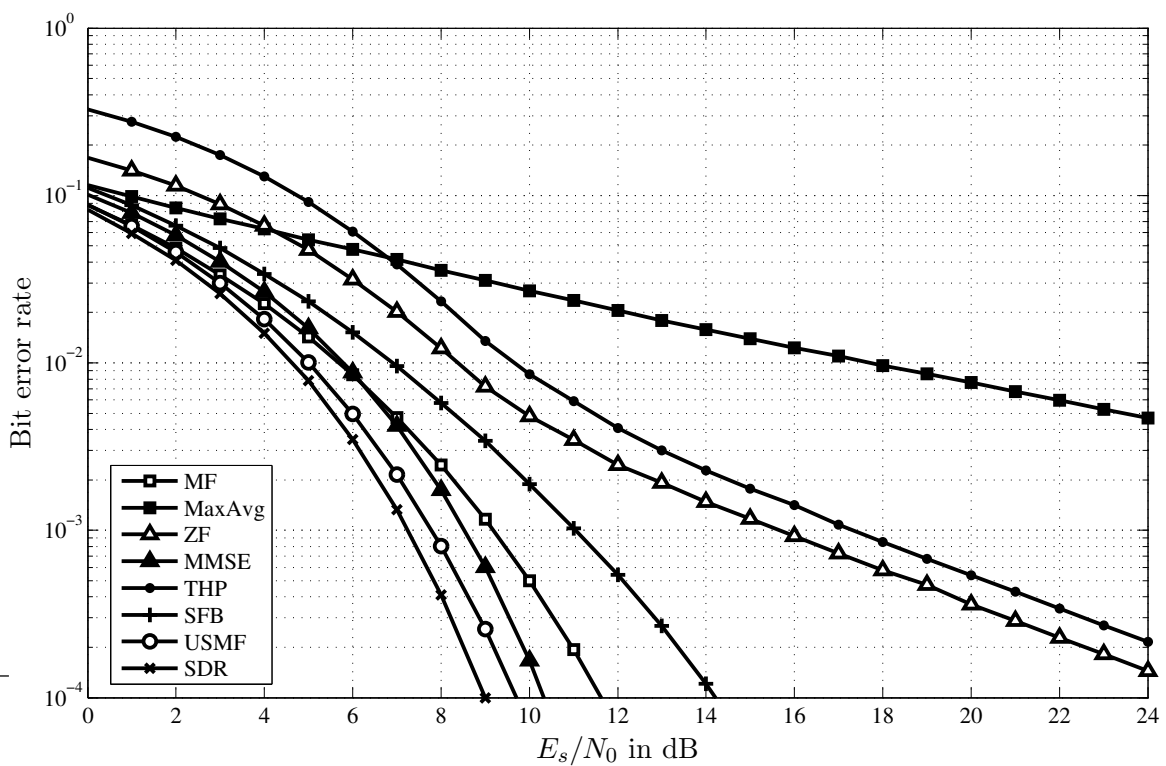


Figure 3.4. BER performance of multicast beamforming: QPSK, LOS, and S1.

Figs. 3.5 and 3.6 present, respectively, the BER results for a 16-QAM modulation scheme in both NLOS and LOS scenarios. Since a larger amount of bits is transmitted per symbol, this modulation scheme becomes more efficient than QPSK only for larger SNR values. For this reason the curves are all shifted to the right. Nevertheless, the relative performance among the algorithms is practically the same as that of the QPSK modulation scheme, for both NLOS and LOS scenarios.

In order to assess the performance impact of having users with difference path-gains, scenario S2 has been simulated considering QPSK modulation and the NLOS channel model. The results are shown in Fig. 3.7, and it is seen that a relative behavior among the algorithms similar to scenario S1 is achieved. The main differences compared to S1 are: the THP algorithm presents the third best performance for large SNR values; the MF and MaxAvg algorithms achieve approximately the same results, with their curves overlapping in Fig. 3.7, and are both outperformed by the SFB algorithm. The first difference is due to the fact that the modulo-based non-linear THP algorithm can deal better with large differences among the channel gains of the different users than the other linear algorithms, with the exception of those which are specifically designed for multicast. Regarding the overlapping of MF and MaxAvg, it happens since MF is based on the sum of the individual channel vectors of the users, and when there is a large difference in terms of channel gains, practically only the strongest channels will be representative, similarly to the MaxAvg, which concentrates the energy on the dominant eigenvector. The SFB algorithm, which uses predefined weight vectors, is not so strongly biased towards the dominant users, therefore achieving better results than MF and MaxAvg.

Table 3.2 presents a summary of the algorithms' performance for the considered modulation schemes and channel profiles for scenario S1. The results correspond to the E_s/N_0 required in order to achieve an uncoded BER of 10^{-3} . It should be noticed that, in the case of other system configurations, e.g. considering the use of coding schemes, different BER requirements, among others, the difference among the algorithms may be reduced. Moreover, the BER performance is not the only decisive factor for choosing the most adequate algorithm. The computational complexity, which will be discussed later in this chapter, must also be taken into account.

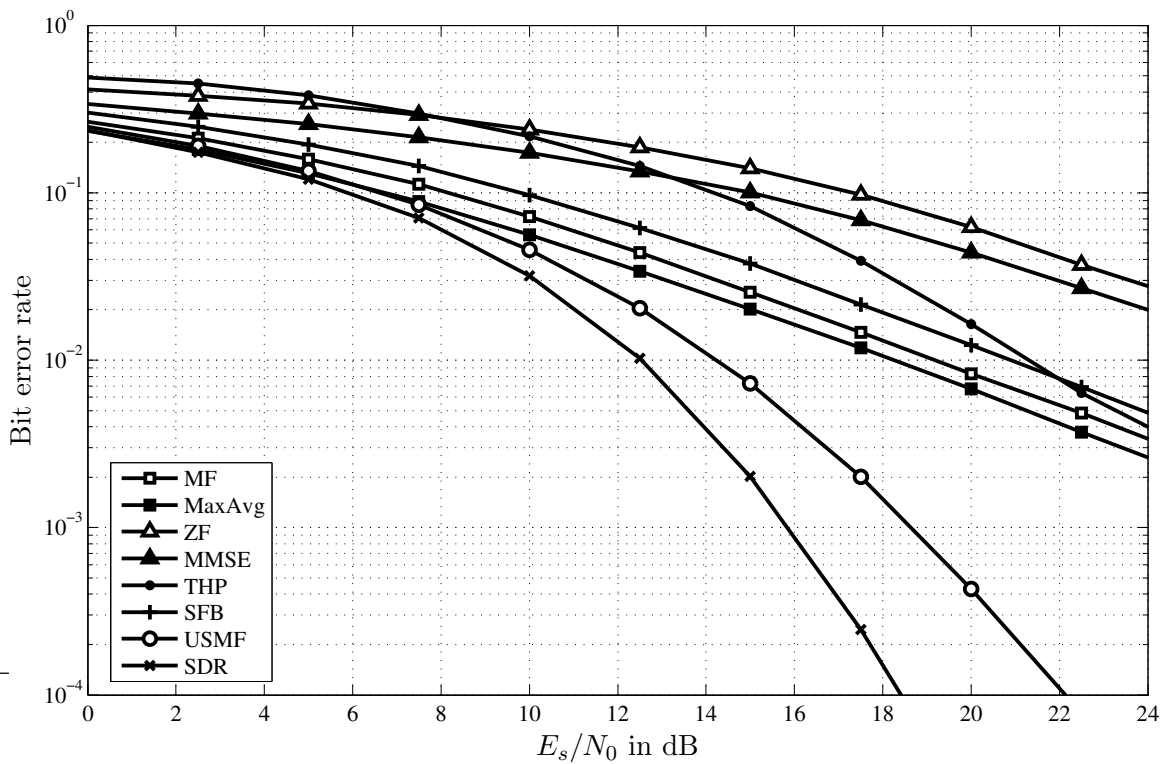


Figure 3.5. BER performance of multicast beamforming: 16-QAM, NLOS, and S1.

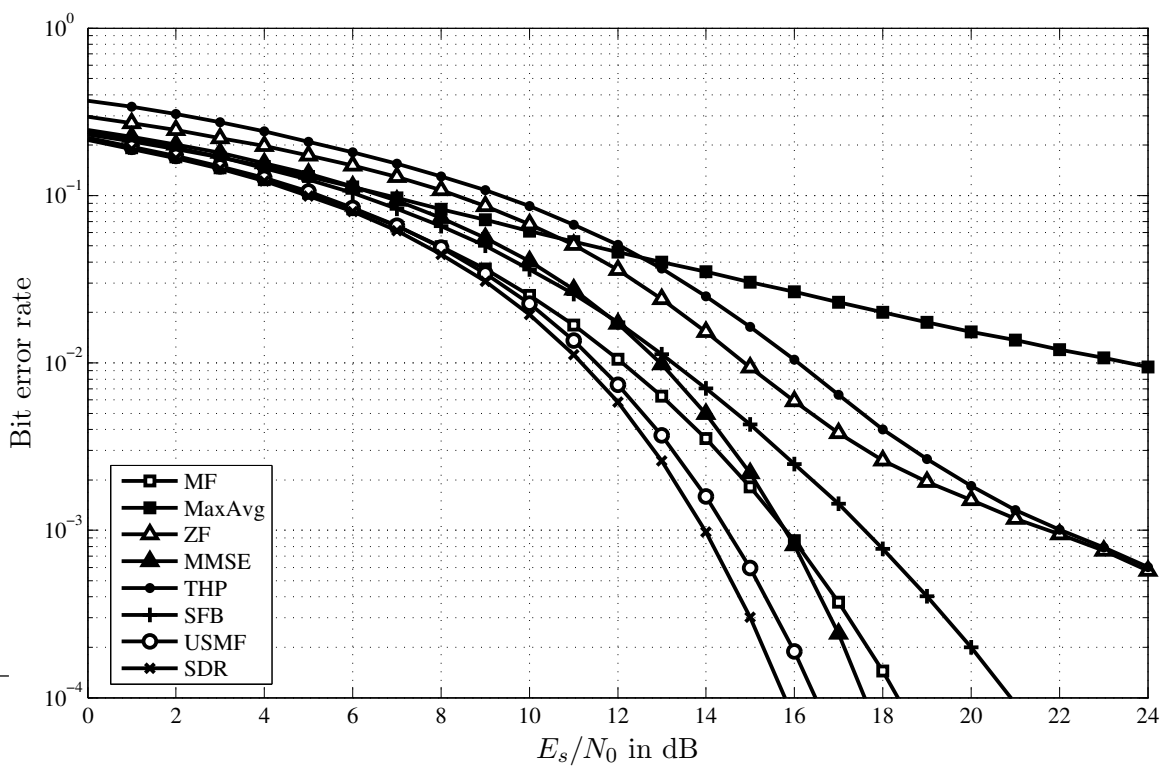


Figure 3.6. BER performance of multicast beamforming: 16-QAM, LOS, and S1.

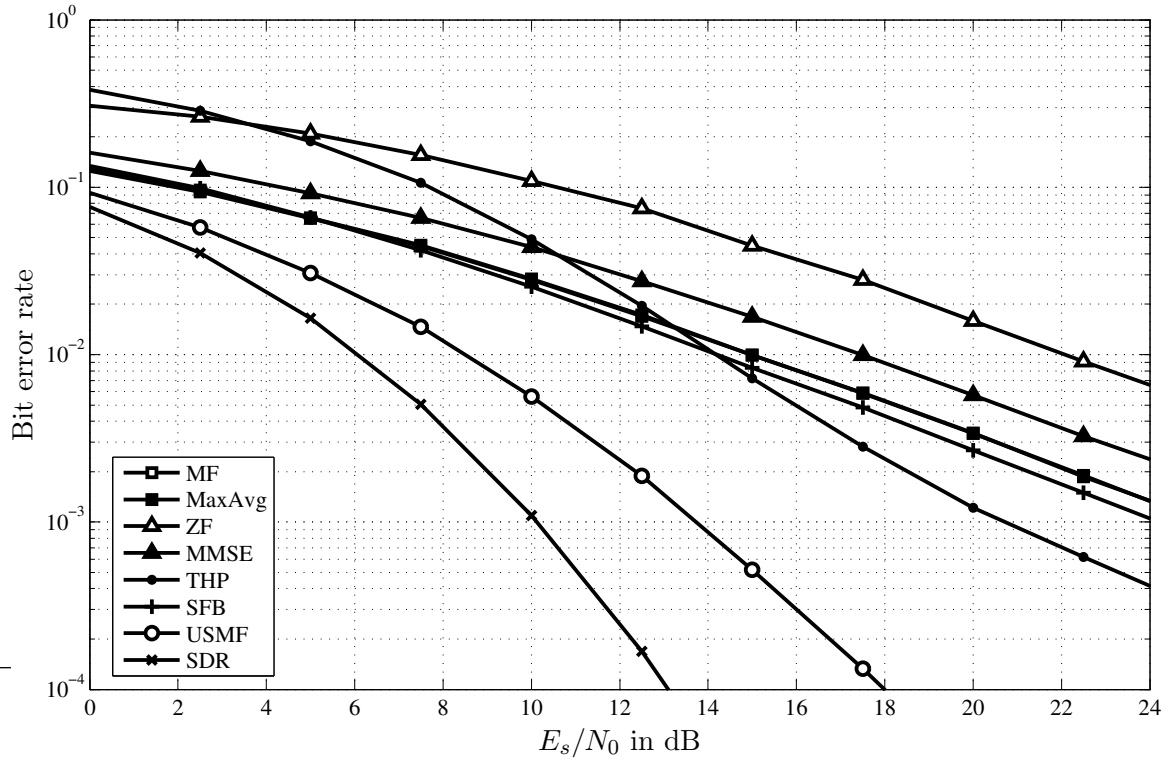


Figure 3.7. BER performance of multicast beamforming: QPSK, NLOS, and S2.

Table 3.2. E_s/N_0 in dB required in order to provide an uncoded BER of 10^{-3} .

	QPSK NLOS	QPSK LOS	16-QAM NLOS	16-QAM LOS
MF	23.2	9.2	29.0	15.8
MaxAvg	22.2	> 35.0	27.9	> 35.0
ZF	32.3	15.5	> 35.0	21.4
MMSE	28.3	8.5	> 35.0	15.8
THP	24.8	17.2	28.7	22.1
SFB	24.8	11.0	30.8	17.6
USMF	12.1	7.8	18.6	14.5
SDR	9.2	7.2	15.8	14.0

3.5.3 Worst-user SNR analysis

In this section, the impact of the multicast group size on the worst-user SNR of the algorithms is analyzed. This investigation is motivated by the fact that, in practice, the multicast group may be composed of a number N of users much larger than the number L of transmit antennas at the base station, differently from the previous section, in which it was assumed that $N = L$. Since the ZF, MMSE, and THP algorithms have the

limitation that the number of users cannot exceed the number of transmit antennas, they are not considered within this section. The following algorithms are taken into account: MF, MaxAvg, SFB, USMF, and SDR.

The investigation considers an E_s/N_0 of 10dB, 4 and 8 transmit antennas at the base station, and scenario S1. The fixed 10dB value was chosen so as to represent a mid-range E_s/N_0 , which might often be verified in practice. The results are presented in terms of the worst-user SNR. For each channel realization, the SNR is measured at each user terminal of the multicast group, and the minimum among these measures is taken as the worst-user SNR metric, which is then averaged over the number of channel realizations. Since only SNR values are considered, and no bit errors are accounted for, the results are valid irrespective of the modulation scheme. It should be noticed that, due to the array gain, the SNR measured at the user terminals may achieve values above 10dB. More specifically, array gains in the order of 6dB and 9dB are expected for the 4 and 8-antenna scenarios, respectively.

Figs. 3.8 and 3.9 depict the average worst-user SNR as a function of the number of users within the multicast group for the NLOS and LOS scenarios, respectively, considering different algorithms and a 4-antenna array. For all algorithms it can be seen that the more users there are within a group, the lower the SNR that can be guaranteed. Moreover, the relative behavior among the algorithms, for both NLOS and LOS scenarios, is the same as that verified through the BER evaluation, which will be discussed in the following.

In Fig. 3.8, it can be seen that SDR presents the best results. The USMF algorithm is the one that best approaches the SDR performance. The other three algorithms, the MaxAvg, MF, and SFB, present worse results, with the average worst-user SNR falling below 0dB for large group sizes. The simulation results for the LOS scenario, which are shown in Fig. 3.9, indicate that the absolute performance of all algorithms improves, with the exception of MaxAvg, which suffers a considerable performance degradation. The reasons for the relative performance of the algorithms are the same as those discussed in the previous section.

The performance of USMF within the LOS scenario gets closer to that of SDR as the number of users increases. For large group sizes, USMF even outperforms SDR. Note that the SDR algorithm only achieves the optimal solution for the cases in which a rank 1 matrix is achieved at the end of the numerical optimization. Since the probability of achieving rank 1 matrices decreases for large group sizes, the SDR performance is degraded, relying on randomization methods for improving the obtained solution. It should also be mentioned that, according to [KSL07], it is always possible to find

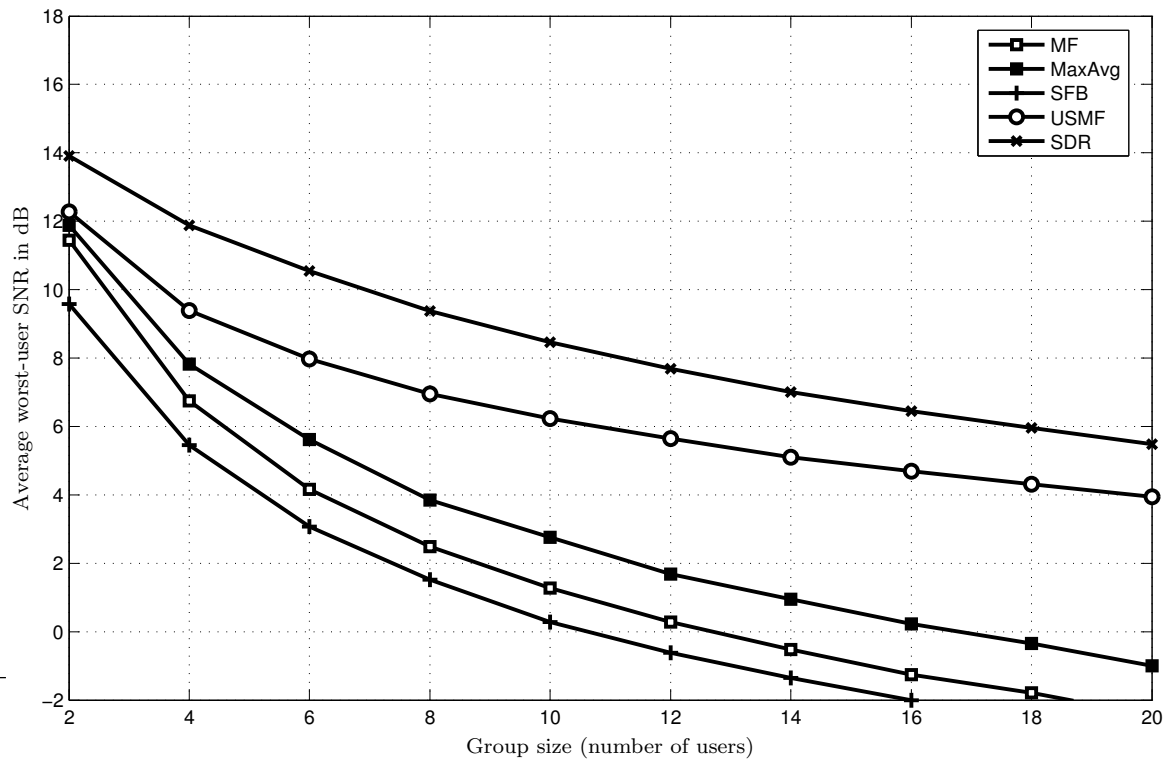


Figure 3.8. Average worst-user SNR for NLOS, $L = 4$, and $E_s/N_0=10\text{dB}$.

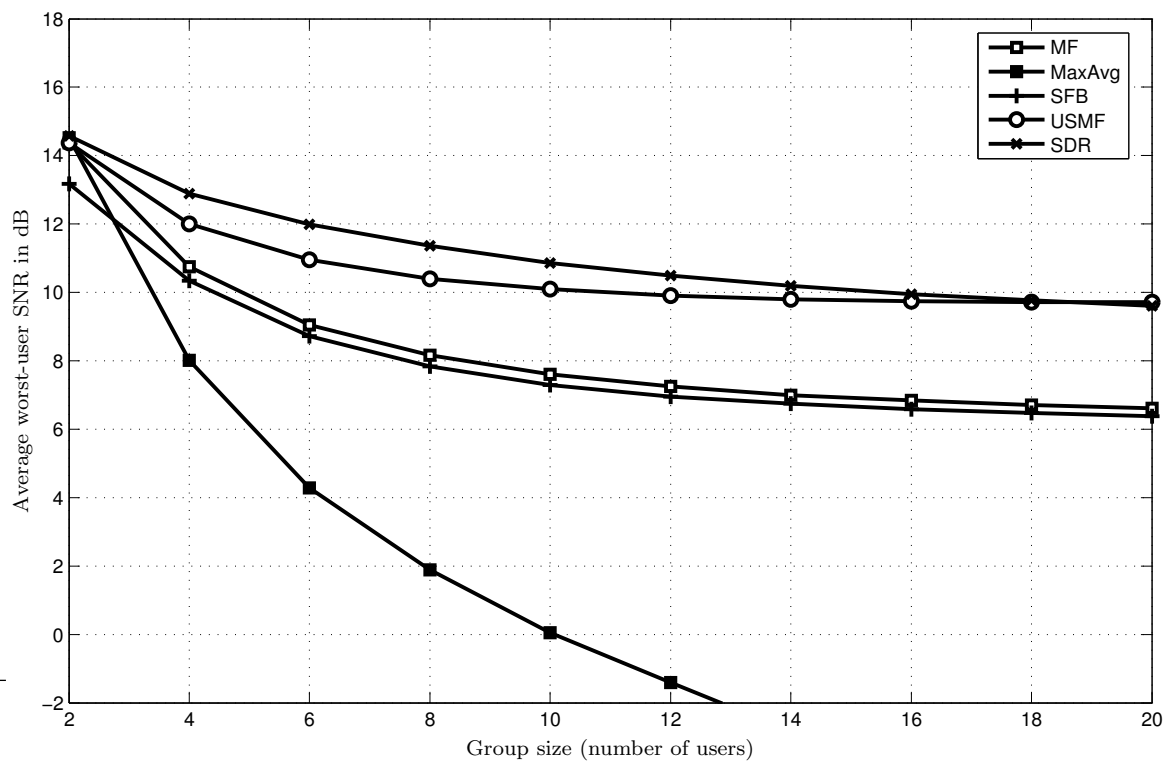


Figure 3.9. Average worst-user SNR for LOS, $L = 4$, and $E_s/N_0=10\text{dB}$.

a rank 1 solution for LOS channels (also known as Vandermonde channels), but the SDR method does not necessarily deliver it. The rank 1 solution can be achieved by postprocessing through spectral factorization, which increases the complexity and has not been considered in the simulations.

Figs. 3.10 and 3.11 also present results for the NLOS and LOS scenarios, respectively, but now considering an 8-antenna array. The same conclusions as those for the 4-antenna case can be drawn from these results. It can also be noticed that the relative performance of USMF with regard to SDR is improved. The reason for this is that the same amount of randomizations was considered by the SDR algorithm for both 4-antenna and 8-antenna cases. As shown in [SDL06], however, more transmit antennas require more randomizations in order to better approximate the optimal solution. The number of randomizations was kept constant for comparison purposes, but it can of course be changed in order to improve the performance of SDR at the cost of increased complexity.

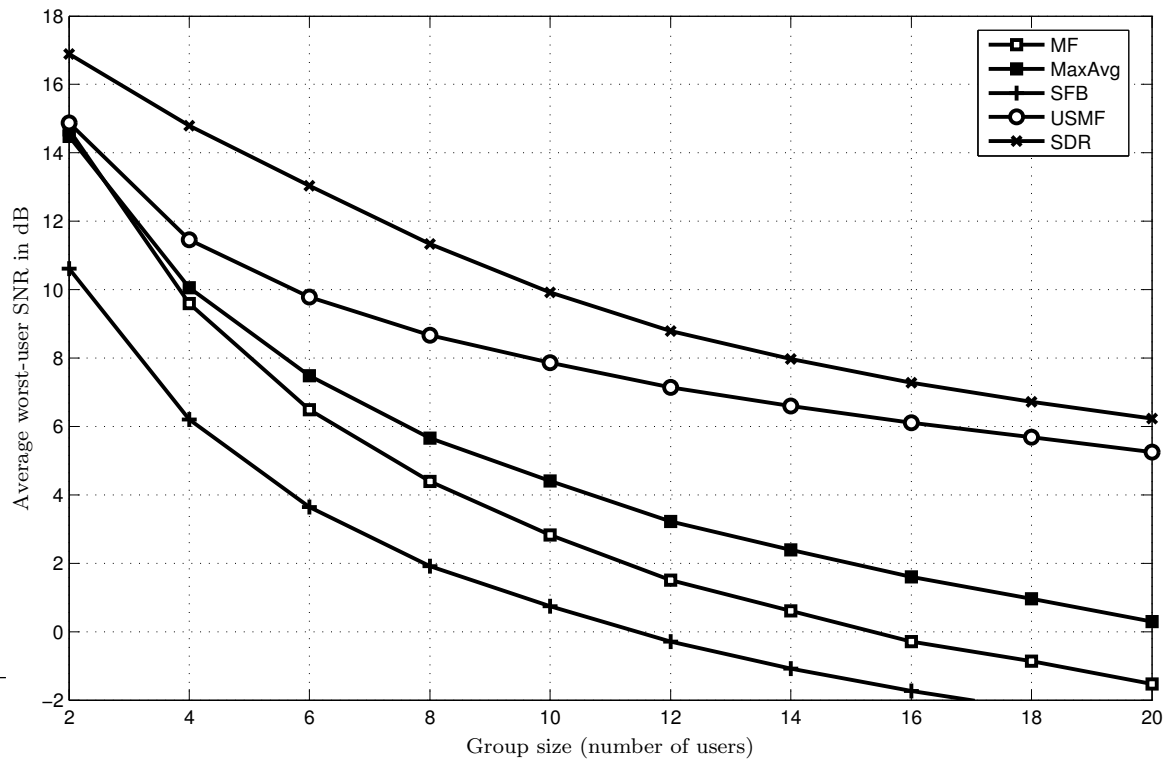


Figure 3.10. Average worst-user SNR for NLOS, $L = 8$, and $E_s/N_0=10$ dB.

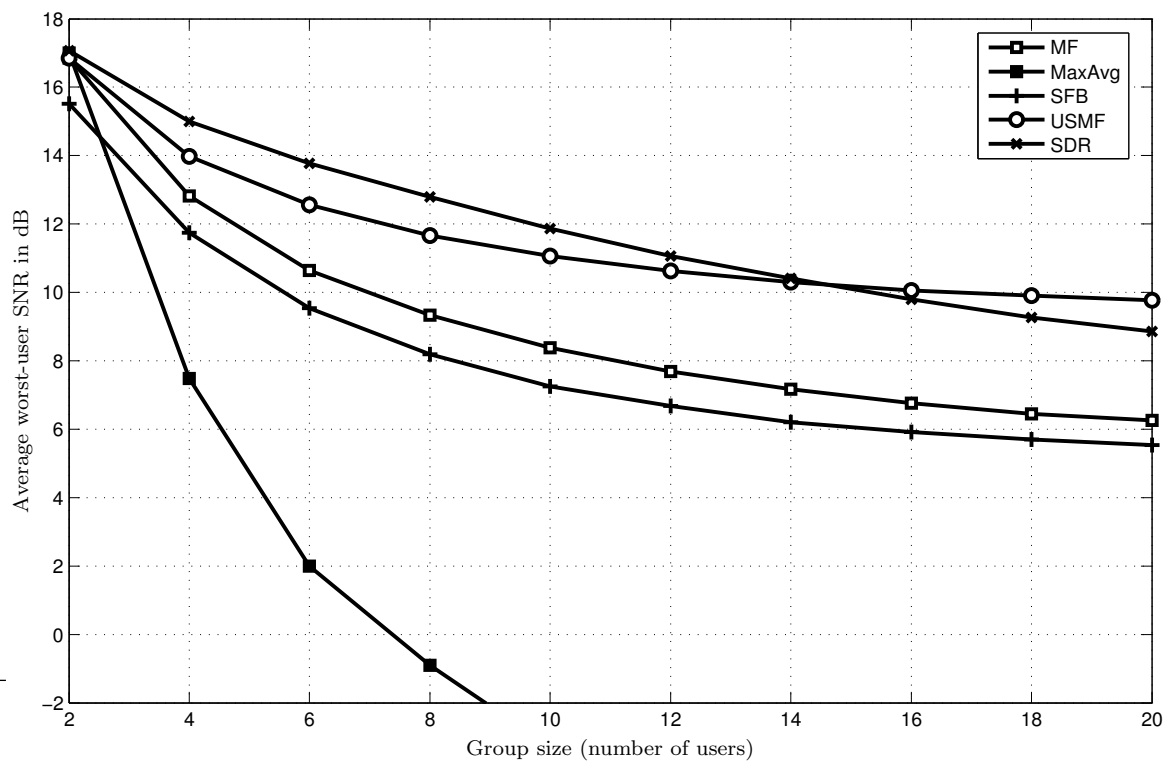


Figure 3.11. Average worst-user SNR for LOS, $L = 8$, and $E_s/N_0=10$ dB.

3.5.4 Remarks on complexity

In order to complement the performance analysis, this section takes into account the complexity of the different beamforming algorithms. With these results at hand, it is possible to identify which algorithms present the best trade-off between complexity and performance.

The complexity of an algorithm is here measured in terms of the required number of complex multiplications. Divisions and square roots have the same complexity as a multiplication, when they are efficiently implemented using Newton's method [BV04], and therefore are counted as such. Additions and subtractions are not taken into account and it is assumed that the algorithms are implemented as efficiently as possible. Repeated operations do not increase the complexity, i.e., when the same computation is employed at several points within the algorithm, its computational cost is computed only once, since its result can be stored in memory and reused when necessary.

Table 3.3 shows the complexity of all algorithms in terms of the number of complex multiplications, as well as the order of complexity according to the big O notation [GL96]. The algorithms are sorted in the table according to their increased order of complexity. Note that, in the complexity analysis of the THP algorithm, the suboptimal ordering procedure of [Joh04] is taken into account. An upper bound for the complexity order of SDR is given in [SDL06] in terms of the number of arithmetic operations, but since the comparison in Table 3.3 only takes into account the number of multiplications, a factor of 1/2 is introduced in order to roughly approximate the number of multiplications. For more details on the complexity of mathematical functions and operations, see Appendix A.2.

Table 3.3. Computational complexity of the beamforming algorithms.

Alg.	Number of complex multiplications	Complexity order
MF	$NL + 2L + 2$	$\mathcal{O}(NL)$
SFB	$NL^2 + NL + 2L + 2$	$\mathcal{O}(NL^2)$
MaxAvg	$\frac{1}{2}NL^2 + \frac{1}{2}NL + L + \mathcal{O}(L^3)$	$\mathcal{O}(\frac{1}{2}NL^2 + L^3)$
ZF	$\frac{1}{2}NL^2 + L^3 + L^2 + \frac{3}{2}NL + 2L + 2$	$\mathcal{O}(\frac{1}{2}NL^2 + L^3)$
MMSE	$\frac{1}{2}NL^2 + L^3 + L^2 + \frac{3}{2}NL + 2L + 2$	$\mathcal{O}(\frac{1}{2}NL^2 + L^3)$
USMF	$2N^3L + N^3 - \frac{1}{2}N^2L + \frac{3}{2}N^2 + \frac{1}{2}NL - \frac{5}{2}N + 2L + 2$	$\mathcal{O}(2N^3L)$
THP	$3N^4 + \frac{1}{6}N^3 + N^2L + \frac{3}{2}N^2 + 2NL + \frac{13}{3}N + 2 + \mathcal{O}(\frac{1}{3}N^3)$	$\mathcal{O}(3N^4)$
SDR	-	$\mathcal{O}(\frac{1}{2}(N + L^2)^{3.5})$

The MF and SFB algorithms are the ones presenting the lowest complexity, whereas SDR is the most complex one. The MaxAvg, ZF, and MMSE algorithms have the same complexity order, higher than SFB but still lower than USMF. The THP has a complexity comparable to that of USMF.

3.6 Conclusions

In this chapter, the single-group multicast problem has been investigated. The following algorithms, known from the unicast case, have been formulated for the single-group multicast case: Matched Filter (MF), linear Zero-Forcing (ZF), linear Minimum Mean Square Error (MMSE), Tomlinson-Harashima Precoding (THP), and Switched Fixed Beams (SFB). Additionally, an algorithm specifically designed for the multicast case, called User-Selective Matched Filter (USMF) has been proposed. These newly proposed algorithms have been extensively analyzed in terms of performance and complexity, for both Non-Line-Of-Sight (NLOS) and Line-Of-Sight (LOS) scenarios, and their relative behavior has been explained. The main conclusions may be summarized as follows:

- For the NLOS scenario, the USMF algorithm presents a much better performance than the other proposed algorithms, reasonably approaching the performance of the more complex Semi-Definite Relaxation (SDR) algorithm.
- The LOS scenario has a rather positive impact on several of the proposed algorithms, such as the USMF, MMSE, MF, and SFB. The USMF gets much closer to SDR, and the other mentioned algorithms also follow closely.
- With regard to the impact of the group size on the worst-user SNR performance, it has been shown that the USMF algorithm presents the best trade-off between complexity and performance. For large group sizes, the other proposed algorithms have their performance significantly degraded, while some of them actually have a group size limitation, such as the ZF, MMSE, and THP algorithms.

Chapter 4

Adaptive multi-group multicast beamforming

4.1 Introduction

In this chapter, the theme of multi-group multicast beamforming is approached. It is an extension of the single-group beamforming, discussed in the previous chapter, to the case in which multiple multicast groups share the same radio resource. The motivation is to exploit the spatial dimension provided by the multiple antennas in order to provide an efficient utilization of the radio resources. The challenge is to design efficient algorithms capable of suppressing the inter-group interference, while at the same time providing the best possible quality to the users of the different multicast groups. The optimization problem is formulated in Section 4.2. Some solutions to this problem have been proposed in works such as [KSL05, KSL07, GS05a, GS06], which are briefly discussed in Section 4.3. It is shown in this chapter that algorithms originally designed for the multi-user unicast scenario can be extended for the multi-group multicast case. Formulations of both linear and non-linear algorithms for the multi-group multicast case are proposed in Sections 4.4 and 4.5, respectively. The linear algorithms are the Matched Filter (MF), linear Zero-Forcing (ZF), linear Minimum Mean Square Error (MMSE), and SINR Balancing (SB), while the non-linear ones are based on Tomlinson-Harashima Precoding (THP) and Vector Precoding (VP). Additionally, modified versions of these algorithms – referred to as Multicast-Aware (MA) algorithms – are proposed in order to improve the performance of the multicast services. An analysis of the performance and complexity of the algorithms is presented in Section 4.6. The results demonstrate that the linear MA algorithms achieve significant performance gains with regard to the original ones, but the same is not true for the non-linear MA algorithms, which is due to a number of reasons which are discussed throughout the chapter. Finally, the main conclusions are summarized in Section 4.7.

4.2 Problem formulation

In a multi-group multicast scenario, differently from the single-group case, there are several data streams being transmitted simultaneously on the same radio resource,

each targeted at a different multicast group. Due to this simultaneous transmission of different streams at the same time and at the same resource, each receiver sees the streams that are intended for other groups as interference. This inter-group interference has a significant impact on the solution of the optimization problem.

The single-group optimization problem specified in (3.1) determines a single beamforming vector. Now, since this is a multi-group case, a beamforming vector is considered to be associated to each data stream. These beamforming vectors can be concatenated into matrix $\mathbf{M}' \in \mathbb{C}^{L \times K}$. The optimization problem for determining the beamforming matrix \mathbf{M}' that maximizes the worst-user Signal-to-Interference plus Noise Ratio (SINR) can be written as

$$\begin{aligned} \mathbf{M}'_{\text{opt}} &= \underset{\mathbf{M}'}{\operatorname{argmax}} \min_n \gamma_n, \quad n = 1, \dots, N \\ \text{subject to: } &\sigma_s^2 \operatorname{tr}(\mathbf{M}'^H \mathbf{M}') \leq P, \end{aligned} \quad (4.1)$$

where γ_n is given by

$$\gamma_n = \frac{\sigma_s^2 |\mathbf{h}_n \mathbf{m}'_{b_n}|^2}{\sum_{k=1, k \neq b_n}^K \sigma_s^2 |\mathbf{h}_n \mathbf{m}'_k|^2 + \sigma_z^2}, \quad \text{for } n = 1, \dots, N. \quad (4.2)$$

Another possible optimization problem corresponds to the minimization of the transmit power subject to individual user quality constraints. It can be written as

$$\begin{aligned} \mathbf{M}'_{\text{opt}} &= \underset{\mathbf{M}'}{\operatorname{argmin}} \operatorname{tr}(\mathbf{M}'^H \mathbf{M}'), \\ \text{subject to: } &\gamma_n \geq \gamma_{\text{tgt}} \quad n = 1, \dots, N, \end{aligned} \quad (4.3)$$

where γ_n is defined in (4.2) and γ_{tgt} corresponds to the desired target SINR.

Both optimization problems correspond to quadratically constrained quadratic programming problems [BV04]. The second problem, expressed in (4.3), was claimed to be NP-hard by Karipidis et al. in [KSL05]. The equivalence of both problems for the single-group beamforming case indicates that the first problem, expressed in (4.1), might be NP-hard as well.

Regarding the receive processing optimization, the procedure described in Section 2.3 that results in (2.19) is taken into account by all algorithms, unless otherwise explicitly stated by the algorithm description. The receive filter $\mathbf{D} \in \mathbb{C}^{N \times N}$ is given by

$$\mathbf{D} = \operatorname{diag}(\mathbf{h}_1 \mathbf{m}'_{b_1}, \dots, \mathbf{h}_N \mathbf{m}'_{b_N})^{-1}, \quad (4.4)$$

which can be alternatively expressed as

$$\mathbf{D} = \operatorname{diag}((\mathbf{H} \mathbf{M}' \odot \mathbf{T}^+) \mathbf{1})^{-1}, \quad (4.5)$$

where the symbol \odot denotes the entry-wise matrix product, also known as Hadamard or Schur product, $\mathbf{H} \in \mathbb{C}^{N \times L}$ is the channel matrix, and $\mathbf{T}^+ \in \mathbb{R}^{N \times K}$ is the right pseudoinverse of the transformation matrix defined in (2.9).

4.3 State-of-the-art

In this section, a review of the state-of-the-art in multi-group multicast beamforming is presented, which complements the short review presented by Table 1.1 of Chapter 1.

The multi-group multicast beamforming problem has first been discussed by Lopez in [Lop02], where the use of null space projection algorithms has been suggested for eliminating the interference among the data streams of different groups. After the null space projections, an equivalent channel matrix \mathbf{HM} is achieved, whose non-zero elements are grouped into “array processing subblocks”. These subblocks determine the type of transmit processing technique to be employed, which can be: single-group multicast beamforming, single-user unicast beamforming, or non-linear precoding for a group of unicast users. This approach has served as inspiration for the algorithms which will be presented in Sections 4.4.2.2 and 4.5.3.

A precoding strategy based on Dirty Paper Coding (DPC) [Cos83] for the multi-group multicast scenario has been proposed by Khisti in [Khi04]. This precoding strategy, however, is based on sum rate maximization, which is not adequate to the optimization problems discussed in Section 4.2.

In [KSL05], Karipidis et al. proposed a method based on Semi-Definite Relaxation (SDR) for the multi-group multicast optimization problem of minimizing the transmit power subject to SINR constraints expressed in (4.3). It corresponds to an extension of the single-group multicast beamforming algorithm in [SD04, SDL06], and is based on the multi-user unicast case presented in [BO99]. Similar to the single-group multicast case, the rank 1 relaxation allows the problem to be solved efficiently through semi-definite optimization methods. If the obtained solution has rank 1, then it corresponds to the optimal solution, otherwise randomization techniques need to be employed in order to improve the solution [SD04, KSL05]. The problem is that, differently from the single-group case, it is no longer possible to simply scale the generated randomized beamforming vectors, due to the inter-group interference. In [KSL05], the problem of converting each candidate vector into a feasible solution is called “multi-group power control” and is expressed as a Linear Programming (LP) problem, which can also be solved through semi-definite optimization. This additional optimization problem,

however, increases the complexity of the algorithm. The specific case of multi-group multicast beamforming for Vandermonde channel matrices is approached in [KSL06, KSL07], where it is shown that the relaxed problem always leads to rank 1 matrices, meaning that the optimal solution is always achieved for this case.

Gao and Schubert proposed in [GS05a] another solution to problem (4.3) than that of [KSL05]. The difference with regard to [KSL05] is that DPC is employed and a block-triangular channel is taken into account. Such a channel structure allows a group-by-group algorithm, since the interference from previous groups is known. The beamforming vectors are successively determined for each group by employing single-group beamforming based on SDR [SD04]. The power allocated to each beamforming vector is also determined successively through a simple algorithm.

In [GS06], the same SDR approach of [KSL05] is employed to solve problem (4.3), but instead of solving the “multi-group power control” through semi-definite programming, an iterative power allocation method based on worst-case interference functions is proposed.

With regard to the problem of maximizing the worst-user SINR expressed in (4.1), differently from the single-group multicast case, its solution cannot be directly obtained by scaling the solution of (4.3). It has been shown in [GS06] and [KSL07], however, that it can be solved through a bisection method. The idea is to specify an SINR interval within which the optimal solution must lie, and to determine the solution of problem (4.3) when considering the middle point of the interval as the target SINR. The interval is then successively bisected, based on whether the required amount of power P_{req} exceeds the transmit power constraint P or not. For each interval middle point, the corresponding problem (4.3) is solved. The bisection proceeds until a desired precision is reached with regard to $|P_{\text{req}} - P|$.

Another method for determining a solution to (4.1), which is based on the alternating optimization procedure of [SB04], has been proposed in [GS06]. It employs an iterative power allocation algorithm, which determines the power allocation vector and the maximum achievable worst-user SINR, given a fixed set of beamforming vectors. Additionally, given a certain SINR target, the SDR approach of [GS05a] is used to determine the beamforming vectors. The power allocation and beamforming algorithms are alternately executed, until the worst-user SINR stops increasing.

The extension of multi-user unicast beamforming techniques to the multi-group multicast case, however, has not been investigated by previous works. For this reason,

formulations of linear and non-linear beamforming algorithms for the multi-group multicast scenario are proposed in the next sections. Additionally, it is shown that these algorithms can be enhanced, in general, by introducing modifications that aim at improving the performance of multicast services. These enhanced algorithms are further referred to as Multicast-Aware (MA) algorithms.

4.4 Linear algorithms

4.4.1 Matched filter

The derivation of the Matched Filter (MF) for the multi-group multicast scenario is based on the optimization problem for the multi-user unicast case presented in [Joh04]. It aims at maximizing the SNR perceived at each terminal, without taking the inter-group interference into account. The unicast problem for determining the modulation matrix \mathbf{M} can be expressed as

$$\mathbf{M}_{\text{MF}} = \underset{\mathbf{M}}{\operatorname{argmax}} \frac{|\mathbb{E}\{\mathbf{s}^H \mathbf{y}\}|^2}{\mathbb{E}\{\|\mathbf{s}\|^2\} \mathbb{E}\{\|\mathbf{z}\|^2\}}, \quad \text{subject to: } \mathbb{E}\{\|\mathbf{M}\mathbf{s}\|^2\} \leq P. \quad (4.6)$$

The multicast optimization can be obtained by substituting the modulation matrix \mathbf{M} and symbol vector \mathbf{s} by the reduced modulation matrix \mathbf{M}' and reduced symbol vector \mathbf{s}' , respectively. Recalling from (2.15) that $\mathbf{s} = \mathbf{T}^+ \mathbf{s}'$, the multicast problem is given by

$$\mathbf{M}'_{\text{MF}} = \underset{\mathbf{M}'}{\operatorname{argmax}} \frac{|\mathbb{E}\{(\mathbf{T}^+ \mathbf{s}')^H \mathbf{y}\}|^2}{\mathbb{E}\{\|\mathbf{T}^+ \mathbf{s}'\|^2\} \mathbb{E}\{\|\mathbf{z}\|^2\}}, \quad \text{subject to: } \mathbb{E}\{\|\mathbf{M}' \mathbf{s}'\|^2\} \leq P. \quad (4.7)$$

The cost function of the optimization problem corresponds to an equivalent group SINR, denoted by γ_{eq} , which can be further expressed as

$$\gamma_{\text{eq}} = \frac{|\mathbb{E}\{\mathbf{s}'^H \mathbf{T}^{+,T} (\mathbf{H} \mathbf{M}' \mathbf{s}' + \mathbf{z})\}|^2}{\mathbb{E}\{\mathbf{s}'^H \mathbf{T}^{+,T} \mathbf{T}^+ \mathbf{s}'\} \mathbb{E}\{\mathbf{z}^H \mathbf{z}\}} = \frac{|\operatorname{tr}(\mathbf{H} \mathbf{M}' \mathbf{R}'_s \mathbf{T}^{+,T})|^2}{\operatorname{tr}(\mathbf{T}^+ \mathbf{R}'_s \mathbf{T}^{+,T}) \operatorname{tr}(\mathbf{R}_z)}, \quad (4.8)$$

where $\mathbf{R}_z = \mathbb{E}\{\mathbf{z}\mathbf{z}^H\}$ and $(\cdot)^{X,Y}$ corresponds to the sequential application of matrix operators X and Y . Note that, differently from the single-group multicast case, the optimization now involves the determination of a matrix, instead of a vector, which is due to the multiple data streams. As a matter of fact, the cost function in (4.8) resembles rather that of the multi-user unicast case in [Joh04] than that of the single-group multicast case. The application of the same Lagrange optimization procedure as in [Joh04] leads to the following solution:

$$\mathbf{M}'_{\text{MF}} = \sqrt{\frac{P}{\sigma_s^2 \operatorname{tr}(\mathbf{H} \mathbf{H}^H \mathbf{T}^+ \mathbf{T}^{+,T})}} \mathbf{H}^H \mathbf{T}^+. \quad (4.9)$$

4.4.2 Zero-forcing based algorithms

4.4.2.1 Zero-forcing

The Zero-Forcing (ZF) optimization problem for the multi-group scenario, assuming that $\mathbf{s} = \mathbf{T}^+\mathbf{s}'$, can be written as

$$\mathbf{M}'_{\text{ZF}} = \text{E}\{\|\hat{\mathbf{s}} - \mathbf{T}^+\mathbf{s}'\|^2\}, \quad \text{subject to: } \begin{cases} \text{E}\{\|\mathbf{M}'\mathbf{s}'\|^2\} \leq P \\ \hat{\mathbf{s}}|_{\mathbf{z}=\mathbf{0}} = \mathbf{T}^+\mathbf{s}' \end{cases}, \quad (4.10)$$

where the second constraint corresponds to the zero-forcing constraint, which means that in the absence of noise the estimated symbol vector $\hat{\mathbf{s}}$ must be equal to the complete symbol vector with repeated entries $\mathbf{T}^+\mathbf{s}'$. Similarly to the single-group case, it is here assumed that the receive filter for each user is given by a scalar $\beta \in \mathbb{C}$, i.e., $\mathbf{D} = \beta\mathbf{I}$. The second constraint can be further expressed as

$$\hat{\mathbf{s}}|_{\mathbf{z}=\mathbf{0}} = \mathbf{T}^+\mathbf{s}' \implies \beta\mathbf{H}\mathbf{M}'\mathbf{s}' = \mathbf{T}^+\mathbf{s}' \implies \beta\mathbf{H}\mathbf{M}' = \mathbf{T}^+. \quad (4.11)$$

The MSE cost function, substituting $\hat{\mathbf{s}}$ and taking into account the zero-forcing constraint, is given by

$$\text{E}\{\|\beta\mathbf{H}\mathbf{M}'\mathbf{s}' + \mathbf{z} - \mathbf{T}^+\mathbf{s}'\|^2\} = \text{E}\{\|\mathbf{z}\|^2\} = \text{tr}(\mathbf{R}_z). \quad (4.12)$$

The Lagrangian function can be expressed as

$$\text{L}(\mathbf{M}', \mu, \mathbf{\Lambda}) = \text{tr}(\mathbf{R}_z) + \mu(\text{tr}(\mathbf{M}'^{\text{H}}\mathbf{M}'\mathbf{R}'_s) - P) + \text{tr}(\mathbf{\Lambda}(\mathbf{T}^+ - \beta\mathbf{H}\mathbf{M}')), \quad (4.13)$$

where $\mu \in \mathbb{R}$ and $\mathbf{\Lambda} \in \mathbb{C}^{K \times N}$ are Lagrange multipliers. Note that the Lagrange multipliers associated to the zero-forcing constraint are now grouped within a matrix, instead of within a vector as in the single-group case. Again, the optimization procedure employed in [Joh04] for the multi-user unicast case can be employed to obtain the solution to the multi-group multicast problem, which is given by

$$\mathbf{M}'_{\text{ZF}} = \sqrt{\frac{P}{\sigma_s^2 \text{tr}((\mathbf{H}\mathbf{H}^{\text{H}})^{-1}\mathbf{T}^+\mathbf{T}^{+\text{T}})}} \mathbf{H}^{\text{H}}(\mathbf{H}\mathbf{H}^{\text{H}})^{-1}\mathbf{T}^+. \quad (4.14)$$

For this algorithm, the receive filter expression in (4.4) can be simplified as

$$\mathbf{D}_{\text{ZF}} = \sqrt{\frac{\sigma_s^2 \text{tr}((\mathbf{H}\mathbf{H}^{\text{H}})^{-1}\mathbf{T}^+\mathbf{T}^{+\text{T}})}{P}} \mathbf{I}. \quad (4.15)$$

4.4.2.2 Multicast-aware zero-forcing

The algorithm presented in the previous section corresponds to a direct method of implementing the zero-forcing filter based on channel inversion. Another possible method is to make use of null-space projections [SH02, SSH04] in order to eliminate the interference. In [SH02, SSH04], a null-space method called Block Diagonalization (BD) is proposed for the MIMO multi-user scenario. The idea of BD is to suppress only the interference among streams of different users, i.e., no energy is spent on mitigating the interference among the streams of a same user. The assumption is that this remaining intra-user interference can be suppressed by implementing receive processing techniques at each multi-antenna user terminal.

The MIMO multi-user scenario is to some extent analogous to the multi-group multicast scenario. For the latter, it is only necessary to suppress the interference among different groups. The users belonging to the same group do not require interference cancellation. Actually, since they expect the same data stream, no further interference suppression is required at the receiver side. In this section, an algorithm based on null-space projections, which has been first introduced by the author of this thesis in [SK06b], is proposed for the multi-group multicast scenario. This algorithm will be referred to as multicast-aware zero-forcing (MA-ZF).

It is assumed that $\mathbf{M}' \in \mathbb{C}^{L \times K}$ and $\mathbf{m}'_k \in \mathbb{C}^L$ denote, respectively, the complete beamforming matrix and the beamforming vector of the k^{th} multicast group.

Let $\mathbf{H}_k \in \mathbb{C}^{g_k \times L}$ and $\tilde{\mathbf{H}}_k \in \mathbb{C}^{(N-g_k) \times L}$ denote, respectively, the channel matrix of all users belonging to group k and all users not belonging to group k . The latter can be written as

$$\tilde{\mathbf{H}}_k = [\mathbf{H}_1^T, \dots, \mathbf{H}_{k-1}^T, \mathbf{H}_{k+1}^T, \dots, \mathbf{H}_K^T]^T. \quad (4.16)$$

The channel $\tilde{\mathbf{H}}_k$ can be decomposed using Singular Value Decomposition (SVD) as follows:

$$\tilde{\mathbf{H}}_k = \tilde{\mathbf{U}}_k \tilde{\mathbf{S}}_k [\tilde{\mathbf{V}}_k^{(1)}, \tilde{\mathbf{V}}_k^{(0)}]^H, \quad (4.17)$$

where $\tilde{\mathbf{U}}_k \in \mathbb{C}^{(N-g_k) \times (N-g_k)}$ is a unitary matrix, $\tilde{\mathbf{S}}_k \in \mathbb{R}^{(N-g_k) \times L}$ is a diagonal matrix, $\tilde{\mathbf{V}}_k^{(1)} \in \mathbb{C}^{L \times \tilde{r}_k}$ and $\tilde{\mathbf{V}}_k^{(0)} \in \mathbb{C}^{L \times (L-\tilde{r}_k)}$ contain the right singular vectors of $\tilde{\mathbf{H}}_k$, with \tilde{r}_k denoting the rank of matrix $\tilde{\mathbf{H}}_k$. Matrix $\tilde{\mathbf{V}}_k^{(0)}$ constitutes an orthogonal basis for the null space of $\tilde{\mathbf{H}}_k$. Due to this property, $\tilde{\mathbf{V}}_k^{(0)}$ can be used for specifying a beamforming vector that cancels the interference from the other groups of users. If $L - \tilde{r}_k = 1$, then $\tilde{\mathbf{V}}_k^{(0)}$ can be used directly as the beamforming vector, otherwise, if $L - \tilde{r}_k > 1$, then there are some degrees of freedom for determining a suitable beamforming vector. Note that $\tilde{r}_k = N - g_k$, when assuming that matrix \mathbf{H} has full row rank.

The multiplication of the channel matrix \mathbf{H}_j by $\tilde{\mathbf{V}}_k^{(0)}$, for all $j \neq k$, results in a matrix of zeros $\mathbf{0} \in \mathbb{R}^{g_j \times (L - \tilde{r}_k)}$. The product $\mathbf{H}_k \tilde{\mathbf{V}}_k^{(0)}$, on the other hand, can be seen as an equivalent channel matrix $\mathbf{H}_k^{(\text{eq})} \in \mathbb{C}^{g_k \times (L - \tilde{r}_k)}$ after the null space projection. When multiplying \mathbf{H}_k by $\tilde{\mathbf{V}}_k^{(0)}$ it is assured that the interference from the data streams of other users will be totally suppressed. For this reason, each multicast group can be processed individually, i.e., the single-group beamforming algorithms of Section 3.4 can be applied to the equivalent channel $\mathbf{H}_k^{(\text{eq})}$ of each group k . Let $\mathbf{m}_k^{(\text{eq})} \in \mathbb{C}^{(L - \tilde{r}_k)}$ denote the equivalent beamforming vector obtained after applying single-group beamforming to $\mathbf{H}_k^{(\text{eq})}$. The resulting beamforming vector for group k is then given by

$$\mathbf{m}'_k = \tilde{\mathbf{V}}_k^{(0)} \mathbf{m}_k^{(\text{eq})}, \quad (4.18)$$

and the beamforming matrix \mathbf{M}' is

$$\mathbf{M}' = [\tilde{\mathbf{V}}_1^{(0)} \mathbf{m}_1^{(\text{eq})}, \dots, \tilde{\mathbf{V}}_K^{(0)} \mathbf{m}_K^{(\text{eq})}]. \quad (4.19)$$

In order to better illustrate how the MA-ZF algorithm works, consider the parameters of the exemplary scenario of Section 2.3: $N = 4$, $K = 3$, $\mathbf{g} = [1, 1, 2]^T$, $\mathbf{b} = [1, 2, 3, 3]^T$. Assuming that the channel matrix is full rank, the elements required for calculating \mathbf{M}' have the following dimensions:

$$\begin{aligned} \mathbf{H}_1 &\in \mathbb{C}^{1 \times 4}, & \tilde{\mathbf{H}}_1 &\in \mathbb{C}^{3 \times 4}, & \tilde{\mathbf{V}}_1^{(0)} &\in \mathbb{C}^{4 \times 1}, & \mathbf{m}_1^{(\text{eq})} &\in \mathbb{C}^{1 \times 1}, \\ \mathbf{H}_2 &\in \mathbb{C}^{1 \times 4}, & \tilde{\mathbf{H}}_2 &\in \mathbb{C}^{3 \times 4}, & \tilde{\mathbf{V}}_2^{(0)} &\in \mathbb{C}^{4 \times 1}, & \mathbf{m}_2^{(\text{eq})} &\in \mathbb{C}^{1 \times 1}, \\ \mathbf{H}_3 &\in \mathbb{C}^{2 \times 4}, & \tilde{\mathbf{H}}_3 &\in \mathbb{C}^{2 \times 4}, & \tilde{\mathbf{V}}_3^{(0)} &\in \mathbb{C}^{4 \times 2}, & \mathbf{m}_3^{(\text{eq})} &\in \mathbb{C}^{2 \times 1}, \end{aligned} \quad (4.20)$$

and the product $\mathbf{H}\mathbf{M}'$ is given by

$$\mathbf{H}\mathbf{M}' = \begin{bmatrix} \mathbf{H}_1 \tilde{\mathbf{V}}_1^{(0)} \mathbf{m}_1^{(\text{eq})} & \mathbf{H}_1 \tilde{\mathbf{V}}_2^{(0)} \mathbf{m}_2^{(\text{eq})} & \mathbf{H}_1 \tilde{\mathbf{V}}_3^{(0)} \mathbf{m}_3^{(\text{eq})} \\ \mathbf{H}_2 \tilde{\mathbf{V}}_1^{(0)} \mathbf{m}_1^{(\text{eq})} & \mathbf{H}_2 \tilde{\mathbf{V}}_2^{(0)} \mathbf{m}_2^{(\text{eq})} & \mathbf{H}_2 \tilde{\mathbf{V}}_3^{(0)} \mathbf{m}_3^{(\text{eq})} \\ \mathbf{H}_3 \tilde{\mathbf{V}}_1^{(0)} \mathbf{m}_1^{(\text{eq})} & \mathbf{H}_3 \tilde{\mathbf{V}}_2^{(0)} \mathbf{m}_2^{(\text{eq})} & \mathbf{H}_3 \tilde{\mathbf{V}}_3^{(0)} \mathbf{m}_3^{(\text{eq})} \end{bmatrix} = \begin{bmatrix} x & 0 & 0 \\ 0 & x & 0 \\ 0 & 0 & x \\ 0 & 0 & x \end{bmatrix}, \quad (4.21)$$

where x indicates non-zero values.

Another aspect concerning the MA-ZF algorithm is that, differently from the ZF filter, the received power is not balanced among the users. In the case of ZF, all users receive the same power, which is due to the channel inversion step. The approach based on null-space projections, however, does not make any such guarantees regarding the receive power. For this reason, it is necessary to perform power loading on matrix \mathbf{M}' . In [SSH04], the power loading is done according to the waterfilling algorithm [PF05], which aims at maximizing the sum throughput. A more fair power loading, which

balances the received power among the users, is considered here instead. The power loading matrix $\mathbf{\Gamma} \in \mathbb{R}^{K \times K}$ is given by

$$\mathbf{\Gamma} = \text{diag}(\min(|\mathbf{H}_1 \tilde{\mathbf{V}}_1^{(0)} \mathbf{m}_1^{(\text{eq})}|), \dots, \min(|\mathbf{H}_K \tilde{\mathbf{V}}_K^{(0)} \mathbf{m}_K^{(\text{eq})}|))^{-1}, \quad (4.22)$$

where the modulo operator $|\cdot|$ is assumed to be applied element-wise. This power loading ensures that the same amount of power is given to the worst user of each multicast group. Additionally, the matrix $\mathbf{M}'\mathbf{\Gamma}$ still has to be normalized by a scalar factor $\beta \in \mathbb{R}$ in order to satisfy the transmit power constraint, which is given by

$$\beta = \sqrt{\frac{P}{\sigma_s^2 \text{tr}(\mathbf{M}'^H \mathbf{M}' \mathbf{\Gamma}^2)}}. \quad (4.23)$$

The beamforming solution for the MA-ZF algorithm can finally be summarized as

$$\mathbf{M}'_{\text{MA-ZF}} = \beta \mathbf{M}' \mathbf{\Gamma}, \quad (4.24)$$

where β , \mathbf{M}' , and $\mathbf{\Gamma}$ are defined, respectively, in (4.23), (4.19), and (4.22).

4.4.3 Minimum mean square error based algorithms

4.4.3.1 Minimum mean square error

The Minimum Mean Square Error (MMSE) optimization problem for the multi-group scenario, assuming that $\mathbf{s} = \mathbf{T}^+ \mathbf{s}'$ and that each receiver implements a scalar filter $\beta \in \mathbb{C}$, can be written as

$$\{\mathbf{M}'_{\text{MMSE}}, \beta_{\text{MMSE}}\} = \underset{\{\mathbf{M}', \beta\}}{\text{argmin}} \mathbb{E}\{\|\hat{\mathbf{s}} - \mathbf{T}^+ \mathbf{s}'\|^2\}, \quad \text{subject to: } \mathbb{E}\{\|\mathbf{M}' \mathbf{s}'\|^2\} \leq P, \quad (4.25)$$

The MSE cost function can be further expressed as

$$\begin{aligned} \mathbb{E}\{\|\hat{\mathbf{s}} - \mathbf{T}^+ \mathbf{s}'\|^2\} &= \mathbb{E}\{\|(\beta \mathbf{H} \mathbf{M}' - \mathbf{T}^+) \mathbf{s}' + \beta \mathbf{z}\|^2\} \\ &= \mathbb{E}\{\mathbf{s}'^H (\beta \mathbf{H} \mathbf{M}' - \mathbf{T}^+)^H (\beta \mathbf{H} \mathbf{M}' - \mathbf{T}^+) \mathbf{s}' + |\beta|^2 \mathbf{z}^H \mathbf{z}\} \\ &= \text{tr}(|\beta|^2 \mathbf{M}'^H \mathbf{H}^H \mathbf{H} \mathbf{M}' \mathbf{R}'_s - 2\text{Re}(\beta \mathbf{T}^{+,T} \mathbf{H} \mathbf{M}' \mathbf{R}'_s) + \mathbf{T}^{+,T} \mathbf{T}^+ \mathbf{R}'_s + |\beta|^2 \mathbf{R}_z). \end{aligned} \quad (4.26)$$

The Lagrangian function is given by

$$L(\mathbf{m}, \beta, \mu) = \mathbb{E}\{\|\hat{\mathbf{s}} - \mathbf{T}^+ \mathbf{s}'\|^2\} + \mu(\text{tr}(\mathbf{M}'^H \mathbf{M}' \mathbf{R}'_s) - P), \quad (4.27)$$

where $\mu \in \mathbb{R}$ is a Lagrange multiplier. Similarly to the MF and ZF algorithms, the optimization procedure employed in [Joh04] for the multi-user unicast case can be

employed to obtain the solution to the multi-group multicast problem, which is given by

$$\mathbf{M}'_{\text{MMSE}} = \sqrt{\frac{P}{\sigma_s^2 \text{tr} \left(\mathbf{H} \left(\mathbf{H}^H \mathbf{H} + \frac{N\sigma_z^2}{P} \mathbf{I} \right)^{-2} \mathbf{H}^H \mathbf{T} + \mathbf{T}^+, \mathbf{T} \right)}} \left(\mathbf{H}^H \mathbf{H} + \frac{N\sigma_z^2}{P} \mathbf{I} \right)^{-1} \mathbf{H}^H \mathbf{T}^+, \quad (4.28)$$

with the receive filter expressed as

$$\mathbf{D}_{\text{MMSE}} = \sqrt{\frac{\sigma_s^2 \text{tr} \left(\mathbf{H} \left(\mathbf{H}^H \mathbf{H} + \frac{N\sigma_z^2}{P} \mathbf{I} \right)^{-2} \mathbf{H}^H \mathbf{T} + \mathbf{T}^+, \mathbf{T} \right)}{P}} \mathbf{I}. \quad (4.29)$$

4.4.3.2 Multicast-aware minimum mean square error

In this section, the MMSE algorithm is enhanced for the multi-group multicast scenario. The proposed multicast-aware MMSE (MA-MMSE) algorithm is based on the same method of null-space projections described in Section 4.4.2.2. The difference is that, instead of making the projections with regard to the original channel, an equivalent regularized channel is taken into account. The null space projections totally suppress the inter-group interference of the equivalent channel. However, since it is not equal to the original channel, a similar effect as that of the MMSE algorithm is achieved, in which there appears a residual inter-group interference. Moreover, since the projections are done on a regularized channel, the drawbacks of an ill-conditioned matrix are avoided.

Let $\mathbf{H}^{(\text{R})} \in \mathbb{C}^{N \times N}$ denote the regularized channel. It is defined as

$$\mathbf{H}^{(\text{R})} = \mathbf{H} \mathbf{H}^H + \frac{N\sigma_z^2}{P} \mathbf{I}, \quad (4.30)$$

where the same regularization factor as that of the MMSE algorithm [Joh04] is considered. Matrix $\tilde{\mathbf{H}}_k \in \mathbb{C}^{(N-g_k) \times N}$ and its SVD are given by

$$\tilde{\mathbf{H}}_k = [\mathbf{H}_1^{(\text{R}),\text{T}}, \dots, \mathbf{H}_{k-1}^{(\text{R}),\text{T}}, \mathbf{H}_{k+1}^{(\text{R}),\text{T}}, \dots, \mathbf{H}_K^{(\text{R}),\text{T}}]^{\text{T}}, \quad (4.31\text{a})$$

$$\tilde{\mathbf{H}}_k = \tilde{\mathbf{U}}_k \tilde{\mathbf{S}}_k [\tilde{\mathbf{V}}_k^{(1)}, \tilde{\mathbf{V}}_k^{(0)}]^{\text{H}}, \quad (4.31\text{b})$$

where $\mathbf{H}_k^{(\text{R})} \in \mathbb{C}^{g_k \times N}$, $\tilde{\mathbf{U}}_k \in \mathbb{C}^{(N-g_k) \times (N-g_k)}$, $\tilde{\mathbf{S}}_k \in \mathbb{R}^{(N-g_k) \times N}$, $\tilde{\mathbf{V}}_k^{(1)} \in \mathbb{C}^{N \times \tilde{r}_k}$, $\tilde{\mathbf{V}}_k^{(0)} \in \mathbb{C}^{N \times (N-\tilde{r}_k)}$, and \tilde{r}_k denotes the rank of matrix $\tilde{\mathbf{H}}_k$.

The multicast beamforming optimization, which can be implemented according to any of the algorithms in Section 3.4, is done for each group considering the equivalent

channel after the null-space projection $\mathbf{H}_k^{(\text{eq})} = \mathbf{H}_k^{(\text{R})} \tilde{\mathbf{V}}_k^{(0)} \in \mathbb{C}^{g_k \times (N - \tilde{r}_k)}$, and resulting in the beamforming vector $\mathbf{m}_k^{(\text{eq})} \in \mathbb{C}^{(N - \tilde{r}_k)}$.

The beamforming matrix $\mathbf{M}'_{\text{MA-MMSE}} \in \mathbb{C}^{L \times K}$ of the MA-MMSE algorithm can finally be written as

$$\mathbf{M}'_{\text{MA-MMSE}} = \beta \mathbf{H}^{\text{H}} \mathbf{M}' \mathbf{\Gamma} \quad (4.32)$$

with

$$\beta = \sqrt{\frac{P}{\sigma_s^2 \text{tr}(\mathbf{M}'^{\text{H}} \mathbf{H} \mathbf{H}^{\text{H}} \mathbf{M}' \mathbf{\Gamma}^2)}}, \quad (4.33a)$$

$$\mathbf{M}' = [\tilde{\mathbf{V}}_1^{(0)} \mathbf{m}_1^{(\text{eq})}, \dots, \tilde{\mathbf{V}}_K^{(0)} \mathbf{m}_K^{(\text{eq})}], \quad (4.33b)$$

$$\mathbf{\Gamma} = \text{diag}(\min(|\mathbf{H}_1^{(\text{R})} \tilde{\mathbf{V}}_1^{(0)} \mathbf{m}_1^{(\text{eq})}|), \dots, \min(|\mathbf{H}_K^{(\text{R})} \tilde{\mathbf{V}}_K^{(0)} \mathbf{m}_K^{(\text{eq})}|))^{-1}, \quad (4.33c)$$

where $\beta \in \mathbb{R}$, $\mathbf{M}' \in \mathbb{C}^{N \times K}$, and $\mathbf{\Gamma} \in \mathbb{R}^{K \times K}$.

4.4.4 SINR balancing based algorithms

4.4.4.1 SINR balancing

Different solutions to the SINR Balancing (SB) problem have been proposed in the literature for the multi-user unicast scenario, such as in [BO99, SB04]. In [BO99], the problem of minimizing the transmit power subject to the condition that the users achieve a certain SINR target, is written as a semidefinite optimization problem, which can be solved through efficient semidefinite programming techniques. In [SB04], a different methodology for solving this problem, as well as the problem of maximizing the worst-user SINR subject to a transmit power constraint, is proposed. It takes advantage of the uplink/downlink duality and consists of an alternating optimization procedure, which adjusts both the unit-norm beamformers and the power allocation among the streams, converging to the optimal solution after only a few iterations. In this section, the alternate optimization algorithm is briefly reviewed and applied to the multi-group multicast case.

Let $\mathbf{U} \in \mathbb{C}^{L \times N}$ denote the unit-norm beamforming matrix, whose n^{th} column $\mathbf{u}_n \in \mathbb{C}^L$ is given by

$$\mathbf{u}_n = \frac{\mathbf{m}_n}{\|\mathbf{m}_n\|}, \quad (4.34)$$

and let $\mathbf{p} \in \mathbb{R}^N$ denote the power allocation vector, whose n^{th} element $p_n \in \mathbb{R}$ is

$$p_n = \sigma_s^2 \|\mathbf{m}_n\|^2. \quad (4.35)$$

From (4.34) and (4.35), it also follows that

$$\mathbf{m}_n = \sqrt{(p_n/\sigma_s^2)} \mathbf{u}_n. \quad (4.36)$$

The multi-group unicast SINR balancing optimization problem can be written as

$$\begin{aligned} \{\mathbf{p}_{\text{SB}}, \mathbf{U}_{\text{SB}}\} &= \underset{\{\mathbf{p}, \mathbf{U}\}}{\text{argmax}} \min_n \gamma_n, \quad \text{for } n = 1, \dots, N, \\ &\text{subject to: } \mathbf{1}^T \mathbf{p} \leq P. \end{aligned} \quad (4.37)$$

where the unicast SINR γ_n is given by

$$\gamma_n = \frac{p_n \mathbf{u}_n^H \mathbf{G}_n \mathbf{u}_n}{\sum_{i=1, i \neq n}^N p_i \mathbf{u}_i^H \mathbf{G}_n \mathbf{u}_i + 1}, \quad (4.38)$$

and $\mathbf{G}_n = (\mathbf{h}_n^H \mathbf{h}_n) / \sigma_z^2 \in \mathbb{C}^{L \times L}$ denotes the normalized Gram matrix of the channel. Note that, when this SINR calculation is applied to the multicast case, pessimistic values are achieved, since even multicast users belonging to the same group are assumed to be interferers.

With the power and beamforming vectors being regarded separately, according to (4.34) and (4.35), the optimization problem is separated into two parts: power allocation and unit-norm beamforming determination. These two parts are explained in the following, and then the alternating optimization procedure is described.

The power allocation vector \mathbf{p} , given a fixed unit-norm beamforming matrix \mathbf{U} , can be determined by employing centralized power control [Zan92]. Let $\mathbf{S} \in \mathbb{R}^{N \times N}$ denote a diagonal matrix corresponding to the signal part of the transmission, and $\mathbf{\Psi} \in \mathbb{R}^{N \times N}$ the interference part. The elements of \mathbf{S} and $\mathbf{\Psi}$ are given by

$$S_{i,j} = \begin{cases} \mathbf{u}_i^H \mathbf{G}_i \mathbf{u}_i, & i = j \\ 0, & i \neq j \end{cases}, \quad \Psi_{i,j} = \begin{cases} 0, & i = j \\ \mathbf{u}_j^H \mathbf{G}_i \mathbf{u}_j, & i \neq j \end{cases}. \quad (4.39)$$

Assuming that all users achieve the same maximal SINR value γ_{\max} , the following equation holds

$$\mathbf{S} \mathbf{p} = \gamma_{\max} (\mathbf{\Psi} \mathbf{p} + \mathbf{1}) \implies \gamma_{\max}^{-1} \mathbf{p} = \mathbf{S}^{-1} \mathbf{\Psi} \mathbf{p} + \mathbf{S}^{-1} \mathbf{1}. \quad (4.40)$$

In order to achieve the maximal SINR, the power vector needs to employ the total available power P , i.e., $\mathbf{1}^T \mathbf{p} = P$. When left-multiplying (4.40) by $\mathbf{1}^T$ it becomes

$$\gamma_{\max}^{-1} = P^{-1} \mathbf{1}^T \mathbf{S}^{-1} \mathbf{\Psi} \mathbf{p} + P^{-1} \mathbf{1}^T \mathbf{S}^{-1} \mathbf{1}. \quad (4.41)$$

According to [SB04], an eigensystem can be formed based on (4.40) and (4.41):

$$\mathbf{\Upsilon} \mathbf{p}_{\text{ext}} = \gamma_{\text{max}}^{-1} \mathbf{p}_{\text{ext}}, \quad (4.42)$$

where $\mathbf{p}_{\text{ext}} = [\mathbf{p}^T \ 1]^T \in \mathbb{R}^{N+1}$ is an extended power vector, and $\mathbf{\Upsilon} \in \mathbb{R}^{(N+1) \times (N+1)}$ is an extended coupling matrix given by

$$\mathbf{\Upsilon} = \begin{bmatrix} \mathbf{S}^{-1} \mathbf{\Psi} & \mathbf{S}^{-1} \mathbf{1} \\ P^{-1} \mathbf{1}^T \mathbf{S}^{-1} \mathbf{\Psi} & P^{-1} \mathbf{1}^T \mathbf{S}^{-1} \end{bmatrix}. \quad (4.43)$$

The solution of the eigensystem leads to the optimal power vector, which is given by the first N components of the principal eigenvector of $\mathbf{\Upsilon}$ [SB04].

Next, the unit-norm beamforming optimization problem is discussed. Given a fixed power allocation, it has been shown in [SB04] for the unicast case that, due to the uplink/downlink duality, the optimal unit-norm beamformers can be obtained by performing maximization of the uplink SINR of each user independently. The optimization problem is expressed as

$$\begin{aligned} \mathbf{u}_{n,\text{opt}} &= \underset{\mathbf{u}_n}{\text{argmax}} \frac{\mathbf{u}_n^H \mathbf{G}_n \mathbf{u}_n}{\mathbf{u}_n^H \mathbf{Q}_n \mathbf{u}_n}, \quad \text{subject to: } \|\mathbf{u}_n\|^2 = 1, \\ \text{with } \mathbf{Q}_n &= \sum_{i=1, i \neq n}^N (q_i \mathbf{G}_i) + \mathbf{I}, \end{aligned} \quad (4.44)$$

where $\mathbf{q} \in \mathbb{R}^N$ represents the uplink power allocation vector, which may be obtained as the first N components of the principal eigenvector of the extended uplink coupling matrix $\mathbf{\Upsilon}^{(\text{ul})} \in \mathbb{R}^{(N+1) \times (N+1)}$ given by

$$\mathbf{\Upsilon}^{(\text{ul})} = \begin{bmatrix} \mathbf{S}^{-1} \mathbf{\Psi}^T & \mathbf{S}^{-1} \mathbf{1} \\ P^{-1} \mathbf{1}^T \mathbf{S}^{-1} \mathbf{\Psi}^T & P^{-1} \mathbf{1}^T \mathbf{S}^{-1} \end{bmatrix}. \quad (4.45)$$

The solution of (4.44) corresponds to the dominant generalized eigenvector of the pair $(\mathbf{G}_n, \mathbf{Q}_n)$.

Concluding the section, the alternating optimization algorithm is now explained. The algorithm consists of the alternating execution of the power allocation and unit-norm beamforming procedures, such as described in [SB04]. The dominant eigenvalue λ_{max} of the power allocation problem monotonically decreases after each iteration, so that the stop criterion is defined based on λ_{max} reaching a certain precision ϵ , i.e., $\lambda_{\text{max}}^{(i-1)} - \lambda_{\text{max}}^{(i)} < \epsilon$, where $(\cdot)^{(i)}$ indicates the i^{th} algorithm iteration. Given an arbitrary initial uplink power vector $\mathbf{q}^{(0)}$, the following steps are repeated until the desired precision is reached:

- Calculate $\mathbf{U}^{(i)}$ given the previous vector $\mathbf{q}^{(i-1)}$,
- Calculate $\mathbf{q}^{(i)}$ given matrix $\mathbf{U}^{(i)}$.

At the end, the downlink power allocation \mathbf{p} is calculated for the final matrix \mathbf{U} . The resulting multi-user unicast beamforming matrix $\mathbf{M}_{\text{SB}} \in \mathbb{C}^{L \times N}$ is given by

$$\mathbf{M}_{\text{SB}} = \mathbf{U} \text{diag}(\mathbf{p})^{1/2}. \quad (4.46)$$

When extending this procedure to the multi-group multicast case, there is an issue with the power constraint in (2.21) that needs to be clarified. In order to separate the beamforming matrix into the power and unit-norm beamforming parts, (4.35) has considered the following assumption:

$$\mathbb{E}\{|\|\mathbf{M}\mathbf{s}\|^2\} = \sum_{n=1}^N \sigma_s^2 \mathbf{m}_n^H \mathbf{m}_n, \quad (4.47)$$

which is only valid if the symbols within \mathbf{s} are uncorrelated, which is not true for the multi-group multicast case, since there are repeated symbols within \mathbf{s} . For this reason, an additional power normalization must be performed once after all iterations are concluded. The reduced-form beamforming matrix $\mathbf{M}'_{\text{SB}} \in \mathbb{C}^{L \times K}$ is finally given by

$$\mathbf{M}'_{\text{SB}} = \beta \mathbf{U} \text{diag}(\mathbf{p})^{1/2} \mathbf{T}^+, \quad (4.48)$$

with $\beta \in \mathbb{R}$ defined as

$$\beta = \sqrt{\frac{P}{\sigma_s^2 \text{tr}(\text{diag}(\mathbf{p})^{1/2} \mathbf{U}^H \mathbf{U} \text{diag}(\mathbf{p})^{1/2} \mathbf{T}^+ \mathbf{T}^+, \mathbf{T})}}. \quad (4.49)$$

4.4.4.2 Multicast-aware SINR balancing

In this section, the SINR balancing (SB) algorithm of the previous section is enhanced with the purpose of improving the performance of the multicast users. The proposed multicast-aware SB (MA-SB) algorithm, which has been introduced by the author of this thesis in [SK07b], is based on alternating optimization. MA-SB differs from algorithms proposed by previous works [GS06, KSL07] in that it does not require the application of the bisection method. The algorithms in [GS06, KSL07] actually solve the problem of minimizing the transmit power subject to SINR constraints, and the bisection method is required for iteratively adjusting the SINR target until the maximum worst-user SINR is achieved. MA-SB directly aims at maximizing the minimum SINR, and therefore it does not require the bisection method.

The optimization problem of determining the optimal reduced-form beamforming matrix $\mathbf{M}'_{\text{MA-SB}} \in \mathbb{C}^{L \times K}$ of MA-SB can be written as

$$\begin{aligned} \mathbf{M}'_{\text{MA-SB}} &= \underset{\mathbf{M}'}{\text{argmax}} \min_n \gamma_n, \quad \text{for } n = 1, \dots, N, \\ &\text{subject to: } \sigma_s^2 \text{tr}(\mathbf{M}'^H \mathbf{M}') \leq P. \end{aligned} \quad (4.50)$$

with the SINR γ_n defined as

$$\gamma_n = \frac{\sigma_s^2 \mathbf{m}_{b_n}^H \mathbf{G}_n \mathbf{m}'_{b_n}}{\sum_{k=1, k \neq b_n}^K \sigma_s^2 \mathbf{m}_k^H \mathbf{G}_n \mathbf{m}'_k + 1}, \quad (4.51)$$

and $\mathbf{G}_n = (\mathbf{h}_n^H \mathbf{h}_n) / \sigma_z^2 \in \mathbb{C}^{L \times L}$ denoting the normalized Gram matrix of the channel. Note that (4.50) and (4.51) express the same optimization problem of maximizing the minimum SINR as (4.1) and (4.2), respectively.

Even though the optimization problem is expressed in the reduced form, the proposed MA-SB algorithm is derived based on the complete form of the multi-group multicast scenario. This is necessary in order to make it possible to find a solution based on alternating optimization, similarly to the SB algorithm of the previous section. For this reason, the same notation is considered for the power vector $\mathbf{p} \in \mathbb{R}^N$ and unit-norm beamforming vectors $\mathbf{u}_n \in \mathbb{C}^L$ as defined in (4.35) and (4.34), respectively.

The MA-SB algorithm is described in the following. First, the power allocation procedure for a fixed matrix \mathbf{U} is presented, followed by the unit-norm beamforming given a fixed power allocation \mathbf{p} . These two procedures are alternately executed in an iterative fashion. After all iterations are concluded, a single power redistribution step is introduced in order to balance the SINRs among the unicast users and multicast groups.

In order to express the set of equations that determines the downlink power assignment given a fixed matrix \mathbf{U} , it is initially assumed that all users are unicast and that they achieve the same maximum SINR γ_{max} . Let $\mathbf{S} \in \mathbb{C}^{N \times N}$ denote a diagonal matrix corresponding to the signal part of the transmission, and $\mathbf{\Psi} \in \mathbb{C}^{N \times N}$ the interference part. For the multi-user unicast case, the elements of \mathbf{S} and $\mathbf{\Psi}$ are given in (4.39), and the power vector is determined based on the solution of the eigensystem expressed in (4.42).

For the multi-group multicast case, however, this procedure cannot be directly applied in the reduced form, since the power allocation would have to be done for each group, and not for each user. This results in a number of equations larger than the number of variables, i.e., there are still N SINR values to balance but only $K < N$ power elements to adjust. In this case it is not always possible to guarantee that all users achieve the same SINR and the system cannot be solved as an eigenvalue problem.

In order to simplify the procedure and allow the multi-group multicast power allocation to be also expressed as an eigensystem, it is here assumed that the power allocation

can be done user-wise, i.e., vector \mathbf{p} contains N elements, and the elements of matrices \mathbf{S} and $\mathbf{\Psi}$ are now defined as:

$$S_{i,j} = \begin{cases} \left(\sum_{n=1, b_n=b_i}^N \mathbf{u}_n^H \right) \mathbf{G}_i \left(\sum_{n=1, b_n=b_i}^N \mathbf{u}_n \right), & i = j \\ 0, & i \neq j \end{cases}, \quad (4.52a)$$

$$\Psi_{i,j} = \begin{cases} 0, & b_i = b_j \\ \mathbf{u}_j^H \mathbf{G}_i \mathbf{u}_j, & b_i \neq b_j \end{cases}. \quad (4.52b)$$

Matrices \mathbf{S} and $\mathbf{\Psi}$ are chosen so that when they are substituted in the SINR expression in (4.40), the actual SINR perceived by the users is approximated, while still allowing the system to be solved as an eigenvalue problem. The solution corresponds to the principal eigenvector of the extended coupling matrix, defined in (4.43), but considering the new \mathbf{S} and $\mathbf{\Psi}$ matrices of (4.52). Assuming that

$$\mathbf{m}'_{b_n} = \sum_{i=1, b_i=b_n}^N \mathbf{m}_i = \sum_{i=1, b_i=b_n}^N \sqrt{p_i/\sigma_s^2} \mathbf{u}_i, \quad (4.53)$$

the actual and approximate complete-form SINR expressions are, respectively:

$$\gamma_n = \frac{\left(\sum_{i=1, b_i=b_n}^N \sqrt{p_i} \mathbf{u}_i^H \right) \mathbf{G}_n \left(\sum_{i=1, b_i=b_n}^N \sqrt{p_i} \mathbf{u}_i \right)}{\sum_{k=1, k \neq b_n}^K \left(\sum_{i=1, b_i=k}^N \sqrt{p_i} \mathbf{u}_i^H \right) \mathbf{G}_n \left(\sum_{i=1, b_i=k}^N \sqrt{p_i} \mathbf{u}_i \right) + 1}, \quad (4.54a)$$

$$\gamma_n \simeq \frac{p_n \left(\sum_{i=1, b_i=b_n}^N \mathbf{u}_i^H \right) \mathbf{G}_n \left(\sum_{i=1, b_i=b_n}^N \mathbf{u}_i \right)}{\sum_{k=1, k \neq b_n}^K \left(\sum_{i=1, b_i=k}^N p_i \mathbf{u}_i^H \mathbf{G}_n \mathbf{u}_i \right) + 1}. \quad (4.54b)$$

The approximation of the signal part in (4.54b) corresponds to considering the power of only the n^{th} user and disregarding the power of the other users belonging to the same group. With regard to the interference part, it is a worst-case approximation which considers all interferers as unicast users, instead of taking into account the equivalent group beamforming vectors.

Regarding the determination of the unit-norm beamformers, a similar approach to that of [SB04], which has been presented in the previous section, is considered. The optimization problem for the unit-norm beamformer of user n is written as

$$\mathbf{u}_{n,\text{opt}} = \underset{\mathbf{u}_n}{\operatorname{argmax}} \frac{\mathbf{u}_n^H \mathbf{G}_n \mathbf{u}_n}{\mathbf{u}_n^H \mathbf{Q}_n \mathbf{u}_n}, \quad \text{subject to: } \|\mathbf{u}_n\|^2 = 1, \quad (4.55)$$

$$\text{with } \mathbf{Q}_n = \sum_{i=1, b_i \neq b_n}^N q_i \mathbf{G}_i + \mathbf{I},$$

where $\mathbf{q} \in \mathbb{R}^N$ represents the uplink power allocation vector, which may be determined as the principal eigenvector of the extended uplink coupling matrix defined in (4.45), with the \mathbf{S} and $\mathbf{\Psi}$ matrices given in (4.52a) and (4.52b), respectively. The solution of (4.55) corresponds to the dominant generalized eigenvector of the pair $(\mathbf{G}_n, \mathbf{Q}_n)$. The difference with regard to the multi-user unicast case lies in the definition of matrix \mathbf{Q}_n , which has been modified in order to avoid interference within a same multicast group.

The MA-SB algorithm consists of the alternating optimization of the power allocation and unit-norm beamforming procedures, such as described in [SB04]. Similarly to the previous section, the stop criterion is based on the principal eigenvalue of the extended coupling matrix. Given an arbitrary initial uplink power vector $\mathbf{q}^{(0)}$, the following steps are repeated until the desired precision is reached:

- Calculate $\mathbf{U}^{(i)}$ given the previous vector $\mathbf{q}^{(i-1)}$,
- Calculate $\mathbf{q}^{(i)}$ given matrix $\mathbf{U}^{(i)}$.

At the end, the downlink power allocation \mathbf{p} is calculated for the final matrix \mathbf{U} . The resulting complete-form modulation matrix is given by

$$\mathbf{M}_{\text{MA-SB}} = \beta \mathbf{U} \text{diag}(\mathbf{p})^{1/2}, \quad (4.56)$$

where $\beta \in \mathbb{R}$ is a normalization factor related to the total transmit power constraint, which is given by

$$\beta = \sqrt{\frac{P}{\text{tr}(\text{diag}(\mathbf{p})^{1/2} \mathbf{U}^H \mathbf{U} \text{diag}(\mathbf{p})^{1/2} \mathbf{R}_s)}}. \quad (4.57)$$

Due to the SINR approximation considered for the power allocation procedure, the SINR balancing is not achieved for all users. In fact, it is perceived that the SINR of the unicast users reaches a certain balanced level, and that the average SINR of the users of the multicast group also approaches this level, but not each individual multicast user.

In order to improve the worst-user performance, a power redistribution among the multicast and unicast users is proposed here. This procedure is a further refinement of the algorithm, and is performed only a single time after the iterative algorithm has stopped. Let $\mathbf{p}' \in \mathbb{R}^K$ represent the group power allocation vector and $\mathbf{u}'_k \in \mathbb{C}^L$ the unit-norm beamforming vector of group k , such that $p'_k = \|\mathbf{m}'_k\|^2$, $\mathbf{u}'_k = \mathbf{m}'_k / \|\mathbf{m}'_k\|$, and $\mathbf{U}' = [\mathbf{u}'_1, \dots, \mathbf{u}'_K] \in \mathbb{C}^{L \times K}$. The users with lowest SINR are selected to represent each group, such that $\mathbf{G}'_k = \mathbf{G}_n |_{\gamma_n = \min \gamma_k}$, where $\gamma \in \mathbb{R}^N$ corresponds to the SINR

vector that results from the application of $\mathbf{M}_{\text{MA-SB}}$, and the vector $\boldsymbol{\gamma}_k \in \mathbb{R}^{g_k}$ contains the SINR of the users belonging to group k .

The unit-norm beamforming vectors \mathbf{u}'_k calculated at the last iteration of the alternating optimization are maintained, and the power vector \mathbf{p}' is recalculated by solving the system:

$$\begin{cases} \gamma_{max}^{-1} \mathbf{p}' = \mathbf{S}'^{-1} \boldsymbol{\Psi}' \mathbf{p}' + \mathbf{S}'^{-1} \mathbf{1} \\ \mathbf{1}^T \mathbf{p}' = P \end{cases}, \quad (4.58)$$

for which the elements of $\mathbf{S}' \in \mathbb{R}^{K \times K}$ and $\boldsymbol{\Psi}' \in \mathbb{R}^{K \times K}$ are given by

$$S'_{i,i} = \begin{cases} \mathbf{u}_i^H \mathbf{G}'_i \mathbf{u}'_i, & i = j \\ 0, & i \neq j \end{cases}, \quad \Psi'_{i,j} = \begin{cases} 0, & i = j \\ \mathbf{u}_j^H \mathbf{G}'_i \mathbf{u}'_j, & i \neq j \end{cases}. \quad (4.59)$$

The solution corresponds to the first K elements of the principal eigenvector of the extended coupling matrix $\boldsymbol{\Upsilon}' \in \mathbb{R}^{(K+1) \times (K+1)}$ given by

$$\boldsymbol{\Upsilon}' = \begin{bmatrix} \mathbf{S}'^{-1} \boldsymbol{\Psi}' & \mathbf{S}'^{-1} \mathbf{1} \\ P^{-1} \mathbf{1}^T \mathbf{S}'^{-1} \boldsymbol{\Psi}' & P^{-1} \mathbf{1}^T \mathbf{S}'^{-1} \end{bmatrix}. \quad (4.60)$$

The obtained power re-allocation vector is denoted \mathbf{p}'_{PR} . It is applied to the unit-norm beamforming, without the need of further power normalization, such that the reduced-form modulation matrix is given by

$$\mathbf{M}'_{\text{MA-SB}} = \mathbf{U}' \text{diag}(\mathbf{p}'_{\text{PR}})^{1/2}. \quad (4.61)$$

4.5 Non-linear algorithms

4.5.1 Tomlinson-Harashima precoding based algorithms

4.5.1.1 Tomlinson-Harashima precoding

In this section, the Tomlinson-Harashima Precoding (THP) algorithm is described in the context of the multi-group multicast scenario. In Section 3.4.4, the zero-forcing THP algorithm has already been presented in the context of a single-group multicast scenario. The filter parameters have been considered in the complete form, and it has been discussed that, due to the non-linear precoding of the symbols through the modulo operator located within the feedback filter $\mathbf{F} \in \mathbb{C}^{N \times N}$ shown in Fig. 3.1, the precoded symbol vector $\mathbf{v} \in \mathbb{C}^N$ in (3.41b) does not have repeated entries. For this

reason, the multi-user unicast definition of THP in [WVH04, Joh04] can be directly applied to both single-group and multi-group multicast scenarios.

The expressions for the modulation matrix $\mathbf{M} \in \mathbb{C}^{L \times N}$, the feedback filter $\mathbf{F} \in \mathbb{C}^{N \times N}$, and the receive filter $\mathbf{D} \in \mathbb{C}^{N \times N}$, respectively, are given in (3.43a), (3.43b), and (3.44), which are repeated here for the sake of completeness

$$\mathbf{M}_{\text{THP}} = \sqrt{\frac{P}{\text{tr}(\mathbf{R}_v \mathbf{L}_d^{-2})}} \mathbf{H}^H \mathbf{L}^{H,-1} \mathbf{L}_d^{-1}, \quad (4.62a)$$

$$\mathbf{F}_{\text{THP}} = \mathbf{I} - \mathbf{L} \mathbf{L}_d^{-1}, \quad (4.62b)$$

$$\mathbf{D}_{\text{THP}} = \sqrt{\frac{\text{tr}(\mathbf{R}_v \mathbf{L}_d^{-2})}{P}} \mathbf{I}, \quad (4.62c)$$

where $\mathbf{L} \in \mathbb{C}^{N \times N}$ is a lower triangular matrix that comes from the Cholesky factorization of the channel ($\mathbf{H}\mathbf{H}^H = \mathbf{L}\mathbf{L}^H$) [GL96], $\mathbf{L}_d \in \mathbb{R}^{N \times N}$ is a diagonal matrix containing the elements of the main diagonal of \mathbf{L} , and $\mathbf{R}_v \in \mathbb{C}^{N \times N}$ is the covariance matrix of the precoded data vector \mathbf{v} . For more details, see Section 3.4.4.

4.5.1.2 Multicast-aware Tomlinson-Harashima precoding

In this section, multicast awareness is taken into account by the THP algorithm with the purpose of improving the performance of the multicast users. The proposed algorithm is referred to a multicast-aware THP (MA-THP). Considering the reduced form of the multi-group multicast scenario, the THP transmission chain comprises a linear transmission filter $\mathbf{M}' \in \mathbb{C}^{L \times K}$ as well as a feedback filter $\mathbf{F}' \in \mathbb{C}^{K \times K}$. The former is responsible for eliminating part of the interference, such that the equivalent channel matrix $\mathbf{H}\mathbf{M}'$ is lower triangular. In the case of multi-user unicast, this triangularization can be achieved by employing the QR decomposition or Cholesky factorization [WVH04, Joh04]. For the multi-group multicast scenario, however, these methods do not apply, since $\mathbf{H}\mathbf{M}'$ is no longer a square matrix. Nevertheless, it is still possible to eliminate the interference by performing null space projections, such as in [SK06b, LK05, SSH04]. The MA-THP algorithm proposed in this section, which has been introduced by the author of this thesis in [SK07a], is based on these null space projections.

Let \mathbf{h}_n denote the n^{th} row of matrix \mathbf{H} and \mathbf{m}'_k the k^{th} column of matrix \mathbf{M}' . The following constraints must be satisfied:

$$\mathbf{h}_n \mathbf{m}'_k = 0 \quad \forall n, k \mid b_n < k, \quad (4.63)$$

where $n \in \{1, \dots, N\}$ and $k \in \{1, \dots, K\}$. This can be achieved by projecting each group beamformer \mathbf{m}'_k onto the null space associated to the channels of the users of previous groups.

The feedback matrix $\mathbf{F}' \in \mathbb{C}^{K \times K}$ is responsible for successively cancelling the remaining interference. In order to fulfill the causality constraint [Joh04], \mathbf{F}' must be lower triangular with the main diagonal composed of zeros. Let matrix $\mathbf{P}' \in \mathbb{C}^{K \times K}$ be defined as $\mathbf{P}' = (\mathbf{I} - \mathbf{F}')^{-1}$, then $(\mathbf{I} - \mathbf{F}')$ as well as \mathbf{P}' are also lower triangular but with the main diagonal composed of ones.

The effect that is expected from the transmission processing is that the interference among multicast groups be totally cancelled, therefore \mathbf{P}' must also satisfy

$$\mathbf{H}\mathbf{M}'\mathbf{P}' = \text{diag}_b(\mathbf{H}\mathbf{M}'), \quad (4.64)$$

where the $\text{diag}_b(\cdot)$ operator returns a matrix $\mathbf{Y} = \text{diag}_b(\mathbf{X})$, whose elements satisfy the following expression:

$$(\mathbf{Y})_{n,k} = \begin{cases} (\mathbf{X})_{n,k} & , \quad \text{for } b_n = k \\ 0 & , \quad \text{otherwise} \end{cases}. \quad (4.65)$$

Alternatively, by employing the element-wise product with regard to the transformation matrix \mathbf{T}^+ , (4.64) can also be written as

$$\mathbf{H}\mathbf{M}'\mathbf{P}' = \mathbf{H}\mathbf{M}' \odot \mathbf{T}^+. \quad (4.66)$$

One problem that arises from the fact that \mathbf{P}' has dimension K lower than N is that it is not always possible to find a lower triangular matrix \mathbf{P}' satisfying (4.64). In order to obtain a feasible solution it is necessary to impose additional constraints on matrix \mathbf{M}' . These constraints can be obtained by writing (4.64) with \mathbf{M}' already satisfying (4.63) and \mathbf{P}' as a lower triangular matrix with unit diagonal. For example, considering the exemplary scenario with two unicast users and one multicast group composed of two users, (4.64) could be written as

$$\begin{bmatrix} \mathbf{h}_1\mathbf{m}'_1 & 0 & 0 \\ \mathbf{h}_2\mathbf{m}'_1 & \mathbf{h}_2\mathbf{m}'_2 & 0 \\ \mathbf{h}_3\mathbf{m}'_1 & \mathbf{h}_3\mathbf{m}'_2 & \mathbf{h}_3\mathbf{m}'_3 \\ \mathbf{h}_4\mathbf{m}'_1 & \mathbf{h}_4\mathbf{m}'_2 & \mathbf{h}_4\mathbf{m}'_3 \end{bmatrix} \begin{bmatrix} 1 & 0 & 0 \\ P'_{2,1} & 1 & 0 \\ P'_{3,1} & P'_{3,2} & 1 \end{bmatrix} = \begin{bmatrix} \mathbf{h}_1\mathbf{m}'_1 & 0 & 0 \\ 0 & \mathbf{h}_2\mathbf{m}'_2 & 0 \\ 0 & 0 & \mathbf{h}_3\mathbf{m}'_3 \\ 0 & 0 & \mathbf{h}_4\mathbf{m}'_3 \end{bmatrix}, \quad (4.67)$$

which only has a feasible solution if

$$\frac{\mathbf{h}_3\mathbf{m}'_1}{\mathbf{h}_3\mathbf{m}'_3} = \frac{\mathbf{h}_4\mathbf{m}'_1}{\mathbf{h}_4\mathbf{m}'_3} \quad \text{and} \quad \frac{\mathbf{h}_3\mathbf{m}'_2}{\mathbf{h}_3\mathbf{m}'_3} = \frac{\mathbf{h}_4\mathbf{m}'_2}{\mathbf{h}_4\mathbf{m}'_3}. \quad (4.68)$$

Let $\mathbf{H}_k \in \mathbb{C}^{g_k \times L}$ denote the channel matrix of group k , and $\mathbf{h}_{(k,i)} \in \mathbb{C}^{1 \times L}$ the channel of the i^{th} user within group k . When generalizing the problem, the following set of constraints needs to be taken into account for each group k :

$$\begin{aligned} \frac{\mathbf{h}_{(k,1)} \mathbf{m}'_1}{\mathbf{h}_{(k,1)} \mathbf{m}'_k} &= \frac{\mathbf{h}_{(k,2)} \mathbf{m}'_1}{\mathbf{h}_{(k,2)} \mathbf{m}'_k} = \dots = \frac{\mathbf{h}_{(k,g_k)} \mathbf{m}'_1}{\mathbf{h}_{(k,g_k)} \mathbf{m}'_k}, \\ \frac{\mathbf{h}_{(k,1)} \mathbf{m}'_2}{\mathbf{h}_{(k,1)} \mathbf{m}'_k} &= \frac{\mathbf{h}_{(k,2)} \mathbf{m}'_2}{\mathbf{h}_{(k,2)} \mathbf{m}'_k} = \dots = \frac{\mathbf{h}_{(k,g_k)} \mathbf{m}'_2}{\mathbf{h}_{(k,g_k)} \mathbf{m}'_k}, \\ &\vdots \qquad \qquad \qquad \vdots \qquad \qquad \qquad \ddots \qquad \qquad \qquad \vdots \\ \frac{\mathbf{h}_{(k,1)} \mathbf{m}'_{k-1}}{\mathbf{h}_{(k,1)} \mathbf{m}'_k} &= \frac{\mathbf{h}_{(k,2)} \mathbf{m}'_{k-1}}{\mathbf{h}_{(k,2)} \mathbf{m}'_k} = \dots = \frac{\mathbf{h}_{(k,g_k)} \mathbf{m}'_{k-1}}{\mathbf{h}_{(k,g_k)} \mathbf{m}'_k}. \end{aligned} \quad (4.69)$$

This results in a total of $\sum_{k=1}^K (k-1)(g_k-1)$ additional constraints. Note that only groups with more than one user ($g_k > 1$) and which appear after the first position ($k > 1$) generate these constraints.

Due to this relationship among the beamforming vectors of the different groups, it is not possible to optimize them individually. Let $\mathbf{r}_k \in \mathbb{C}^{g_k \times 1}$ represent the power received by the users within each group, i.e., $\mathbf{r}_k = \text{diag}(\mathbf{H}_k \mathbf{m}'_k \mathbf{m}'_k^H \mathbf{H}_k^H)$. The joint optimization problem corresponds to finding the matrix \mathbf{M}' which maximizes the minimum energy received by the users, i.e.,

$$\begin{aligned} \mathbf{M}'_{\text{opt}} &= \underset{\mathbf{M}'}{\text{argmax}} \min([\mathbf{r}_1^T, \mathbf{r}_2^T, \dots, \mathbf{r}_K^T]^T), \\ &\text{subject to (4.63), (4.69), and } \text{tr}(\mathbf{M}'^H \mathbf{M}' \mathbf{R}'_v) = P, \end{aligned} \quad (4.70)$$

where the $\min(\cdot)$ operator is assumed to return the minimum element of the vector passed as argument.

In order to avoid such a complex optimization procedure, a suboptimum methodology which independently determines each beamforming vector is here proposed. The beamforming vector \mathbf{m}'_k of each group is assumed to lie in the null space of the following vectors:

$$\begin{aligned} \mathbf{h}_n, \quad \forall n \mid b_n < k, \\ \frac{\mathbf{h}_{(i,g_i)}}{\mathbf{h}_{(i,g_i)} \mathbf{m}'_i} - \frac{\mathbf{h}_{(i,j)}}{\mathbf{h}_{(i,j)} \mathbf{m}'_i}, \quad \forall i, j \mid i > k \text{ and } j < g_i, \end{aligned} \quad (4.71)$$

where $n \in \{1, \dots, N\}$, $i \in \{1, \dots, K\}$, and $j \in \{1, \dots, N\}$. The dependency among the beamforming vectors can be resolved by beginning the calculation from the last one ($k = K$) and proceeding until the first one ($k = 1$). After each null space projection, the remaining degrees of freedom for determining \mathbf{m}'_k can be exploited by performing single-group multicast beamforming, which can be done according to the algorithms described in Section 3.4.

Let $\mathbf{H}_k \in \mathbb{C}^{g_k \times L}$ denote the channel matrix of the users belonging to group k and $\tilde{\mathbf{H}}_k \in \mathbb{C}^{(L-A_k) \times L}$ denote the concatenation of the vectors defined in (4.71) for group k . The null space of $\tilde{\mathbf{H}}_k$ can be obtained through SVD, and it is denoted by $\tilde{\mathbf{V}}_k^{(0)} \in \mathbb{C}^{L \times A_k}$. The dimension A_k is given by

$$A_k = L - \sum_{i=1}^{k-1} g_i - \sum_{i=k+1}^K (g_i - 1) = L - N + K + g_k - k, \quad (4.72)$$

assuming that matrix \mathbf{H} has full row rank. The equivalent channel matrix $\mathbf{H}_k^{(\text{eq})} \in \mathbb{C}^{g_k \times A_k}$ after the projection is given by $\mathbf{H}_k^{(\text{eq})} = \mathbf{H}_k \tilde{\mathbf{V}}_k^{(0)}$. The multicast beamforming procedure is done considering $\mathbf{H}_k^{(\text{eq})}$ and results in the beamforming vector $\mathbf{m}_k^{(\text{eq})} \in \mathbb{C}^{A_k \times 1}$. The k^{th} column of the modulation matrix \mathbf{M}' is then set to $\mathbf{m}'_k = \tilde{\mathbf{V}}_k^{(0)} \mathbf{m}_k^{(\text{eq})}$, i.e.,

$$\mathbf{M}' = [\tilde{\mathbf{V}}_1^{(0)} \mathbf{m}_1^{(\text{eq})}, \dots, \tilde{\mathbf{V}}_K^{(0)} \mathbf{m}_K^{(\text{eq})}]. \quad (4.73)$$

It should be noted that the independent optimization of \mathbf{m}'_k balances the energy within each group, but not among different groups, due to the projections required by (4.71). For this reason it is required that the available energy be redistributed among the groups, so that the balancing effect between groups can be achieved. The power redistribution matrix $\mathbf{\Gamma} \in \mathbb{R}^{K \times K}$ is defined as

$$\mathbf{\Gamma} = \text{diag}([\min(|\mathbf{H}_1 \tilde{\mathbf{V}}_1^{(0)} \mathbf{m}_1^{(\text{eq})}|), \dots, \min(|\mathbf{H}_K \tilde{\mathbf{V}}_K^{(0)} \mathbf{m}_K^{(\text{eq})}|)]^T)^{-1}. \quad (4.74)$$

In order to satisfy the transmit power constraint, a scalar variable $\beta \in \mathbb{R}$ is defined as

$$\beta = \sqrt{\frac{P}{\text{tr}(\mathbf{R}'_v \mathbf{M}'^H \mathbf{M}' \mathbf{\Gamma}^2)}}. \quad (4.75)$$

Finally, the matrix $\mathbf{M}'_{\text{MA-THP}} \in \mathbb{C}^{L \times K}$ of the MA-THP algorithm is given by

$$\mathbf{M}'_{\text{MA-THP}} = \beta \mathbf{M}' \mathbf{\Gamma}, \quad (4.76)$$

with β , \mathbf{M}' , and $\mathbf{\Gamma}$, defined, respectively, in (4.75), (4.73), and (4.74).

The matrix $\mathbf{M}'_{\text{MA-THP}}$ lying in the null space of (4.71) allows a feasible solution of (4.64). The filter $\mathbf{F}'_{\text{MA-THP}}$ can then be calculated as

$$\begin{aligned} \mathbf{F}'_{\text{MA-THP}} &= \mathbf{I} - [(\mathbf{H} \mathbf{M}' \mathbf{\Gamma})^+ \text{diag}_b(\mathbf{H} \mathbf{M}' \mathbf{\Gamma})]^{-1} \\ &= \mathbf{I} - [(\mathbf{H} \mathbf{M}' \mathbf{\Gamma})^+ (\mathbf{H} \mathbf{M}' \mathbf{\Gamma} \odot \mathbf{T}^+)]^{-1}. \end{aligned} \quad (4.77)$$

The performance of THP depends strongly on how the data streams are ordered prior to transmission. The best ordering is the one which minimizes the impact of the

null space projections, such that the least amount of energy is lost. The optimum ordering can only be determined by exhaustively searching among all $N!$ possibilities. However, there exist more computationally efficient ordering methods which reasonably approximate the optimal performance [JSBU07]. In the case of MA-THP, the number of possible orderings is reduced from $N!$ to $K!$, since the position of the users within each group does not impact the performance. On the other hand, MA-THP presents the drawback of the additional null space projections. This may lead to cases in which THP outperforms MA-THP.

4.5.2 Vector precoding based algorithms

4.5.2.1 Vector precoding

In this section, the Vector Precoding (VP) algorithm is described and formulated. Similarly to the THP algorithm of Section 4.5.1.1, the multi-user unicast definition of VP is directly applied to the multi-group multicast scenario. The VP technique, which is also known as vector perturbation technique or modulo precoding technique [PHS05, HPS05], can be interpreted as a generalization of the THP algorithm [PJU06, JSBU07]. Fig. 4.1 depicts the transmission chain of the VP algorithm [JSBU07], which reminds of the linear representation of THP shown in Fig. 3.1, but without the feedback loop.

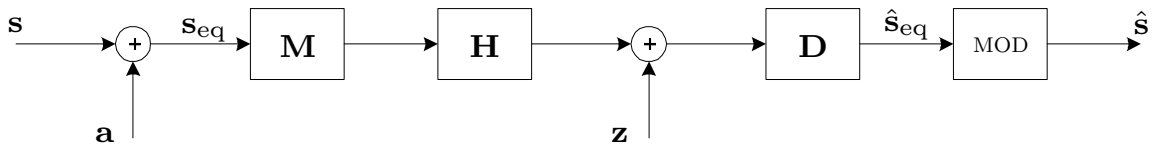


Figure 4.1. VP transmission chain.

A perturbation vector $\mathbf{a} \in \mathbb{C}^N$ is introduced, which has the purpose of modifying the data symbol vector $\mathbf{s} \in \mathbb{C}^N$ such that it becomes approximately orthogonal to the channel inverse \mathbf{H}^{-1} [HPS05], thus improving the energy efficiency of the precoding process. This perturbation depends on the current symbol vector \mathbf{s} , i.e., it needs to be calculated for each transmitted symbol vector. Furthermore, in order to allow the modulo receivers to be capable of detecting the original symbol vector, the perturbation must be of the form

$$\mathbf{a} = \tau(\mathbf{x} + j\mathbf{y}), \quad (4.78)$$

where $\mathbf{x} \in \mathbb{Z}^N$, $\mathbf{y} \in \mathbb{Z}^N$, and $\tau \in \mathbb{R}$ is equivalent to the THP parameter of the same name, which depends on the modulation scheme and is used by the modulo operator.

It is assumed that the linear transmit filter \mathbf{M} implements a zero-forcing algorithm, which is given by

$$\mathbf{M} = \beta \mathbf{H}^H (\mathbf{H} \mathbf{H}^H)^{-1}, \quad (4.79)$$

with $\beta \in \mathbb{R}$. The optimization problem for determining the optimal vector \mathbf{a}_{VP} can be expressed as

$$\mathbf{a}_{\text{VP}} = \underset{\{\mathbf{a}\}}{\operatorname{argmin}} \|\mathbf{M}(\mathbf{s} + \mathbf{a})\|^2, \quad \text{subject to: (4.78)}, \quad (4.80)$$

which, when substituting (4.79) in (4.80), can also be written as

$$\mathbf{a}_{\text{VP}} = \underset{\{\mathbf{a}\}}{\operatorname{argmin}} (\mathbf{s} + \mathbf{a})^H (\mathbf{H} \mathbf{H}^H)^{-1} (\mathbf{s} + \mathbf{a}), \quad \text{subject to: (4.78)}. \quad (4.81)$$

Note that β has been disregarded from (4.81), since it is only an energy normalization parameter. The optimization problem in (4.81) corresponds to a closest point search in a lattice [AEVZ02], which was shown in [Mic01] to be NP-hard. Nevertheless, there exist efficient suboptimal solutions to this problem. The THP algorithm is one of them, representing a practical way of determining \mathbf{a} , which is done through channel triangularization and successive interference cancellation at the feedback filter. THP achieves good results when appropriate ordering strategies are employed [JSBU07]. In [HPS05], the vector perturbation technique is introduced for the multi-user unicast case and an algorithm based on the QR decomposition and successive interference cancellation, similar to THP, is also proposed.

Lattice reduction techniques, such as in [WFH04,PJU06], can also be applied in order to obtain simple and efficient methods for determining the solution to (4.81). Particularly, the Lenstra-Lenstra-Lovász (LLL) algorithm [LLJL82] can be used to find a reduced basis, and the closest point search can be efficiently performed through the Schnorr-Euchner algorithm [SE94].

It is assumed that the frame duration consists of a total of N_s symbol intervals, and that for the whole frame duration the channel does not change significantly. For each discrete-time symbol interval i , the optimal perturbation vector is calculated using one of the aforementioned techniques. The transmit power constraint needs to take into account the average power during the frame period, being expressed as

$$\frac{1}{N_s} \sum_{i=1}^{N_s} \|\mathbf{M} \mathbf{s}_{\text{eq}}[i]\|^2 \leq P. \quad (4.82)$$

Substituting (4.79) in (4.82), and considering that all available power is used, the normalization factor β can be calculated. The resulting modulation matrix $\mathbf{M}_{\text{VP}} \in$

$\mathbb{C}^{L \times N}$ is given by

$$\mathbf{M}_{\text{VP}} = \sqrt{\frac{N_s P}{\sum_{i=1}^{N_s} \mathbf{s}_{\text{eq}}^{\text{H}}[i] (\mathbf{H}\mathbf{H}^{\text{H}})^{-1} \mathbf{s}_{\text{eq}}[i]}} \mathbf{H}^{\text{H}} (\mathbf{H}\mathbf{H}^{\text{H}})^{-1}, \quad (4.83)$$

and the receive filter can be expressed as

$$\mathbf{D}_{\text{VP}} = \sqrt{\frac{\sum_{i=1}^{N_s} \mathbf{s}_{\text{eq}}^{\text{H}}[i] (\mathbf{H}\mathbf{H}^{\text{H}})^{-1} \mathbf{s}_{\text{eq}}[i]}{N_s P}} \mathbf{I}. \quad (4.84)$$

4.5.2.2 Multicast-aware vector precoding

In this section, the multicast-aware VP (MA-VP) algorithm is proposed. The VP algorithm presented in the previous section uses ZF for determining the beamforming matrix. The MA-VP algorithm, however, considers the MA-ZF approach for calculating matrix $\mathbf{M}' \in \mathbb{C}^{L \times K}$.

Let $\mathbf{s}' \in \mathbb{C}^K$ denote the reduced form of the symbol vector, then the perturbation vector also has a reduced dimension $\mathbf{a}' \in \mathbb{C}^K$, and the precoded symbol vector $\mathbf{s}'_{\text{eq}} \in \mathbb{C}^K$ is defined as $\mathbf{s}'_{\text{eq}} = \mathbf{s}' + \mathbf{a}'$.

Matrix $\tilde{\mathbf{H}}_k \in \mathbb{C}^{(N-g_k) \times L}$ and its SVD are given by

$$\tilde{\mathbf{H}}_k = [\mathbf{H}_1^T, \dots, \mathbf{H}_{k-1}^T, \mathbf{H}_{k+1}^T, \dots, \mathbf{H}_K^T]^T, \quad (4.85a)$$

$$\tilde{\mathbf{H}}_k = \tilde{\mathbf{U}}_k \tilde{\mathbf{S}}_k [\tilde{\mathbf{V}}_k^{(1)}, \tilde{\mathbf{V}}_k^{(0)}]^{\text{H}}, \quad (4.85b)$$

where $\mathbf{H}_k \in \mathbb{C}^{g_k \times L}$, $\tilde{\mathbf{U}}_k \in \mathbb{C}^{(N-g_k) \times (N-g_k)}$, $\tilde{\mathbf{S}}_k \in \mathbb{R}^{(N-g_k) \times L}$, $\tilde{\mathbf{V}}_k^{(1)} \in \mathbb{C}^{L \times \tilde{r}_k}$, $\tilde{\mathbf{V}}_k^{(0)} \in \mathbb{C}^{L \times (L-\tilde{r}_k)}$, and \tilde{r}_k denotes the rank of matrix $\tilde{\mathbf{H}}_k$.

The multicast beamforming optimization, which can be implemented according to any of the algorithms in Section 3.4, is done for each group considering the equivalent channel after the null-space projection $\mathbf{H}_k^{(\text{eq})} = \mathbf{H}_k \tilde{\mathbf{V}}_k^{(0)} \in \mathbb{C}^{g_k \times (N-\tilde{r}_k)}$, and resulting in the beamforming vector $\mathbf{m}_k^{(\text{eq})} \in \mathbb{C}^{(N-\tilde{r}_k)}$.

The beamforming matrix $\mathbf{M}'_{\text{MA-VP}} \in \mathbb{C}^{L \times K}$ of the MA-VP algorithm can be written as

$$\mathbf{M}'_{\text{MA-VP}} = \beta \mathbf{M}' \mathbf{\Gamma}, \quad (4.86)$$

with

$$\mathbf{M}' = [\tilde{\mathbf{V}}_1^{(0)} \mathbf{m}_1^{(\text{eq})}, \dots, \tilde{\mathbf{V}}_K^{(0)} \mathbf{m}_K^{(\text{eq})}], \quad (4.87\text{a})$$

$$\mathbf{\Gamma} = \text{diag}(\min(|\mathbf{H}_1 \tilde{\mathbf{V}}_1^{(0)} \mathbf{m}_1^{(\text{eq})}|), \dots, \min(|\mathbf{H}_K \tilde{\mathbf{V}}_K^{(0)} \mathbf{m}_K^{(\text{eq})}|))^{-1}, \quad (4.87\text{b})$$

where $\beta \in \mathbb{R}$, $\mathbf{M}' \in \mathbb{C}^{L \times K}$, and $\mathbf{\Gamma} \in \mathbb{R}^{K \times K}$. The β parameter depends on the perturbation vector and is calculated at the end of the section.

The perturbation vector \mathbf{a}' must have integer components, such that

$$\mathbf{a}' = \tau(\mathbf{x} + \mathbf{j}\mathbf{y}), \quad (4.88)$$

where $\mathbf{x} \in \mathbb{Z}^K$, $\mathbf{y} \in \mathbb{Z}^K$, and $\tau \in \mathbb{R}$. The optimal \mathbf{a}' corresponds to the solution of the following optimization problem

$$\mathbf{a}'_{\text{MA-VP}} = \underset{\{\mathbf{a}'\}}{\text{argmin}} \|\mathbf{M}'\mathbf{\Gamma}(\mathbf{s}' + \mathbf{a}')\|^2, \quad \text{subject to: (4.88)}. \quad (4.89)$$

Assuming a frame duration of N_s symbol intervals, the optimal perturbation vector is calculated for each discrete-time symbol interval i using one of the techniques mentioned in the previous section, e.g., Schnorr-Euchner algorithm [SE94]. The energy normalization parameter β is given by

$$\beta = \sqrt{\frac{N_s P}{\sum_{i=1}^{N_s} \mathbf{s}'_{\text{eq}}[i]^H \mathbf{\Gamma} \mathbf{M}'^H \mathbf{M}' \mathbf{\Gamma} \mathbf{s}'_{\text{eq}}[i]}}. \quad (4.90)$$

4.5.3 Hybrid linear and non-linear precoding

Another possible beamforming approach for the multi-group multicast case is to employ a mix of linear and non-linear precoding schemes. Assuming a scenario in which there are several unicast users, i.e., more than one multicast group of size 1, the term “unicast group” is adopted to denote the set of all unicast users. The idea is to employ linear precoding to mitigate the interference among the multicast groups and the unicast group, and non-linear precoding to mitigate the interference within the unicast group. The proposed Hybrid Linear and Non-linear Precoding (HLNP) algorithm specifically considers the MA-ZF and THP algorithms as the linear and non-linear parts, respectively. Other combinations of algorithms are possible as well, but will not be regarded here.

In order to simplify the notation, regarding the position of the users within the vectors and matrices that describe the system, it is assumed that the unicast group comes

first, and it is then followed by the multicast groups. Note that the ordering among groups is not relevant, since the inter-group interference is assumed to be removed by the linear filter. However, it still plays an important role within the unicast group, since the THP algorithm performs successive interference cancellation.

Let N_{uc} indicate the number of unicast users, then each beamforming vector $\mathbf{m}'_k \in \mathbb{C}^{L \times 1}$ must lie in the null space of

$$\begin{aligned} & \mathbf{h}_n, \\ & \forall n \in \{1, \dots, N_{\text{uc}}\} \mid n < k, \\ & \forall n \in \{N_{\text{uc}} + 1, \dots, N\} \mid b_n \neq k. \end{aligned} \quad (4.91)$$

These null space projections result in an \mathbf{HM}' matrix with a triangular block corresponding to the unicast users. This can be illustrated for the exemplary scenario of Section 2.3, which has two unicast users ($N_{\text{uc}} = 2$) and one multicast group with two users, as follows

$$\mathbf{HM}' = \begin{bmatrix} \mathbf{h}_1 \mathbf{m}'_1 & \mathbf{h}_1 \mathbf{m}'_2 & \mathbf{h}_1 \mathbf{m}'_3 \\ \mathbf{h}_2 \mathbf{m}'_1 & \mathbf{h}_2 \mathbf{m}'_2 & \mathbf{h}_2 \mathbf{m}'_3 \\ \mathbf{h}_3 \mathbf{m}'_1 & \mathbf{h}_3 \mathbf{m}'_2 & \mathbf{h}_3 \mathbf{m}'_3 \\ \mathbf{h}_4 \mathbf{m}'_1 & \mathbf{h}_4 \mathbf{m}'_2 & \mathbf{h}_4 \mathbf{m}'_3 \end{bmatrix} = \begin{bmatrix} x & 0 & 0 \\ x & x & 0 \\ 0 & 0 & x \\ 0 & 0 & x \end{bmatrix}, \quad (4.92)$$

where x indicates non-zero values.

Let $\mathbf{H}_k \in \mathbb{C}^{g_k \times L}$ denote the channel matrix of the users belonging to group k and $\tilde{\mathbf{H}}_k \in \mathbb{C}^{(L-A_k) \times L}$ denote the concatenation of the vectors defined in (4.91) for group k . The null space of $\tilde{\mathbf{H}}_k$ can be obtained through SVD, and it is denoted by $\tilde{\mathbf{V}}_k^{(0)} \in \mathbb{C}^{L \times A_k}$. The dimension A_k is given by

$$A_k = \begin{cases} L - N + N_{\text{uc}} - k + 1, & \text{for } k \leq N_{\text{uc}} \\ L - N + g_k, & \text{for } k > N_{\text{uc}} \end{cases}, \quad (4.93)$$

assuming that matrix \mathbf{H} has full row rank. The equivalent channel matrix $\mathbf{H}_k^{(\text{eq})} \in \mathbb{C}^{g_k \times A_k}$ after the projection is given by $\mathbf{H}_k^{(\text{eq})} = \mathbf{H}_k \tilde{\mathbf{V}}_k^{(0)}$. It is assumed that one of the multicast beamforming algorithms of Section 3.4 is applied considering $\mathbf{H}_k^{(\text{eq})}$, which results in the beamforming vector $\mathbf{m}_k^{(\text{eq})} \in \mathbb{C}^{A_k \times 1}$. The k^{th} column of the modulation matrix \mathbf{M}' is then set to $\mathbf{m}'_k = \tilde{\mathbf{V}}_k^{(0)} \mathbf{m}_k^{(\text{eq})}$, i.e.,

$$\mathbf{M}' = [\tilde{\mathbf{V}}_1^{(0)} \mathbf{m}_1^{(\text{eq})}, \dots, \tilde{\mathbf{V}}_K^{(0)} \mathbf{m}_K^{(\text{eq})}]. \quad (4.94)$$

In order to balance the energy among the multicast groups, the power redistribution matrix $\mathbf{\Gamma} \in \mathbb{R}^{K \times K}$ is defined as

$$\mathbf{\Gamma} = \text{diag}([\min(|\mathbf{H}_1 \tilde{\mathbf{V}}_1^{(0)} \mathbf{m}_1^{(\text{eq})}|), \dots, \min(|\mathbf{H}_K \tilde{\mathbf{V}}_K^{(0)} \mathbf{m}_K^{(\text{eq})}|)]^T)^{-1}. \quad (4.95)$$

In order to satisfy the transmit energy constraint, a variable $\beta \in \mathbb{R}$ is defined as

$$\beta = \sqrt{\frac{P}{\text{tr}(\mathbf{R}'_v \mathbf{M}'^H \mathbf{M}' \mathbf{\Gamma}^2)}}. \quad (4.96)$$

Finally, the matrix $\mathbf{M}'_{\text{HLNP}} \in \mathbb{C}^{L \times K}$ of the HLNP algorithm is given by

$$\mathbf{M}'_{\text{HLNP}} = \beta \mathbf{M}' \mathbf{\Gamma}, \quad (4.97)$$

with β , \mathbf{M}' , and $\mathbf{\Gamma}$, defined, respectively, in (4.96), (4.94), and (4.95).

Let $\mathbf{H}_{\text{uc}} \in \mathbb{C}^{N_{\text{uc}} \times L}$, $\mathbf{M}'_{\text{uc}} \in \mathbb{C}^{L \times N_{\text{uc}}}$, and $\mathbf{F}'_{\text{uc}} \in \mathbb{C}^{N_{\text{uc}} \times N_{\text{uc}}}$ denote the channel, modulation, and feedback matrices of all unicast users, respectively. The expression for the global feedback filter $\mathbf{F}'_{\text{MA-HLNP}} \in \mathbb{C}^{K \times K}$ can be expressed as

$$\begin{aligned} \mathbf{F}'_{\text{uc}} &= \mathbf{I} - \text{diag}(\mathbf{H}_{\text{uc}} \mathbf{M}'_{\text{uc}})^{-1} \mathbf{H}_{\text{uc}} \mathbf{M}'_{\text{uc}}, \\ \mathbf{F}'_{\text{HLNP}} &= \begin{bmatrix} \mathbf{F}'_{\text{uc}} & \mathbf{0} \\ \mathbf{0} & \mathbf{0} \end{bmatrix}, \end{aligned} \quad (4.98)$$

where the $\mathbf{0}$ entries correspond to null matrices of appropriate dimension.

The transmitter structure of the THP algorithm shown in Fig. 3.1 is also valid for this case, since the feedback matrix, and consequently the modulo operator, will not have any impact on the multicast groups. The receiver structure of THP is also valid for the HLNP algorithm. In the case of multi-group multicast, the receiver structure can be additionally simplified, since the receivers do not need to implement the modulo operator.

4.6 Performance and complexity analysis

4.6.1 Analysis assumptions

The scenario, in which the performance of the algorithms of Sections 4.4 and 4.5 is analyzed through simulations, consists of a single cell equipped with an L -element uniform linear antenna array and N single antenna mobile terminals, which belong to one of K multicast groups. The distribution of users among groups is characterized by the vectors $\mathbf{b} \in \mathbb{Z}^N$ and $\mathbf{g} \in \mathbb{Z}^K$ described in Section 2.3. The group configurations considered by the performance analysis are summarized in Table 4.1. The configurations specified by rows 1, 2, and 3, are further referred to as C_1 , C_2 , and C_3 , respectively.

Table 4.1. Group configurations considered by the performance analysis.

Config.	$\{L, N, K\}$	\mathbf{b}	\mathbf{g}	Description
C_1	$\{4, 4, 3\}$	$[1, 2, 3, 3]^T$	$[1, 1, 2]^T$	Two unicast users and a two-user multicast group.
C_2	$\{6, 6, 4\}$	$[1, 2, 3, 3, 4, 4]^T$	$[1, 1, 2, 2]^T$	Two unicast users and two two-user multicast groups.
C_3	$\{6, 6, 3\}$	$[1, 2, 2, 3, 3, 3]^T$	$[1, 2, 3]^T$	One unicast user, a two-user multicast group, and a three-user multicast group.

In the single-group multicast case, since all users belong to the same group, there is no interference among users. In the multi-group multicast case, however, there exists interference among users of different groups, i.e., inter-group interference. Due to this inter-group interference, situations in which the number of users is larger than the number of transmit antennas are not taken into account by this section, since such cases are expected to achieve a poor performance.

The same simulation assumptions as presented in Section 3.5 are also valid for the analysis conducted in this chapter. The channel model takes into account the propagation effects described in Section 3.5. The Rician factor κ of (3.51) determines the strength of the LOS component within the fast fading model. Regarding the path-loss model, only scenario S1 of Section 3.5.1 is taken into account, since it has been verified that scenario S2 does not have a significant impact on the relative performance of the algorithms.

The results are presented in terms of the uncoded Bit Error Rate (BER), which is defined by (3.54). The simulations take into account both QPSK and 16-QAM modulation schemes, and the constellation is normalized such that the average symbol power is $\sigma_s^2 = 1$. The total transmit power is equal to the summed power of all different symbols. Since a different symbol is transmitted to each multicast group, the total transmit power is given by the power of each symbol multiplied by the number K of multicast groups, i.e., $P = K\sigma_s^2 = K$. The τ parameter, which is specified in more details on Appendix A.1 and is required by the modulo operations of the non-linear algorithms, is set to $2\sqrt{2}$ for QPSK and $8/\sqrt{10}$ for 16-QAM [Joh04].

The simulation analysis is divided into two parts. The first part presented in Section 4.4 considers the following linear algorithms: the Matched Filter (MF), the Zero-Forcing (ZF), the Multicast-Aware Zero Forcing (MA-ZF), the Minimum Mean Square Error (MMSE), the Multicast-Aware Minimum Mean Square Error (MA-MMSE), the

SINR Balancing (SB), the Multicast-Aware SINR Balancing (MA-SB), and an implementation of the bisection method based on semi-definite relaxation (Bisec-SDR) proposed in [GS06, KSL07] and discussed in Section 4.3. The second part presented in Section 4.5 analyzes the following non-linear algorithms: the Tomlinson-Harashima Precoding (THP), the Multicast-Aware Tomlinson Harashima Precoding (MA-THP), the Vector Precoding (VP), the Multicast-Aware Vector Precoding (MA-VP), and the Hybrid Linear and Non-linear Precoding (HLNP).

Regarding the implementation of the algorithms, the following assumptions are taken into account:

- Regarding the Multicast-Aware (MA) algorithms, their single-group beamforming part must be specified. The SDR approach of [SDL06] has been chosen, since for small group sizes it almost always converges to the optimal solution.
- A total of 5 iterations is assumed for the alternating optimization procedure of the SB and MA-SB algorithms.
- The Bisec-SDR algorithm is executed until a precision of $|P_{\text{req}} - P| \leq 10^{-3}$ is reached, and the solution to the power minimization problem is obtained through the SDR approach of [KSL07].
- The THP, MA-THP, and HLNP algorithms assume suboptimal stream ordering [Joh04]. This reduces the number of evaluated orderings from $N!$ to N for THP, from $K!$ to K for MA-THP, and from $N_{\text{uc}}!$ to N_{uc} for HLNP.
- The perturbation vector of the VP and MA-VP algorithms is determined based on the Integer Least Squares (ILS) solver of the MILES optimization package [CZ06] for MATLAB, which implements the LLL reduction and a modified version of the Schnorr-Euchner algorithm.

4.6.2 Performance of linear algorithms

In this section, the performance of the linear multi-group multicast beamforming algorithms is analyzed. The performance in terms of the BER is shown in Figs. 4.2 and 4.3 for the QPSK and 16-QAM modulation schemes, respectively. The user configuration C_1 and an NLOS scenario are assumed. The BER is depicted as a function of the E_s/N_0 , which represents the ratio of the symbol energy to the spectral noise density.

From Fig. 4.2 it can be seen that the MF is the algorithm presenting the worst performance by far, which is due to the fact that it does not implement any interference mitigation mechanism. The MF has a high error rate – above 10% – and not even high

E_s/N_0 values are capable of improving its error floor. The ZF algorithm presents better performance than MF, as expected, since the channel inversion totally mitigates the interference among users. The MA-ZF algorithm, which is an enhanced version of ZF for the multi-group multicast scenario, clearly outperforms ZF. The subsequent ordering of the algorithms, in terms of their increasing performance, is given by: SB, MMSE, MA-MMSE, MA-SB, and Bisec-SDR. Some explanations are given in the following.

The Multicast-Aware (MA) algorithms present significant performance gains with regard to their respective non-MA counterparts, which is due to the implemented multicast-aware enhancements. The most noticeable gain, of approximately 9dB, is the one achieved by MA-SB with regard to SB. When comparing the non-MA algorithms, it is seen that their order of increasing performance is given by $\{ZF \rightarrow SB \rightarrow MMSE\}$. For the MA algorithms, the order is given by $\{MA-ZF \rightarrow MA-MMSE \rightarrow MA-SB\}$. The advantage of MMSE over ZF, as well as the advantage of MA-MMSE over MA-ZF, was expected and it is mainly due to the introduction of the regularization factor, which avoids the inversion of ill-conditioned matrices. With regard to the SB algorithm, if only unicast users were taken into account, then SB would achieve the best performance. For the multi-group multicast case, however, it turns out being an inadequate strategy, since its optimization is based on an SINR calculation that assumes that all users interfere with each other. The MA-SB algorithm provides, in general, a better approximation to the real SINR, thus approaching the optimal case and outperforming the other linear MA algorithms. The Bisec-SDR algorithm presents the best performance, but at the cost of a much higher complexity, as it will be discussed later in the complexity analysis section.

When changing the modulation scheme from QPSK to 16-QAM, the achieved results are shown in Fig. 4.3. Besides the expected performance losses due to the higher order modulation, it can be seen that the MA-SB algorithm gets closer to the Bisec-SDR, with the difference between them dropping to less than 1dB. Furthermore, the relative performance among the MA algorithms and among the non-MA algorithms is still the same as in the previous case. What can be perceived is that the MA-ZF algorithm outperforms both the MMSE and SB algorithms for high E_s/N_0 values. This tendency could already be seen in Fig. 4.2 for the QPSK modulation, but in the case of 16-QAM it happens much sooner.

The results for configurations C_2 and C_3 are shown in Figs. 4.4 and 4.5, respectively, for QPSK modulation. When comparing the absolute results displayed in both these figures and in Fig. 4.2, it can be seen that, when considering the MA algorithms, C_3 presents better results than C_2 , which has better results than C_1 . The reason for this behavior lies in the number of available degrees of freedom of the antenna array for

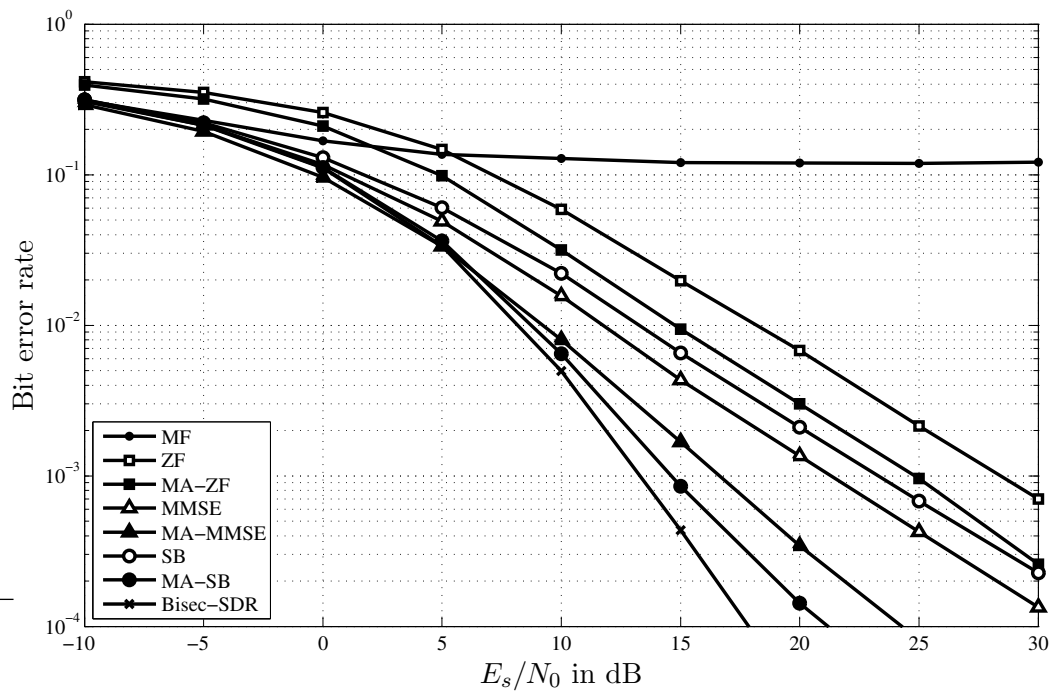


Figure 4.2. BER performance of linear multi-group multicast beamforming: QPSK, NLOS, C_1 , cf. Table 4.1.

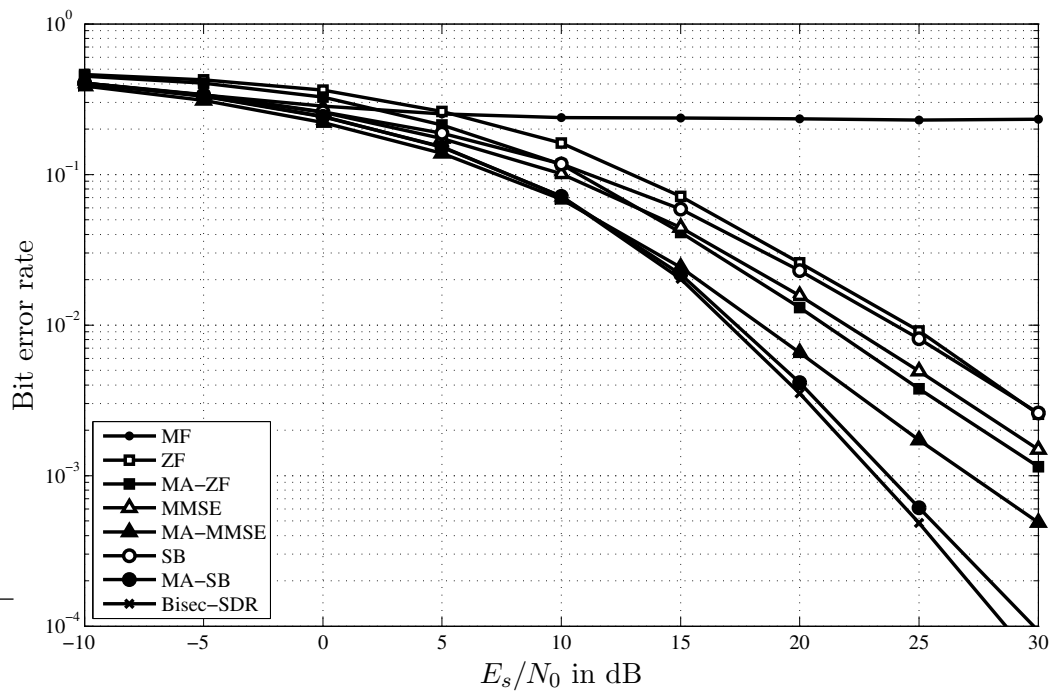


Figure 4.3. BER performance of linear multi-group multicast beamforming: 16-QAM, NLOS, C_1 , cf. Table 4.1.

each configuration. This measure can be expressed as the ratio between the number of transmit antennas and the number of multicast groups, i.e., L/K . The calculation of this measure for each configuration leads to: $L_{C_3}/K_{C_3} > L_{C_2}/K_{C_2} > L_{C_1}/K_{C_1}$, which is in accordance with the achieved results. Another reason for the performance improvement of the MA algorithms when going from C_1 to C_3 is due to the increased number of multicast users, which leads to a more significant impact of the multicast enhancements on the results. Note that the MA-SB algorithm is an exception, which is discussed in the following.

The relative performance among the algorithms shown in Fig. 4.4 for configuration C_2 is similar to that obtained for C_1 in Fig. 4.2. The MA-SB algorithm has a performance close to that of Bisec-SDR, and MA-MMSE is the third best algorithm. However, in Fig. 4.5, which depicts configuration C_3 , it is seen that the performance of MA-SB becomes worse, being even surpassed by that of the MA-MMSE algorithm. This occurs due to the fact that the MA-SB algorithm is based on an approximate SINR, and the accuracy of this approximation increases with the increasing number K of multicast groups. The closer K gets to the number N of users, the closer the SINR approximation gets to the actual SINR. The other way around, when K is reduced, the SINR approximation becomes more inaccurate, thus resulting in worse performance results. A similar behavior is verified for the SB algorithm, which also takes into account an SINR that coincides with the real value only for the unicast case, i.e., when $K = N$.

In order to analyze the impact of the channel correlation on the performance of the algorithms, the Rician factor κ of (3.51) is gradually varied between NLOS ($\kappa \rightarrow 0$) and LOS ($\kappa \rightarrow \infty$) scenarios, given a fixed E_s/N_0 . Fig. 4.6 shows the results when considering configuration C_1 , QPSK modulation, and $E_s/N_0 = 20$ dB. It can be seen that, with increasing κ , the BER of all algorithms increases. Up to $\kappa = 1$ the impact is not really relevant, but then it starts to significantly degrade the BER, leading to exceedingly high error rates as the pure LOS scenario is approached. Differently from the single-group case, for which the presence of LOS represented an improvement in terms of BER, the opposite behavior is observed for the multi-group scenario. Due to the increased channel correlation, it becomes more difficult to suppress the inter-group interference, thus resulting in a poor performance. Regarding the relative performance among the algorithms, it is similar to that of Fig. 4.2, but with the following two exceptions for large κ values: the ZF is outperformed by MF, due to the highly ill-conditioned channel matrix, and the MA-MMSE gets worse than MMSE, due to the inefficiency of applying single-group beamforming on an equivalent regularized LOS channel. For $\kappa \geq 100$ the MC-SB algorithm achieves practically the same performance as Bisec-SDR.

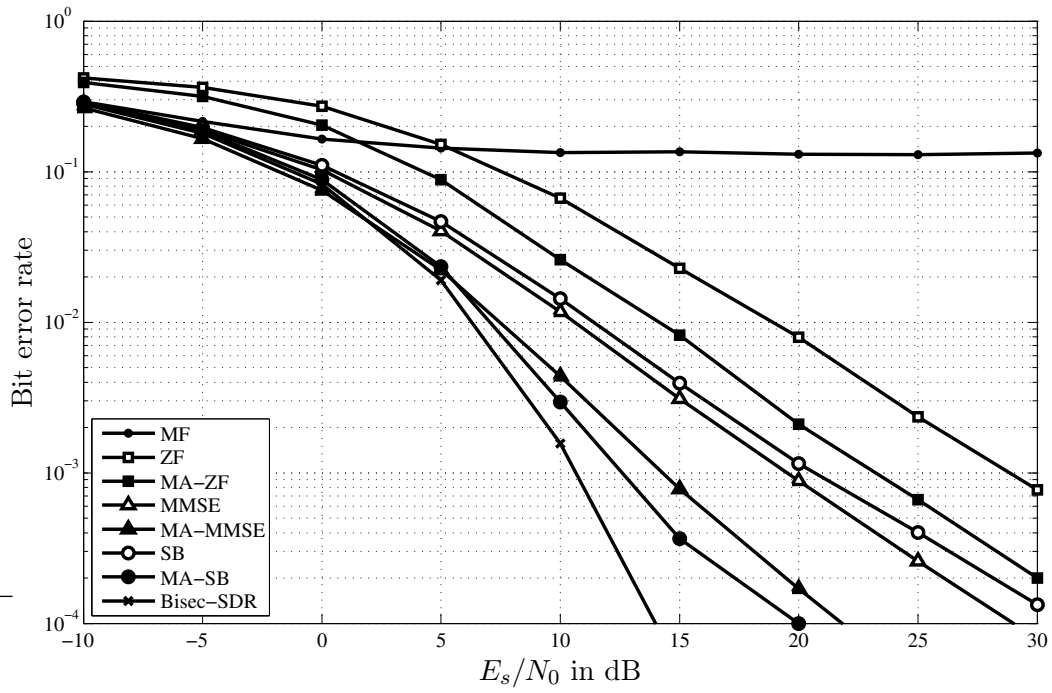


Figure 4.4. BER performance of linear multi-group multicast beamforming: QPSK, NLOS, C_2 , cf. Table 4.1.

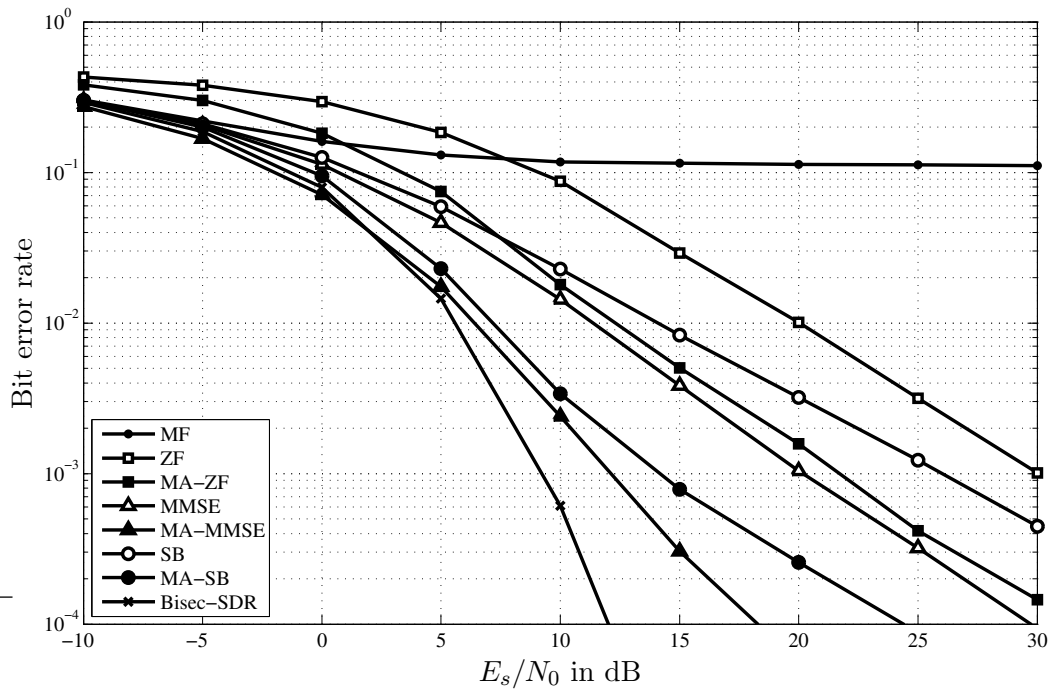


Figure 4.5. BER performance of linear multi-group multicast beamforming: QPSK, NLOS, C_3 , cf. Table 4.1.

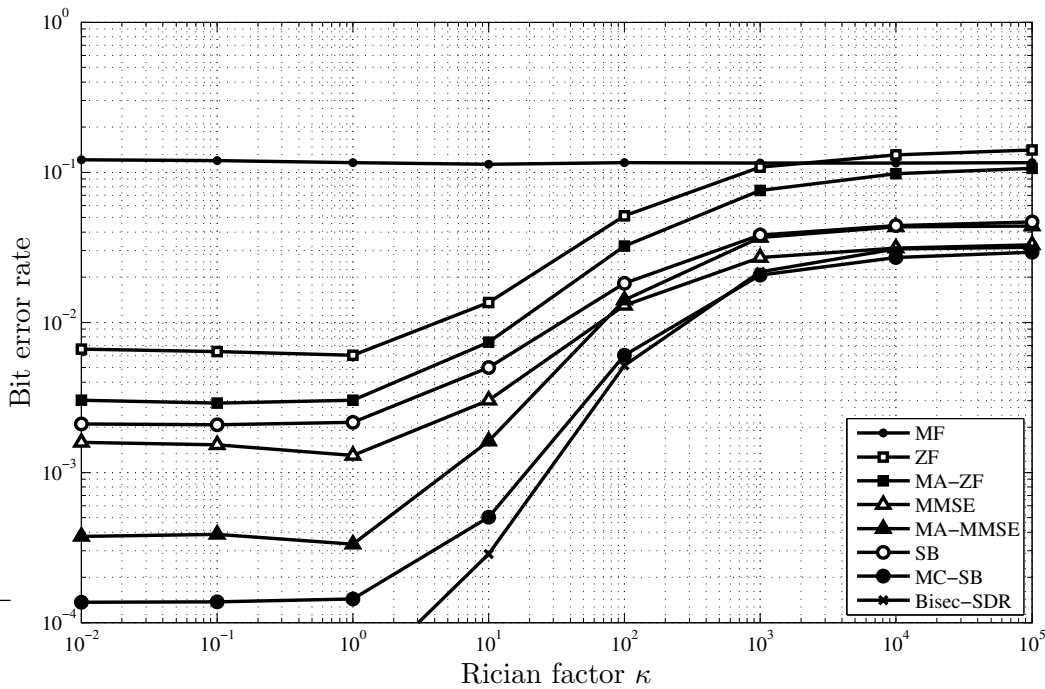


Figure 4.6. Impact of Rician factor κ on the BER of linear multi-group multicast beamforming: QPSK, $E_s/N_0 = 20\text{dB}$, C_1 , cf. Table 4.1.

4.6.3 Performance of non-linear algorithms

The performance of the non-linear algorithms is now analyzed considering the same simulation scenarios as in the previous analysis of the linear algorithms. Figs. 4.7 and 4.8 show the BER results as a function of the E_s/N_0 for QPSK and 16-QAM modulation schemes, respectively, assuming NLOS and user configuration C_1 .

From both Figs. 4.7 and 4.8, it can be seen that the best performance is achieved by the VP algorithm, followed by MA-VP, THP, MA-THP, and HLNP. Differently from the results achieved by the linear algorithms, the non-linear Multicast-Aware (MA) algorithms present worse performance than their respective counterparts without multicast awareness. In the following, these results are discussed in more details.

The verified decreasing order of performance $\{\text{VP}, \text{THP}, \text{HLNP}\}$ was already expected, since the VP algorithm solves a complex optimization problem for determining its solution, the THP algorithm finds the solution based on a less complex suboptimal successive methodology, and the HLNP is a hybrid algorithm that loses some of the advantages of non-linear algorithms by introducing a linear part.

In the case of the MA-THP algorithm, as mentioned in Section 4.5.1.2, a reason for this poor performance can be attributed to the additional null space projections spec-

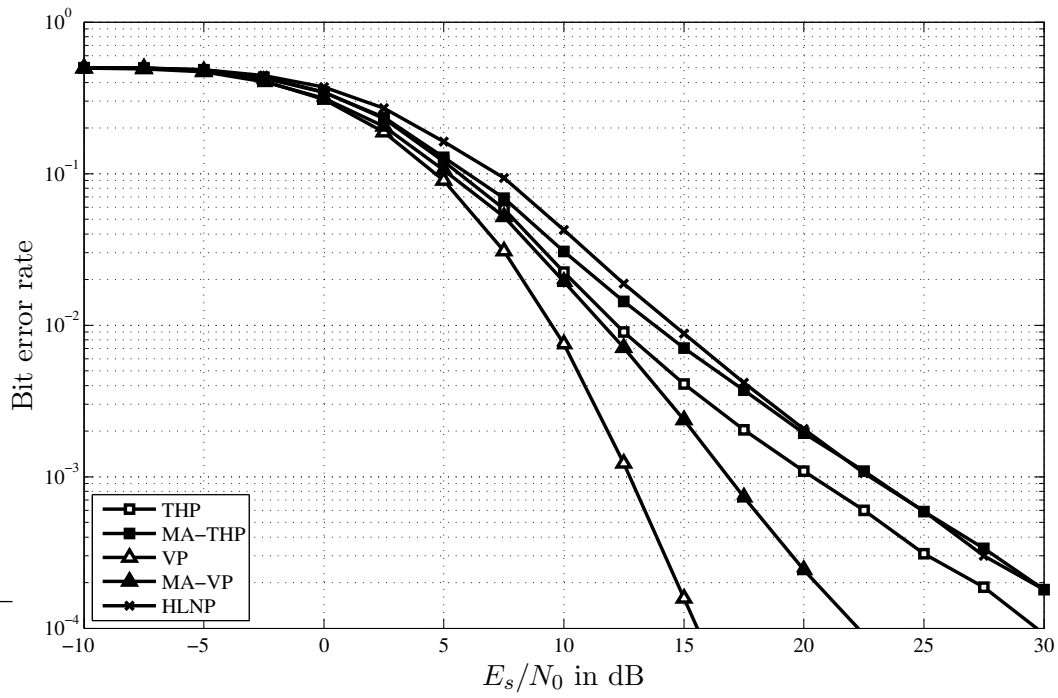


Figure 4.7. BER performance of non-linear multi-group multicast beamforming: QPSK, NLOS, C_1 , cf. Table 4.1.

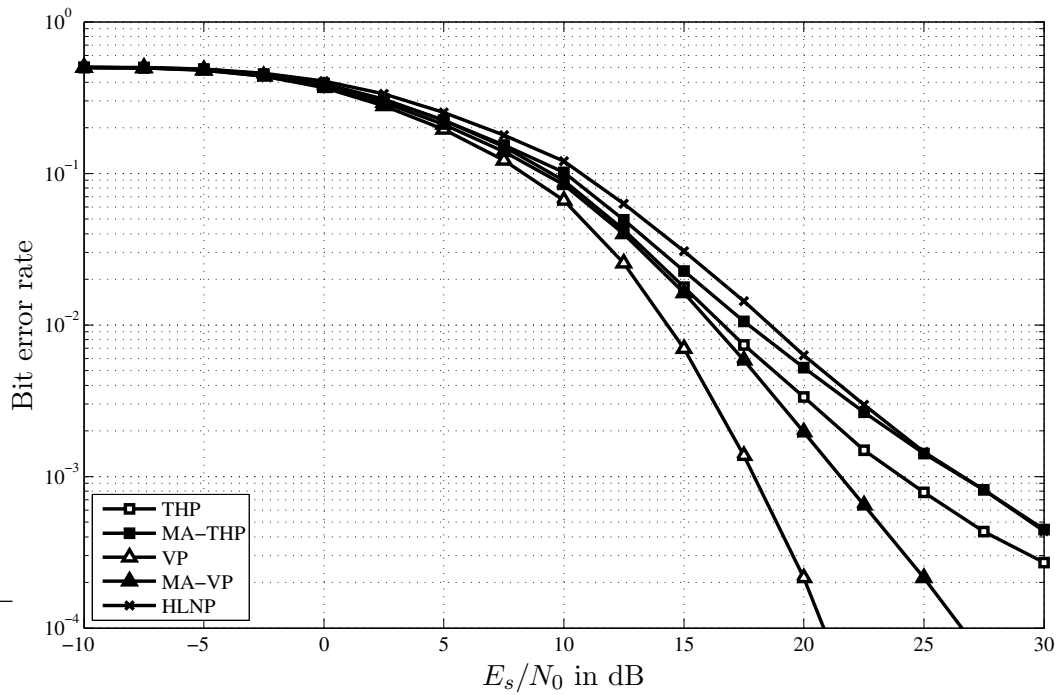


Figure 4.8. BER performance of non-linear multi-group multicast beamforming: 16-QAM, NLOS, C_1 , cf. Table 4.1.

ified in (4.71), which are required in order to achieve a feasible feedback matrix. By analyzing the MA-THP algorithm in more details, it can be verified that there are particular channel realizations in which MA-THP outperforms THP, i.e., in which the gains provided by the multicast awareness outweigh the drawbacks of the additional null space projections. The problem is how to identify, based on the channel knowledge, which algorithm would be more adequate without having to explicitly apply each one and compare the results. Nevertheless, it has been shown by the author of this thesis in [SK07a] that the combination of both MA-THP and THP, which is done by selecting the best algorithm for each iteration of the ordering procedure, only leads to slight performance gains with regard to THP.

Since the feedback filter structure is not present in the MA-VP algorithm, the problem associated with the additional null space projections of MA-THP does not concern MA-VP. The drawback of the MA-VP approach is that, in spite of the single-group beamforming and the reduced number of null space projections with regard to VP, the reduced dimensions of the modulation matrix and signal vector severely limit the degrees of freedom in determining the perturbation vector. It should be mentioned that there are particular channel realizations in which MA-VP outperforms VP, but on average the opposite behavior is verified.

Fig. 4.8 shows the performance results for 16-QAM. In comparison to Fig. 4.7, besides the expected BER degradation, due to the higher modulation order, it can be seen that the relative performance of the algorithms remains the same.

The results for user configurations C_2 and C_3 are depicted in Figs. 4.9 and 4.10, respectively, for the QPSK modulation scheme. It can be seen from Fig. 4.9 that C_2 does not introduce any significant difference with regard to the relative performance among the algorithms, when compared to configuration C_1 . In the case of configuration C_3 , Fig. 4.10 shows that MA-VP is outperformed by THP, and that MA-VP gets closer to the MA-THP and HLNP algorithms. This performance degradation of the non-linear MA algorithms in Fig. 4.10 is a consequence of the reduced dimension of the signal vector ($K = 3$) in comparison to Fig. 4.9 ($K = 4$). The smaller the number of groups, the larger the impact of the previously discussed drawbacks of the non-linear MA algorithms.

The impact of the Rician factor κ on the BER performance of the algorithms, assuming user configuration C_1 , QPSK modulation, and $E_s/N_0 = 20\text{dB}$, is shown in Fig. 4.11. Similar to the corresponding results for the linear algorithms, it can be seen that the BER increases significantly for high values of the Rician factor κ . For values of κ above 10^3 the difference in performance among the algorithms decreases, but the BER values

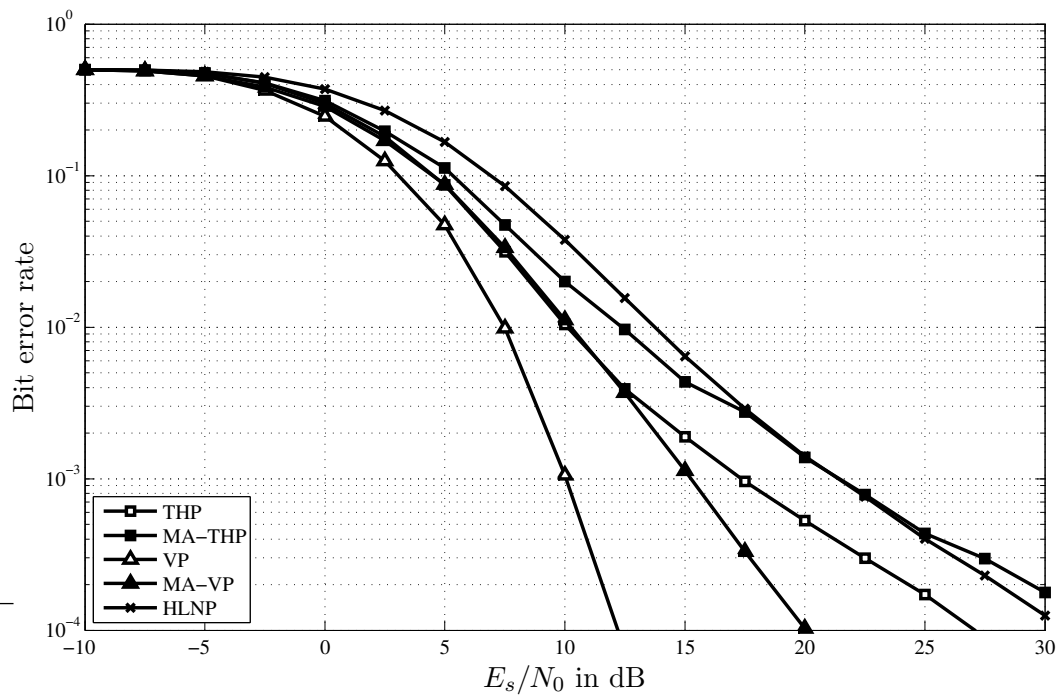


Figure 4.9. BER performance of non-linear multi-group multicast beamforming: QPSK, NLOS, C_2 , cf. Table 4.1.

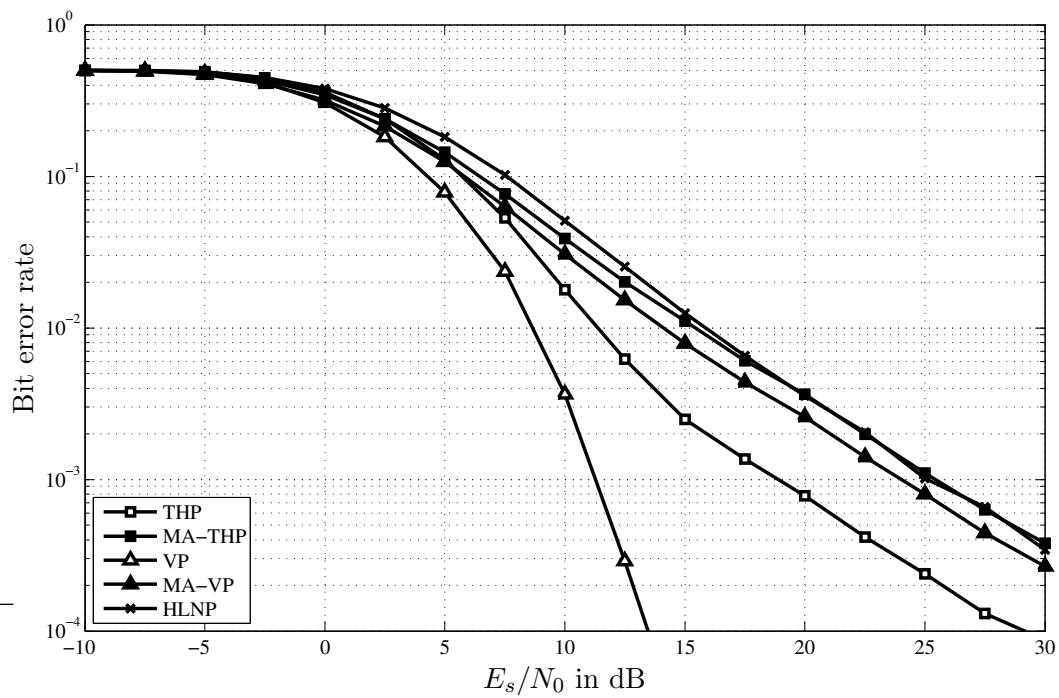


Figure 4.10. BER performance of non-linear multi-group multicast beamforming: QPSK, NLOS, C_3 , cf. Table 4.1.

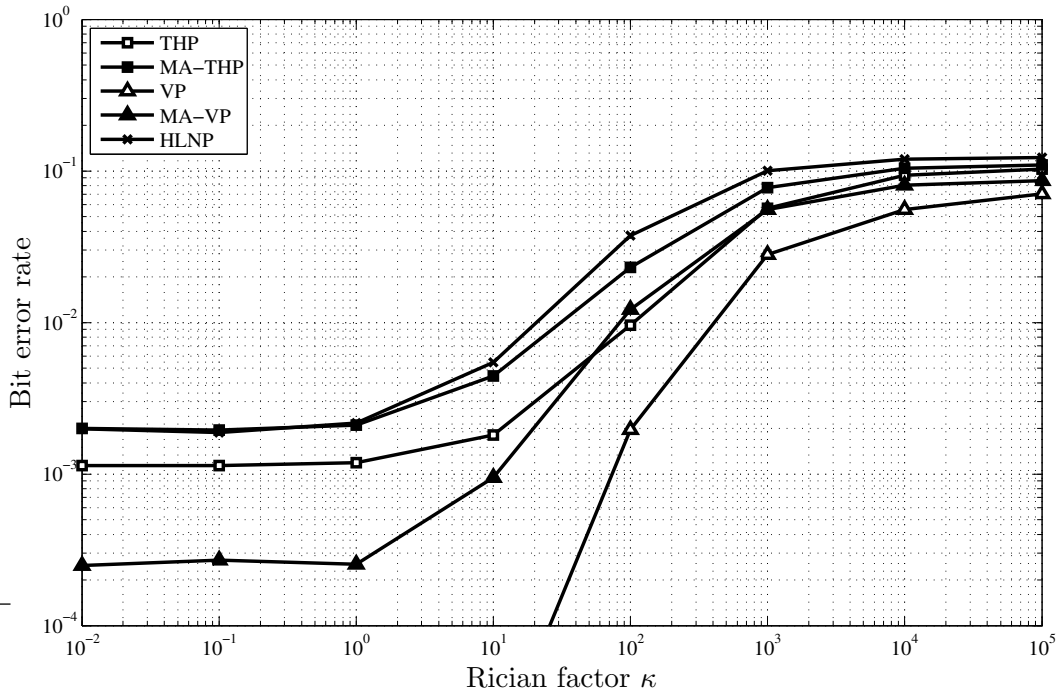


Figure 4.11. Impact of Rician factor κ on the BER of non-linear multi-group multicast beamforming: QPSK, $E_s/N_0 = 20\text{dB}$, C_1 , cf. Table 4.1.

are unacceptably high. For scenarios with too strong LOS components it is not feasible to perform multi-group multicast beamforming, the best alternative being to have a single multicast group per resource and apply single-group multicast beamforming.

Now that the BER performance of all linear and non-linear algorithms has been presented, Table 4.2 summarizes the achieved results in terms of the E_s/N_0 required in order to guarantee a BER of 10^{-3} . An NLOS scenario is assumed, as well as different user configurations and modulation schemes. A comparison among the algorithms reveals that the best non-linear algorithm – VP – outperforms the best linear algorithm – Bisec-SDR – in almost all cases, except for configuration C_3 with QPSK modulation. The third best performance is obtained by the MA-SB algorithm. It should be noted, however, that the advantage of VP and Bisec-SDR with regard to MA-SB comes at the cost of a significantly higher computational complexity, which will be discussed in the next section.

Table 4.2. E_s/N_0 in dB required in order to provide an uncoded BER of 10^{-3} .

Algorithm		QPSK, C_1	16-QAM, C_1	QPSK, C_2	QPSK, C_3
Linear	MF	∞	∞	∞	∞
	ZF	28.4	34.2	28.8	30.0
	MA-ZF	24.8	30.6	23.2	21.7
	MMSE	21.3	31.9	19.5	20.2
	MA-MMSE	16.6	27.1	14.3	12.1
	SB	23.3	34.4	20.7	26.0
	MA-SB	14.6	23.7	12.6	14.2
	Bisec-SDR	13.3	23.2	10.7	9.2
Non-linear	THP	20.3	24.1	17.5	19.0
	MA-THP	22.8	26.7	21.3	25.4
	VP	12.7	17.9	10.1	11.3
	MA-VP	16.8	21.5	15.2	24.0
	HLNP	22.8	26.6	21.5	25.1

4.6.4 Remarks on complexity

In this section, the complexity order of the algorithms is analyzed and compared. The following assumptions are considered when calculating the complexity order:

- The MA-ZF, MA-MMSE, MA-THP, and HLNP algorithms have their complexity order determined essentially by the following two procedures: the null-space projections and the single-group beamforming. The null space projections are implemented through SVD, whose complexity is given in Appendix A.2. The term $\mathcal{O}(\text{SGB}_{A \times B})$ expresses the complexity order of a single-group beamforming algorithm, taking into account an equivalent channel matrix with dimensions $A \times B$. This equivalent channel is explained in more details in Sections 4.4.2.2, 4.4.3.2, 4.5.1.2, and 4.5.3. This complexity depends on the chosen single-group beamforming algorithm, which can be any of those presented in Chapter 3.
- The α parameter of the SB and MA-SB algorithms refers to the number of iterations considered by the alternating optimization procedure.
- According to [KSL05, KSL07], the Bisec-SDR algorithm, which maximizes the minimum SINR for a given channel model, has its complexity divided into two

parts: the number of iterations required for convergence, and the number of arithmetic operations required by each iteration. The first part takes into account a precision of 10^{-3} . With regard to the second part, the complexity order given in [KSL07] is expressed in terms of the number of arithmetic operations, i.e., both sums and multiplications are considered. Since in this section only the number of multiplications is taken into account, a factor of $1/2$ is introduced in order to roughly approximate the number of multiplications from the number of arithmetic operations.

- The complexity order of the VP and MA-VP algorithms is mainly determined by the integer least squares optimization problem associated to the calculation of the perturbation vector. According to [JSBU07] this problem does not have polynomial complexity. The exact expression for the complexity order is not trivial to be derived. For a general comparison, it suffices to say that it has non-polynomial complexity and the complexity order is significantly higher than that of the other analyzed algorithms.

The complexity of the algorithms is shown in Table 4.3. It is expressed in terms of the complexity order and makes use of the big O notation. The algorithms are presented according to their increased order of complexity. Note that this order depends on the previously discussed assumptions concerning each algorithm.

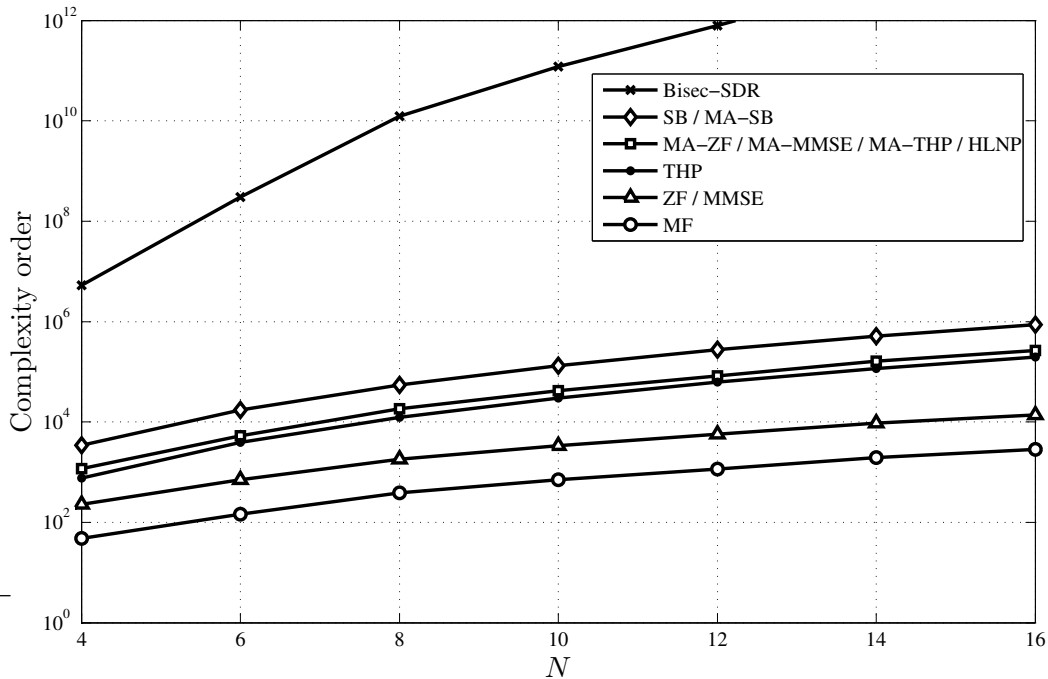
In order to provide a better insight in the complexity of the different algorithms, Fig. 4.12 shows the complexity order as a function of the number N of users. Note that the y-axis is shown in logarithmic scale. The number L of transmit antennas is set to be equal to the number N of users, and the number K of groups is adjusted in such a way that half of the users are unicast users and the other half is roughly divided into equally sized multicast groups with at least 2 users per group. It is assumed that $\alpha = 5$ and the USMF is selected as the single-group beamforming algorithm. The choice of USMF is due to the fact that it presents a much lower complexity than SDR and, as shown in Section 3.5, it provides a reasonable approximation to the SDR performance.

The lowest complexity is presented by the MF algorithm, which is due to the fact that it does not mitigate the interference. The drawback of its low complexity, as the previous performance analysis has shown, is that it achieves the worst BER results.

The ZF and MMSE algorithms introduce a channel inversion in order to mitigate the inter-group interference, for this reason they present a higher complexity than MF. Both ZF and MMSE have the same complexity order, since the only difference between

Table 4.3. Computational complexity of the beamforming algorithms.

Algorithm	Complexity order
MF	$\mathcal{O}(NLK)$
ZF	$\mathcal{O}(NLK + L^3 + L^2K + LK^2 + \frac{1}{2}NL^2)$
MMSE	$\mathcal{O}(NLK + L^3 + L^2K + LK^2 + \frac{1}{2}NL^2)$
THP	$\mathcal{O}(3N^4)$
MA-ZF	$\mathcal{O}(4L^3K + 2NL^2K) + \sum_{k=1}^K \mathcal{O}(\text{SGB}_{g_k \times (L-N+g_k)})$
MA-MMSE	$\mathcal{O}(6N^3K) + \sum_{k=1}^K \mathcal{O}(\text{SGB}_{g_k \times g_k})$
MA-THP	$\mathcal{O}(3K^4 + 4L^3K + 2NL^2K - L^2K^2) + \sum_{k=1}^K \mathcal{O}(\text{SGB}_{g_k \times A_k})$
HLNP	$\mathcal{O}(3N_{\text{uc}}^4 + 4L^3K + 2NL^2K - L^2N_{\text{uc}}^2) + \sum_{k=1}^K \mathcal{O}(\text{SGB}_{g_k \times A_k})$
SB	$\mathcal{O}(\frac{5}{3}\alpha NL^3 + \alpha N^2L^2)$
MA-SB	$\mathcal{O}(\frac{5}{3}\alpha NL^3 + \alpha N^2L^2)$
Bisec-SDR	$\mathcal{O}(3\sqrt{KL}) \mathcal{O}(\frac{1}{2}(L^2K + N)^{3.5})$
VP	Non-polynomial
MA-VP	Non-polynomial

Figure 4.12. Complexity order of the algorithms as a function of the number of users N , assuming that $L = N$.

them lies on the regularization factor, which does not increase the complexity order. The THP algorithm has a complexity higher than both ZF and MMSE, which can be attributed to the stream ordering procedure performed by THP.

Next, the MA-ZF, MA-MMSE, MA-THP, and HLNP, present practically the same complexity order, being slightly higher than that of THP. These algorithms have the null-space projections and single-group beamforming procedures in common, which are the preponderant factors for their complexity order, and for this reason they present an equivalent complexity order.

The alternating optimization employed by the SB and MA-SB algorithms is responsible for the increased complexity order with regard to the previous group of algorithms – MA-ZF, MA-MMSE, MA-THP, and HLNP. The SB and MA-SB present practically the same complexity order. Both algorithms have a similar structure and the additional power redistribution of MA-SB is only performed once, thus not affecting the complexity order.

Finally, the Bisec-SDR algorithm has a much higher complexity than the other algorithms, except for the non-polynomial VP-based algorithms. This higher complexity of Bisec-SDR is due to the numerical optimization performed by the SDP solver. Even though the complexity order of Bisec-SDR may correspond to an upper complexity bound, as mentioned in [KSL05], the actual complexity is still expected to be higher than that of the other algorithms.

4.7 Conclusions

In this chapter, the multi-group multicast problem has been investigated. Several linear and non-linear algorithms have been formulated for the multi-group multicast case, and multicast-aware enhancements have been proposed. Both the performance and complexity of the algorithms have been analyzed throughout the chapter. The main conclusions may be summarized as follows:

- In terms of performance, the best algorithm is VP, followed by the Bisec-SDR algorithm. The former is a non-linear algorithm that introduces a perturbation vector, which is found as the solution of an integer least squares optimization problem. The latter is a linear algorithm that provides a tight approximation to the problem of maximizing the minimum SINR. Both algorithms, however,

present the drawback of high computational complexity with regard to the other algorithms.

- The proposed multicast-aware enhancements of the linear algorithms – MA-ZF, MA-MMSE, and MA-SB – present significant gains with regard to the original algorithms – ZF, MMSE, and SB. In the case of MA-ZF and MA-MMSE, the performance gain with regard to ZF and MMSE comes at the cost of a certain increase in complexity, due to the null space projections and single-group beamforming procedures. In the case of MA-SB, however, the proposed modifications do not significantly increase the complexity with regard to SB.
- Non-linear multicast-aware algorithms – MA-THP and MA-VP – have also been derived in this chapter. However, it has been shown that their performance is actually worse than that of the THP and VP algorithms, respectively. The reasons for this, in the case of MA-THP, are the drawbacks related to the additional null space projections, whereas for MA-VP the problem is due to the reduced dimension of the perturbation vector. Additionally, a hybrid linear/non-linear algorithm (HLNP) has been derived. Among the non-linear algorithms it presents, as expected, the worst performance, but with regard to the linear algorithms, it outperforms MA-ZF. A comparison of HLNP with MA-MMSE is not fair, since HLNP is based on a ZF criterion. An MMSE version of HLNP is expected to outperform the linear MA-MMSE.
- The best trade-off in terms of performance and complexity is achieved by the proposed MA-SB and MA-MMSE algorithms. The choice among these algorithms depends on the ratio between the number of users and number of multicast groups, i.e., N/K . When regarding both performance and complexity aspects, the MA-MMSE algorithm is more adequate for higher ratios ($K \rightarrow 1$), whereas the MA-SB is advised for lower ratios ($K \rightarrow N$).

Chapter 5

Resource allocation in multi-carrier multicast systems

5.1 Introduction

The two previous chapters have dealt with beamforming techniques for both single-group and multi-group multicast scenarios when assuming a single subcarrier, i.e., the beamforming is done for each subcarrier independently. The issue of how the radio resources are allocated is now addressed in this chapter. The term “radio resources” refers to both the available subcarriers as well as the available transmit power at the base station. Only a few works have dealt with resource allocation specifically for multi-carrier multicast systems, such as [SH04, SPC05] and the author of this thesis in [SK07c]. This topic is further investigated in this chapter, which is organized as follows. In Section 5.2, an overview of the theme of resource allocation in multi-carrier multicast systems is briefly presented. The major contribution of the chapter corresponds to the analysis and proposal of different power allocation techniques for multi-carrier multicast systems, which is presented in Section 5.3. Among the proposed algorithms are: the sum throughput maximization algorithm, which is a generalization of water-filling to the multicast case, a simplified sum throughput maximization algorithm based on group metrics, and a fairness-oriented algorithm. A performance and complexity analysis follows in Section 5.4, which provides a comparison of the proposed algorithms taking into account the trade-off between throughput and fairness. In Section 5.5, some issues are discussed with regard to the allocation of resources in SDMA scenarios. Finally, the main conclusions are drawn in Section 5.6.

5.2 Overview of resource allocation

In this section, an overview of resource allocation in multi-carrier multicast systems is presented. The resource allocation can be divided into two parts: subcarrier allocation and power/bit allocation.

The subcarrier allocation problem in multi-carrier multicast systems, similarly to the unicast case, consists of determining which subcarriers are assigned to which users. The

main difference with regard to unicast is that the same subcarrier may be assigned to users belonging to the same group, since they do not interfere with each other.

In principle, known unicast subcarrier allocation techniques, such as in [WCLM99, BGWM07], can be applied to the multicast case. In order to determine which subcarrier should be allocated to a multicast group, a single metric representative of the whole group is required. This group metric is a parameter that must reflect the characteristics of the group and which also depends on the optimization objective of the allocation algorithm.

Some algorithms specific for the multicast case have been proposed by previous works. In [SH04], Suh and Hwang developed a dynamic subcarrier and bit allocation algorithm for multicast OFDM systems. They tackle the problem of jointly assigning subcarriers, power, and bits, for which a suboptimum strategy similar to that of the unicast case [WCLM99] is proposed. First the subcarrier allocation is performed, and then the bit/power allocation algorithm takes place. The optimization criterion for the subcarrier allocation corresponds to the maximization of the sum throughput subject to transmit power and minimum BER constraints. It should be noticed that, in this case, not necessarily all users of a given multicast group are simultaneously assigned to the same resource. Some users in bad channel conditions may require too much power in order to satisfy the BER constraints, thus not being assigned together with the other group members.

The algorithm proposed in [SPC05], which is an extension of [SH04], incorporates characteristics of proportional fair scheduling into the allocation procedure. The algorithm aims at increasing the data rate of the worst users by allocating additional subcarriers whenever the additional allocations improve the long-term average throughput.

In this chapter, a similar decoupled approach is taken into account, in which the subcarrier allocation is performed first and then is followed by the power allocation procedure. A simple subcarrier allocation algorithm is considered, which is described later in this chapter. Regarding the power allocation, it corresponds to the main focus of the analysis, for which different algorithms are proposed and evaluated. Note that, since a general case of Gaussian signalling is assumed, the bit allocation part is not taken into account.

5.3 Power allocation

5.3.1 System assumptions

The scenario considered in this section corresponds to the downlink of a single cell in a cellular multi-carrier system. A single-antenna base station and single-antenna users are assumed. Note that, in the case of multiple antennas without SDMA, the same algorithms are also applicable, whereas for the SDMA case there are some differences, which are approached later in Section 5.5. There are F available subcarriers and N users within the cell. These N users are grouped into K multicast groups. Since in this case, differently from the previous chapters, a single-antenna base station and multiple subcarriers are considered, the channel matrix is now defined as $\mathbf{H} \in \mathbb{C}^{N \times F}$, i.e., the rows correspond to users and the columns to subcarriers.

It is assumed that the subcarrier allocation has already been performed, and therefore the information concerning which users are associated to which subcarrier is available to the power allocation algorithm. The subcarrier allocation matrix $\mathbf{A} \in \mathbb{Z}^{N \times F}$, with elements $A_{i,j} \in \{0, 1\}$, determines which users are active within each subcarrier, where 0 and 1 correspond to the inactive and active states, respectively. No intracell interference is assumed, therefore only users of the same multicast group may share one subcarrier.

The power allocation problem consists of determining the power vector $\mathbf{p} = [p_1, \dots, p_F]^T \in \mathbb{R}^F$, which indicates the amount of power p_f allocated to each subcarrier f . The allocation can be done according to different optimization criteria, such as the maximization of the throughput or the maximization of the minimum SNR. The algorithms proposed in the following subsections, which have different characteristics with regard to their complexity, capacity, and fairness, are namely: Sum Throughput Maximization, Sum Throughput Maximization based on Group Criterion, and Fair Power Allocation.

5.3.2 Sum throughput maximization

In this section, the Sum Throughput Maximization (STM) algorithm is introduced. This algorithm has the purpose of maximizing the total throughput of the system, which is defined as the sum of the bit rates perceived by the individual users. The throughput of user n associated to subcarrier f is denoted by $R_{n,f}$, and if Gaussian signalling is assumed it can be written as

$$R_{n,f} = \log_2(1 + p_f G_{n,f}), \quad (5.1)$$

where p_f is the power allocated to subcarrier f and $G_{n,f}$ is an element of matrix $\mathbf{G} \in \mathbb{R}^{N \times F}$, which corresponds to the normalized channel gain conditioned to the subcarrier allocation, i.e., $G_{n,f} = (|H_{n,f}|^2 / \sigma_z^2) \cdot A_{n,f}$. In order to compose the matrix \mathbf{G} , channel knowledge is required, which is assumed to be available at the transmitter.

The optimization problem can be expressed as

$$\begin{aligned} \mathbf{p}_{\text{opt}} &= \max_{\mathbf{p}} \sum_{f=1}^F \sum_{n=1}^N \log_2(1 + p_f G_{n,f}), \\ \text{subject to: } &\begin{cases} p_f \geq 0, & \forall f \in \mathcal{F}, \\ \sum_{f=1}^F p_f = P, \end{cases} \end{aligned} \quad (5.2)$$

where the first constraint avoids negative power levels, P is the total available power, and \mathcal{F} denotes the set of all subcarrier indices $f = 1, \dots, F$.

The Lagrangian function $L(\mathbf{p})$ and its partial derivative with regard to p_f can be expressed, respectively, as

$$L(\mathbf{p}) = \sum_{f=1}^F \sum_{n=1}^N \log_2(1 + p_f G_{n,f}) + \sum_{f=1}^F \nu_f p_f - \mu \left(\sum_{f=1}^F p_f - P \right), \quad (5.3a)$$

$$\frac{\partial L(\mathbf{p})}{\partial p_f} = \sum_{n=1}^N \frac{G_{n,f}}{1 + p_f G_{n,f}} + \nu_f - \mu. \quad (5.3b)$$

where $\mu \in \mathbb{R}$ and $\nu_f \in \mathbb{R}$ are Lagrange multipliers. Note that, for simplicity of notation, a $\log_e(2)$ term is omitted from (5.3b), where e is the base of the natural logarithm. This consideration is valid, since the solution of (5.2) is the same independent of the logarithm's base.

The Karush-Kuhn-Tucker (KKT) necessary conditions for optimality [BV04] lead to the following set of equations:

$$\begin{cases} p_f \geq 0, & \forall f \in \mathcal{F}, \end{cases} \quad (5.4a)$$

$$\begin{cases} \sum_{f=1}^F p_f = P, \end{cases} \quad (5.4b)$$

$$\begin{cases} \nu_f \geq 0, & \forall f \in \mathcal{F}, \end{cases} \quad (5.4c)$$

$$\begin{cases} \nu_f p_f = 0, & \forall f \in \mathcal{F}, \end{cases} \quad (5.4d)$$

$$\begin{cases} \partial L(\mathbf{p}) / \partial p_f = 0 & \forall f \in \mathcal{F}. \end{cases} \quad (5.4e)$$

The multiplier ν_f can be isolated by substituting (5.3b) into (5.4e). When inserting the isolated ν_f into (5.4c) and (5.4d), respectively, the following equations are obtained:

$$\mu \geq \sum_{n=1}^N \frac{G_{n,f}}{1 + p_f G_{n,f}}, \quad \forall f \in \mathcal{F}, \quad (5.5a)$$

$$p_f \left(\mu - \sum_{n=1}^N \frac{G_{n,f}}{1 + p_f G_{n,f}} \right) = 0, \quad \forall f \in \mathcal{F}. \quad (5.5b)$$

From both these conditions and (5.4a), it follows that μ is related to the power of each subcarrier f according to

$$\begin{cases} p_f = 0, & \text{for } \mu \geq \sum_{n=1}^N G_{n,f}, \\ \mu = \sum_{n=1}^N \frac{G_{n,f}}{1 + p_f G_{n,f}}, & \text{for } \mu < \sum_{n=1}^N G_{n,f}. \end{cases} \quad (5.6a)$$

$$\quad (5.6b)$$

A single level μ therefore determines the power of all subcarriers. It should be noted that it is not possible to explicitly express p_f as a function of μ in (5.6). However, (5.6b) can be rewritten as the following polynomial in p_f :

$$\sum_{j=1}^N (p_f + G_{j,f}^{-1} - N\mu^{-1}) \prod_{i=1, i \neq j}^N (p_f + G_{i,f}^{-1}) = 0, \quad (5.7)$$

which has degree N and only one positive real root.

The problem now consists of finding an adequate value of μ such that the resulting power vector satisfies the total power constraint. The optimal solution can be numerically calculated by performing a one-dimensional search over μ [BV04].

In order to better illustrate the problem, Fig. 5.1 depicts μ as a function of p_f according to (5.6) for a system containing three subcarriers and $P = 1$. This example represents a particular system snapshot, which is characterized by the instantaneous values of the normalized channel gains $G_{n,f}$. Each curve corresponds to a subcarrier f and monotonically decreases with increasing p_f . For the considered power range, the dashed lines indicate the maximum value of μ of each curve, which is achieved for $p_f = 0$ and is denoted by a_f . From (5.6), it follows that

$$a_f = \sum_{n=1}^N G_{n,f}. \quad (5.8)$$

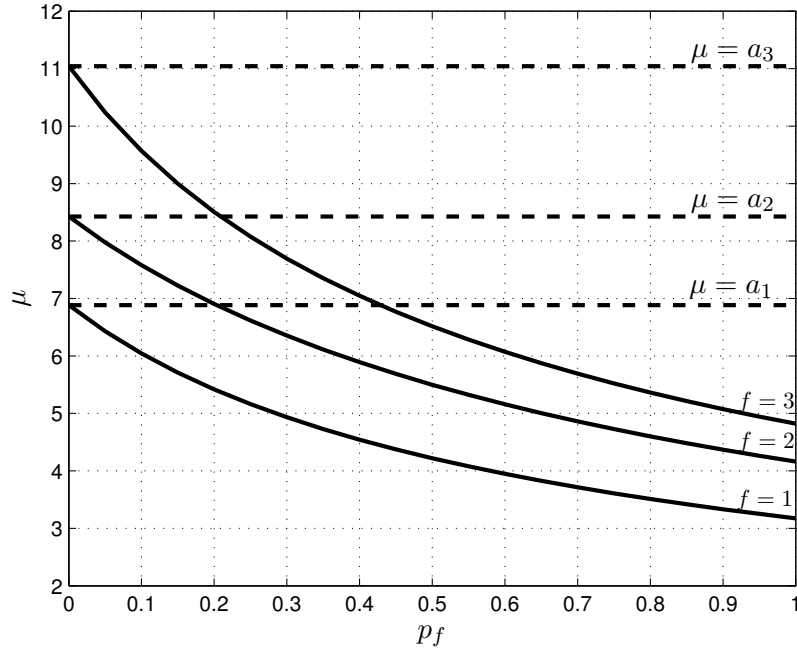


Figure 5.1. Sum throughput maximization for 3 subcarriers and $P = 1$.

By analyzing the problem, it can be seen that a hypothesis testing similar to that of the traditional waterfilling algorithm [PF05] can also be done for this more general unicast/multicast case, with the purpose of reducing the processing time of the one-dimensional search for μ . The algorithm, which is described below, assumes that for a given value of μ , each p_f is obtained by finding the real positive root of (5.7).

1. Assign the subcarrier indices according to the increasing order of a_f .
Set $\tilde{f} = 1$.
2. Set $\mu = a_{\tilde{f}}$ and compute $p_{\tilde{f}+1}, \dots, p_F$.
If $\sum_{f=\tilde{f}+1}^F p_f \leq P$, then proceed to step 3,
otherwise set $\tilde{f} = \tilde{f} + 1$ and repeat step 2.
3. Find $\mu \in]a_{\tilde{f}-1}, a_{\tilde{f}}]$ such that $\sum_{f=\tilde{f}}^F p_f = P$.
Assume that $a_0 = 0$ for the case in which $\tilde{f} = 1$.
Set $p_1, \dots, p_{\tilde{f}-1}$ to zero and compute $p_{\tilde{f}}, \dots, p_F$.

The algorithm does not eliminate the need for a numerical method in order to calculate μ , but as it can be seen from step 3, it may benefit from a narrower search space and

reduced dimension (vector \mathbf{p} with some zero elements), which may result in relevant gains in terms of processing time.

5.3.3 Sum throughput maximization based on group criterion

In this section, the Group Criterion for Throughput Maximization (GCTM) algorithm is presented, which also aims at the maximization of the sum throughput, but corresponds to a simplification of the STM algorithm. It assumes that the users of a multicast group do not have their quality indicators (channel gains) taken into account individually. Instead, for each subcarrier, a single indicator is considered for the whole group.

Let g_f represent the group quality indicator for subcarrier f , then the optimization problem becomes

$$\begin{aligned} \mathbf{p}_{\text{opt}} = \max_{\mathbf{p}} & \sum_{f=1}^F \log_2(1 + p_f g_f), \\ \text{subject to:} & \begin{cases} p_f \geq 0, & \forall f \in \mathcal{F}, \\ \sum_{f=1}^F p_f = P, \end{cases} \end{aligned} \quad (5.9)$$

which can be solved directly by the waterfilling algorithm in [PF05].

The group indicator for each subcarrier can be expressed as a function of the previously defined gain matrix \mathbf{G} , i.e., $g_f = f(\mathbf{G}_f)$, where \mathbf{G}_f is the f^{th} column of matrix \mathbf{G} . The functions considered in this work are the following:

- Maximum (GCTM-Max),
- Minimum (GCTM-Min),
- Arithmetic mean (GCTM-Mean).

More details on which of the STM algorithms with group criteria are more adequate to better approximate the solution of the STM algorithm with individual criteria are presented in Section 5.4.

5.3.4 Fair power allocation

The algorithms considered so far have aimed at the maximization of the sum throughput, which is not a fair criterion in terms of user performance, since the users may achieve bit rates which largely differ from one another. In this section, the Fair Power Allocation (FPA) algorithm is described, which has the purpose of introducing fairness within the power allocation procedure.

The optimization objective of the FPA algorithm is to maximize the lowest SNR within the cell. Let the SNR perceived by user n on subcarrier f be defined as $p_f G_{n,f}$, then the optimization problem can be written as

$$\begin{aligned} \mathbf{p}_{\text{opt}} &= \max_{\mathbf{p}} \min_{\{n,f\}} (p_f G_{n,f}), \\ \text{for } n &= 1, \dots, N \quad \text{and} \quad f = 1, \dots, F, \\ \text{subject to: } &\begin{cases} p_f \geq 0, \quad \forall f \in \mathcal{F}, \\ \sum_{f=1}^F p_f = P, \end{cases} \end{aligned} \quad (5.10)$$

where the \min_+ operator is here assumed to return the minimum non-zero element.

Since the power allocated to a subcarrier does not depend on n , the problem can be rewritten as follows:

$$\begin{aligned} \mathbf{p}_{\text{opt}} &= \max_{\mathbf{p}} \min_f (p_f g'_f), \\ \text{with } g'_f &= \min_n G_{n,f} \end{aligned} \quad (5.11)$$

where the same range of n and f , as well as the same constraints of (5.10), are assumed.

The expression of the optimization problem in (5.11) implies that only the worst user within each subcarrier needs to be considered. The objective is that these worst users in the different subcarriers achieve the same SNR γ for the optimal power vector \mathbf{p}_{opt} , which implies that $p_f g'_f = \gamma$ for all subcarriers. Assuming that $\mathbf{c} \in \mathbb{R}^F$ represents a vector with elements $c_f = g'^{-1}_f$, $\|\cdot\|_1$ denotes the 1-norm of a vector, and $P = \|\mathbf{p}_{\text{opt}}\|_1$ is the total power constraint in vector form, the following system of equations can be established:

$$\begin{cases} \mathbf{p}_{\text{opt}} = \gamma \mathbf{c}, \\ P = \gamma \|\mathbf{c}\|_1, \end{cases} \quad (5.12)$$

whose solution is given by:

$$\mathbf{p}_{\text{opt}} = P \frac{\mathbf{c}}{\|\mathbf{c}\|_1}. \quad (5.13)$$

5.4 Performance and complexity analysis

5.4.1 Analysis assumptions

The system consists of a single cell serving a certain number K of user groups. Among these groups there are K_{uc} unicast groups, each containing one user, and K_{mc} multicast groups, such that $K = K_{\text{uc}} + K_{\text{mc}}$. For simplicity, it is assumed that all multicast groups have the same size, which is denoted by N_{mc} , only one subcarrier is allocated to each group, and the number of available subcarriers is equal to the number of user groups, i.e., $F = K$.

The users are uniformly distributed over one hexagonal sector of a tri-sectorized cell and a single-antenna base station is located at the sector corner. The considered propagation effects include the distance-based path-loss attenuation with exponent $\alpha = 3.5$, as well as uncorrelated Rayleigh fading, which is modelled as a circularly symmetric complex Gaussian random variable with variance σ^2 . The path-loss is modelled by assuming that the cell border is at a distance $r_b = 1$ from the base station and that the fading variance of a user n with distance $r_n \leq r_b$ is given by $\sigma^2 = 1/r_n^\alpha$ [SL04]. Note that the term cell border is used to refer to the corner of the hexagon directly opposite to the corner in which the base station is located. Additive white Gaussian noise is also assumed and the transmit power is adjusted to provide an average SNR of 10dB at the cell border.

A simple subcarrier allocation (SSA) algorithm is implemented, which approximates the maximization of the sum throughput given an equal power distribution. The considered algorithm iteratively allocates a subcarrier to each user group according to the highest average group channel gain. After an allocation, the corresponding user group and subcarrier are no longer taken into account by the further steps. The procedure is repeated until one subcarrier is allocated to each user group.

The evaluation of the results considers two distinct system configurations. The first one, denoted as system configuration SC1, represents a worst-case situation in which the users have path-loss of the same order, with $\sigma^2 = 1$, and no specific subcarrier allocation algorithm is employed (random allocation). This scenario can be interpreted as all users being close to each other. System configuration SC2, on the other hand, takes into account the different path-loss of the users, with $\sigma^2 = 1/r_n^\alpha$, as well as the previously described SSA algorithm.

5.4.2 Performance of the power allocation algorithms

This section presents the performance analysis of the proposed power allocation algorithms in terms of the achievable throughput as well as the fairness among the users. First, the relative performance among the sum throughput maximization algorithms, namely STM and GCTM, is compared for different scenarios, then the FPA algorithm is included and the absolute throughput achieved by all algorithms is analyzed, and finally the algorithms are compared in terms of the worst-user SNR, which corresponds to the fairness criterion.

In Section 5.3.3, the GCTM algorithm has been presented as an alternative to STM for performing the sum throughput maximization, which consists of assuming a single quality indicator for each subcarrier and applying the waterfilling algorithm. Different group criteria can be taken into account, so that their impact is now analyzed.

The performance of GCTM is shown in Fig. 5.2 for the system configurations SC1 and SC2, with $K_{uc} = K_{mc} = 2$ and $F = 4$, and for some different functions $f(\mathbf{G}_f)$, which are namely: maximum (GCTM-Max), minimum (GCTM-Min), and arithmetic mean (GCTM-Mean). The figure depicts the average sum throughput ratio between the GCTM and STM algorithms, i.e., $E\{R_{GCTM}/R_{STM}\}$, as a function of the multicast group size N_{mc} . It is verified that the throughput ratio decreases with increasing N_{mc} . This is due to the fact that, the more users there are within the multicast group, the less representative the group metric becomes.

For configuration SC1, it can be seen that GCTM-Max is the algorithm which best approximates the performance of STM. The performance gets worse for an increasing group size, but is still close to 88% for $N_{mc} = 20$. The GCTM-Min presents the worst result, while GCTM-Mean has an intermediate performance. The min function is a rather inadequate criterion for GCTM, which is explained due to the fact that the waterfilling algorithm may happen to allocate low power to a multicast subcarrier, since the power is adjusted according to the worst user, even if there are other users with very good channel gains which would significantly contribute to increase the average throughput. By considering the mean instead of the min criterion, the power is better distributed among the subcarriers, which leads to better sum throughput results. The max criterion is even better than the mean criterion, since the waterfilling algorithm tends to allocate more power to the subcarriers with users in very good conditions, which contributes to increase the sum throughput.

For configuration SC2, the performance of the algorithms is improved with regard to configuration SC1. This gain in performance is explained by the fact that configuration

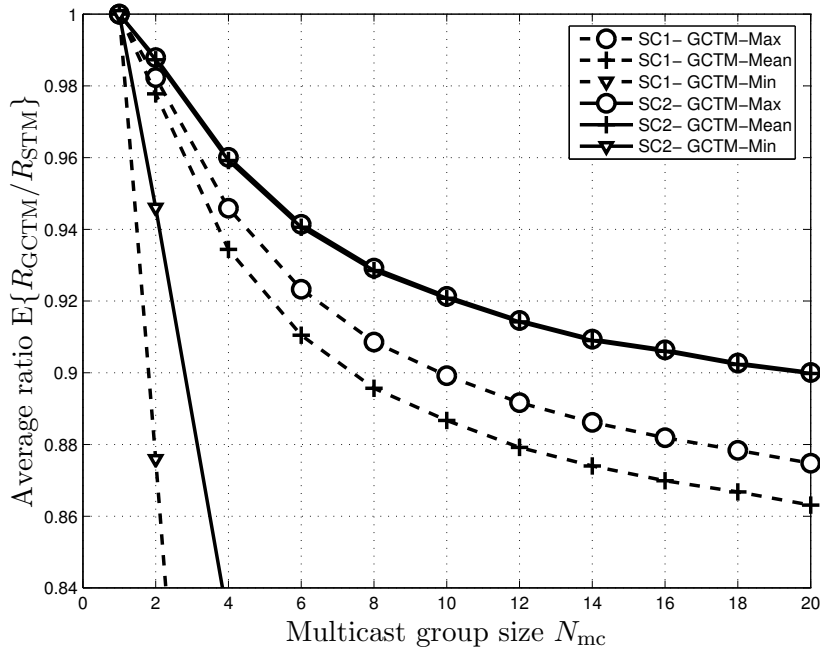


Figure 5.2. Sum throughput ratio between GCTM and STM for different group criteria, for configurations SC1 and SC2, $K_{uc} = K_{mc} = 2$, and $F = 4$.

SC2 implements the subcarrier allocation algorithm SSA, instead of random allocation, as well as the different path-loss perceived by the users. The relative performance of the algorithms is similar to that of SC1, with the difference that the GCTM-Mean and GCTM-Max present approximately the same performance. This is due to the fact that, in the case of configuration SC2, the different path-loss of the users lead to a large variance of the channel gains, which results in the average channel gain being dominated by the largest values.

The cumulative distribution function (CDF) of the average user throughput is shown in Fig. 5.3 for configuration SC2 and a group size of 10 users. The average is taken over the throughput of the users of the multicast group, and each CDF sample corresponds to a different channel realization. Note that the high throughput values are a result of the large amount of multicast users, which have resource sharing capabilities. The STM algorithm, as expected, presents the best average throughput results. The relative behavior among the GCTM and STM curves with regard to Fig. 5.2 is maintained, being GCTM-Max and GCTM-Mean the ones which best approximate the STM algorithm, for the same reasons previously discussed. Regarding the FPA algorithm, it presents worse average throughput performance than the algorithms that aim at throughput maximization, since it aims at providing fairness among the users. The fact that FPA outperforms GCTM-min is explained by the inadequacy of the min criterion to the purpose of maximizing the throughput, which has been previously discussed.

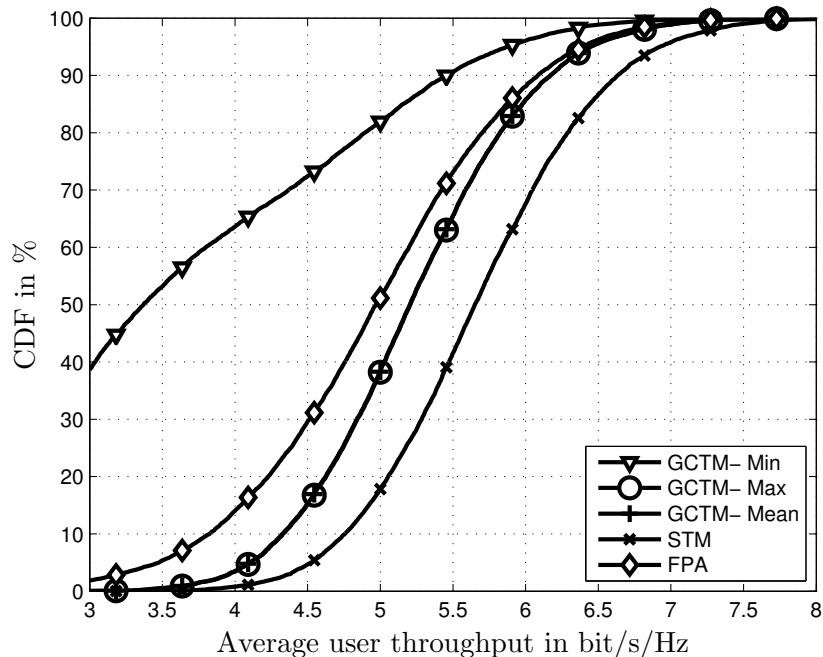


Figure 5.3. CDF of the average user throughput of the different power allocation algorithms for configuration SC2, $K_{uc} = K_{mc} = 2$, $F = 4$, and $N_{mc} = 10$.

In order to compare the degree of fairness of the different algorithms, the measure of the worst-user SNR is employed, which corresponds to the lowest SNR perceived among all users in all subcarriers. In Fig. 5.4, the average worst-user SNR is depicted as a function of the multicast group size N_{mc} for the different power allocation methods. The FPA algorithm presents the best performance in terms of fairness, as already expected, and it presents a gain of roughly 5dB with regard to the GCTM-Max algorithm, which is maintained throughout the whole group size range. When compared to Fig. 5.3, the relative performance of the algorithms is the opposite, with FPA presenting the best performance, then followed by the GCTM-Mean/GCTM-Max algorithms and then the STM algorithm. This order inversion is due to the trade-off between performance and fairness, i.e., when the sum throughput performance improves the fairness gets worse and the other way around. The only exception is the GCTM-Min algorithm, which due to the previously discussed conflict of objectives between the min criterion and the waterfilling algorithm, presents bad results in terms of both performance and fairness.

Fairness is an important aspect to be taken into account, especially for users of multicast services. In the case of error-tolerant hierarchical multicast [PS99, TZ01], it is probably more advantageous to prefer the sum throughput maximization, since the capacity can be maximized at the cost of a few users with low-quality audio/video transmission. However, for services which do not tolerate errors, such as file download,

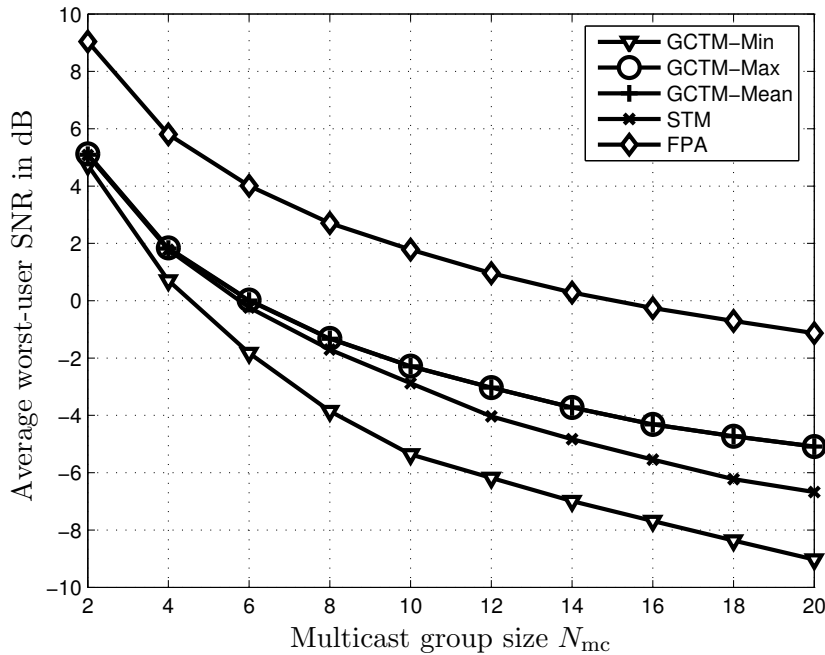


Figure 5.4. Comparison of the different power allocation algorithms in terms of the average worst-user SNR for configuration SC2, $K_{uc} = K_{mc} = 2$, and $F = 4$.

low quality users may compromise the throughput of all other users within the multicast group, due to retransmission mechanisms [JLSX05], and therefore a fair algorithm is certainly more adequate.

5.4.3 Remarks on complexity

In this section, the complexity of the STM algorithm is analyzed. The other algorithms are not considered, because they either have a closed-form solution, in the case of FPA, or their complexity is the same as that of traditional waterfilling [PF05], in the case of GCTM. The FPA algorithm presents a rather low complexity, since it is not an iterative algorithm and only a few operations are required for determining the power allocation vector. Regarding GCTM, it requires at most F iterations, with each iteration also requiring only a few operations. As for STM, it necessarily has a complexity higher than that of GCTM, with both having the same complexity only for the case in which $N_{mc} = 1$.

It has been shown in Section 5.3.2 that the allocation of power based on sum throughput maximization can have its processing effort reduced by employing an algorithm similar to the traditional waterfilling, which consists of iteratively testing the hypothesis that

a certain subcarrier be allocated zero power. The advantage of this approach is the reduction of both the power vector dimension and the range of the search space, which results in decreased computational effort when searching for μ , cf. section 5.3.2.

In the following, it is analyzed to which extent it is expected that the effective power vector length, i.e., the number of non-zero power elements within \mathbf{p} , and the search space be reduced when applying the hypothesis testing of section 5.3.2. The simulation configuration SC1 is considered and among F allocated subcarriers the same number of unicast and multicast groups is assumed, i.e., $K_{uc} = K_{mc} = F/2$, with each multicast group being composed of three users, i.e., $N_{mc} = 3$.

In Fig. 5.5, the effective length of the power allocation vector is shown as a function of the number F of allocated subcarriers for two different cases and considering the STM algorithm. It can be seen that the absolute difference between the total number F of subcarriers and the number of non-zero subcarriers increases for larger values of F . For a small number F of subcarriers the difference is negligible, but for an intermediate/large amount, the reduction of the effective power vector length leads to significant gains in terms of processing effort.

The average ratio between the search space range for the cases with and without hypothesis testing, which can be defined as $E\{(a_{\bar{f}} - a_{\bar{f}-1})/a_F\}$, is shown in Fig. 5.6. The ratio rapidly decreases as a few subcarriers are added. For more than 10 subcarriers it can be seen that the hypothesis testing is capable of reducing the search space to less than 5% of the total range.

Summarizing, the results of Figs. 5.5 and 5.6 show that the proposed enhancements of the STM algorithm can provide a considerable reduction of the computational complexity.

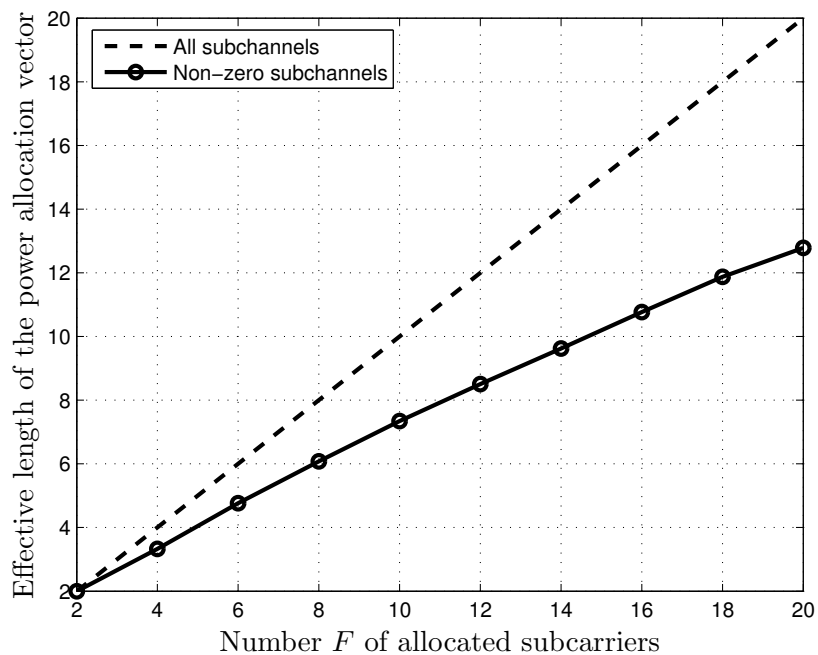


Figure 5.5. Effective length of the power allocation vector for configuration SC1, STM algorithm, $K_{uc} = K_{mc} = F/2$, and $N_{mc} = 3$.

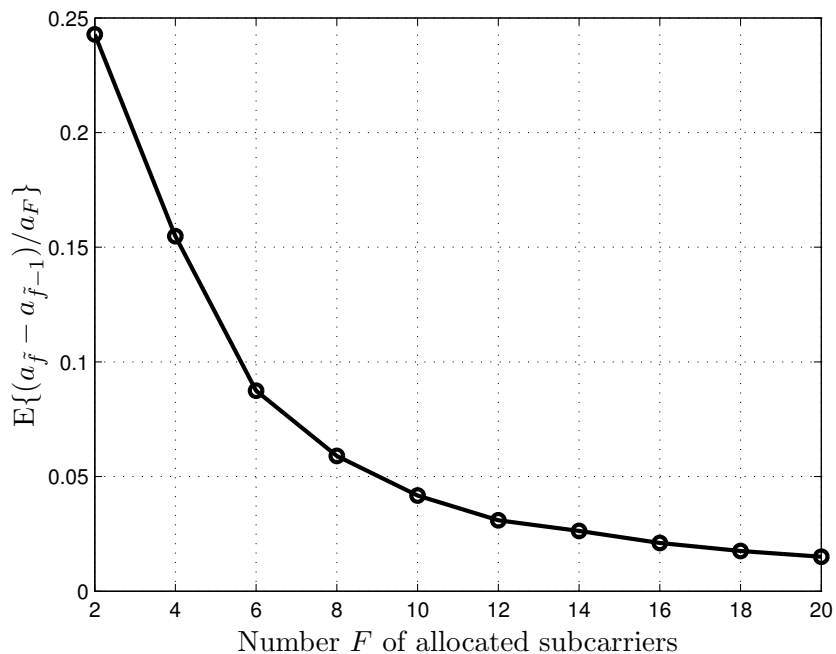


Figure 5.6. Ratio between the search space range with and without hypothesis testing for configuration SC1, STM algorithm, $K_{uc} = K_{mc} = F/2$, and $N_{mc} = 3$.

5.5 Considerations for SDMA scenarios

In SDMA scenarios, multiple multicast groups may share the same radio resource. The motivation is to improve the resource efficiency, but at the cost of increased inter-group interference. Such interference can be mitigated through the multi-group multicast beamforming algorithms presented in Chapter 4.

The decision of which groups to assign to the same resources is expected to have a significant impact on the performance. In the case of unicast users, several algorithms have been proposed by previous works. The term “grouping criterion” is usually employed to describe the measure that quantifies the degree of compatibility among the users, i.e., how efficiently can the interference among the users be mitigated when they share the same resources. In [STKL01, FGH05, YG05], criteria based on the actual calculation of beamforming matrices are proposed for the unicast case, whereas in [Cal04, SS04, MK06], lower-complexity correlation-based algorithms are considered instead. The advantage of correlation-based algorithms is that the channel correlation is an adequate measure for assessing the compatibility among users, while at the same time avoiding the burden of calculating beamforming matrices for the different possible user groupings.

In the case of multiple multicast groups, algorithms similar to the unicast case can be employed as well. The difference is that the compatibility criterion now has to be calculated among all users of different multicast groups, since they are potential interferers. In this case, a “group criterion” can also be taken into account, i.e., the different values can be somehow combined. The derivation of such an allocation algorithm, however, is not the focus of this section. The purpose of this discussion is to show that the sharing of resources by different multicast groups, in spite of the more delicate compatibility issue, still leads to better performances than isolating the groups in different resources. For this matter, two allocation approaches are briefly analyzed in the following:

- MC|UC: This approach consists of separating the users according to their type of service, i.e., Unicast (UC) and Multicast (MC) users are allocated to different time or frequency resources. More specifically, a UC resource can have more than one unicast user and an MC resource can have more than one multicast group. This means that multicast beamforming and traditional unicast SDMA can be employed separately on their respective resources.
- MC+UC: this corresponds to an allocation scheme which allows both unicast and multicast users to share the same resources. The interference within a same

resource is mitigated by multi-group multicast beamforming algorithms, such as those presented in Chapter 4.

In order to evaluate the performance gains that an efficient grouping might provide in terms of the quality of the worst-user, it is here considered that, among all possible groupings, the one providing the highest worst-user throughput is selected. The interference mitigation is done by considering the MA-ZF algorithm described in Section 4.4.2.2. The simulation results consider an exhaustive group search, but other more computationally efficient schemes, such as those previously mentioned for the unicast case, can be employed instead.

Now, the performance of the two considered allocation strategies – MC+UC and MC|UC – is compared. The MC+UC strategy refers to the case in which MC and UC users may share the same resource, whereas for the MC|UC strategy the MC and UC users are active in different resources. For both cases, a maximum of two resources is assumed. The 10th percentile of the worst user throughput, among both MC and UC services, assuming Gaussian signalling and an average E_s/N_0 of 10dB, is presented in Fig. 5.7 as a function of the number of unicast users, while the number of multicast users is fixed to 4. Since this is an SDMA scenario, a multi-antenna base station is taken into account, which in this analysis is assumed to have 8 antenna elements. Note that the throughput is normalized by the number of resources, i.e., divided by two in this case, in order to capture the effect of the time/frequency-multiplexing.

It can be seen, as expected, that the throughput decreases with an increasing number of users. The MC+UC case presents better capacity results than MC|UC for the whole simulated range. For a low number of unicast users the advantage of MC+UC comes from the fact that it is often able to accommodate the users in a single resource, whereas MC|UC always requires two resources. For a higher number of unicast users, the MC|UC strategy concentrates too many interfering users in a same resource, while the other resource is occupied exclusively by the users of the multicast group. The MC+UC, on the other hand, better distributes the users among the resources.

Even though these results correspond to a simplified scenario, they show that an appropriate allocation that allows the sharing of resources is capable of improving the performance of a multi-group multicast system.

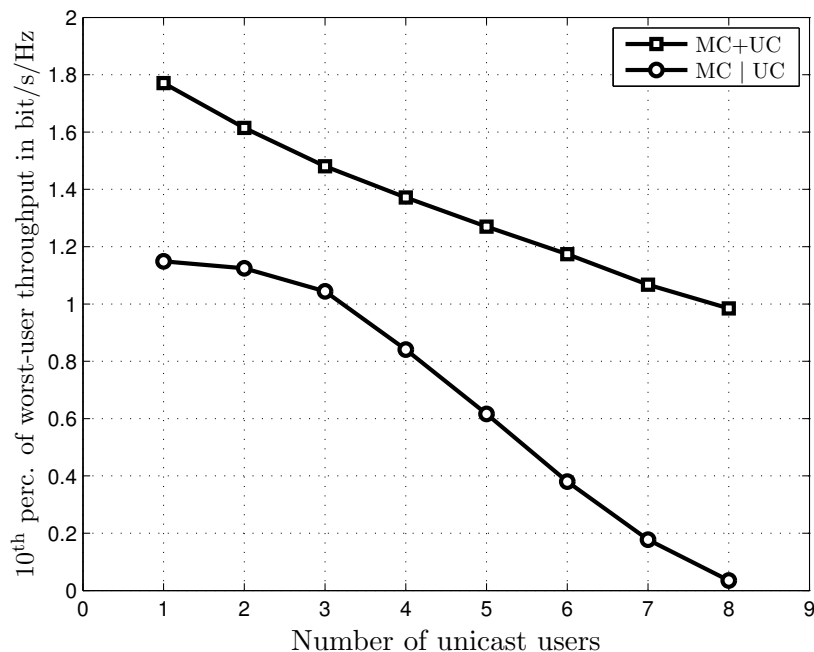


Figure 5.7. Comparison of different grouping strategies in terms of the worst-user throughput, 8-antenna array, 4 multicast users.

5.6 Conclusions

In this chapter, the resource allocation problem has been analyzed for multi-carrier multicast systems, with an emphasis on the power allocation problem. The following power allocation algorithms have been proposed and investigated: sum throughput maximization (STM), group criterion for throughput maximization (GCTM), and fair power allocation (FPA). The first two aim at maximizing the sum capacity, while the last one maximizes the minimum perceived SNR. Next, some of the main conclusions are summarized:

- The solution of the STM problem has been presented, which depends on numerical optimization, and an algorithm similar to the waterfilling hypothesis testing has been proposed for reducing the processing effort. It has been shown that by employing the hypothesis testing, both the effective power vector dimension and the search space range can be significantly reduced, especially for a large number of allocated subcarriers.
- The GCTM algorithm, which consists of a simplification of STM that employs a group quality indicator per subcarrier, has been shown to provide a reasonable

approximation of STM. The best group function was verified to be the maximum channel gain. The performance of the GCTM-Max algorithm is degraded for increased multicast group sizes, but up to an intermediate size it still achieves roughly 90% of the STM performance.

- The fairness of the power allocation algorithms with regard to the worst-user SNR has been compared. It was shown that FPA is able to provide a worst-user SNR at least 5dB higher than the other algorithms, while the STM and GCTM-Max had similar performances, but with the latter being slightly better for large group sizes.
- With regard to the allocation of resources in SDMA scenarios, it has been shown that appropriate allocation algorithms, which allow the sharing of resources by unicast and multicast users, are capable of achieving better performance results than algorithms which, for example, isolate unicast and multicast users in different resources.

Chapter 6

Conclusions

This thesis has dealt with the problem of multicast beamforming for multi-antenna wireless cellular networks. Both single-group and multi-group scenarios have been considered, with the former corresponding to a single multicast group per radio resource and the latter referring to multiple multicast groups per resource.

In order to provide the necessary mathematical framework for the analysis of the algorithms, a general system model has been proposed for the multi-group multicast scenario in Chapter 2. Particular cases, such as the multi-user, single-group, and single-user cases, can be derived from the general model by properly adjusting the system parameters.

Different beamforming algorithms known from the unicast case have been formulated for the single-group multicast case in Chapter 3. Moreover, a new algorithm called User-Selective Matched Filter (USMF), which was specifically designed for the multicast case, has been proposed. The performance of the algorithms has been analyzed in terms of the uncoded Bit Error Rate (BER) and worst-user Signal-to-Noise Ratio (SNR). The results have shown that USMF presents a good trade-off between performance and complexity, outperforming the other algorithms originally proposed for the unicast case and approaching the performance of a more complex algorithm based on Semi-Definite Relaxation (SDR).

The multi-group multicast case allows multiple multicast groups in a same resource. This resource sharing results in inter-group interference, which needs to be suppressed by the beamforming algorithms. In Chapter 4, known algorithms from the unicast case have been formulated for the multi-group multicast scenario. Additionally, these algorithms were further modified with the purpose of improving the performance of the multicast services. These modified algorithms, which were termed Multicast-Aware (MA), in most cases were based on a combination of null space projections and single-group beamforming. In the case of the linear algorithms, the MA extension presents significant performance gains over the non-MA algorithms. For the non-linear algorithms, however, the MA extension has a negative impact instead, which has been shown to be due to the additional null space constraints or the reduced dimension of the symbol vector, depending on the algorithm. The analysis of the results revealed that the best trade-off between performance and complexity was achieved by the linear multicast-aware SINR Balancing (SB) and Minimum Mean Square Error (MMSE) algorithms. It

has been shown that the choice among these algorithms depends on the ratio between the number of users and number of multicast groups.

Since the allocation of resources among the multicast groups is expected to have a significant impact on the performance of the beamforming algorithms, this issue has been addressed in Chapter 5. The analysis focuses on the proposal and evaluation of alternatives for allocating the power among the subcarriers of a multi-carrier multicast system. Different criteria, such as sum throughput maximization and user fairness, have been considered by the algorithms. The throughput maximization algorithm is shown to be an extension of the traditional waterfilling algorithm for the unicast case. For this new algorithm, the hypothesis testing procedure can also be employed in order to reduce the computational complexity. An algorithm based on a group criterion has been proposed as well, which has been shown to achieve a reasonable trade-off between performance and complexity. Additionally, some considerations have been made with regard to the allocation of resources in SDMA scenarios. It has been shown that, in spite of the inter-group interference, the sharing of resources among unicast and multicast users provides better performance than isolating them into different resources.

In summary, this thesis has provided a common framework for the analysis of single-group and multi-group multicast beamforming. The algorithms have been proposed with the purpose of improving the trade-off between performance and complexity, as well as filling the gaps in the literature, while ultimately providing a set of beamforming alternatives as complete as possible. Nevertheless, there are still several open issues and problems to be investigated by further works in the area, such as: the impact of imperfect channel knowledge on the performance of the algorithms, the extension to Multiple Input Multiple Output (MIMO) scenarios, the proposal of efficient resource allocation algorithms for multicast SDMA scenarios, among others.

Appendix

A.1 Considerations on the variance of THP-precoded symbols

In this section, some aspects regarding the variance of THP-precoded symbols are discussed. As shown in Section 3.4.4, the Tomlinson-Harashima precoding algorithm generates a new symbol vector \mathbf{v} , which depends on the modulo operator and the feedback filter \mathbf{F} .

The elements of \mathbf{v} , due to the modulo operator, necessarily lie within the region \mathbb{M} of the complex plane delimited by the τ parameter. As stated in [Joh04], the complex modulo operator $\text{mod}(x)$ and the region \mathbb{M} , respectively, are given by

$$\text{mod}(x) = x - \left\lfloor \frac{\text{Re}(x)}{\tau} + \frac{1}{2} \right\rfloor \tau - j \left\lfloor \frac{\text{Im}(x)}{\tau} + \frac{1}{2} \right\rfloor \tau, \quad (\text{A.1})$$

$$\mathbb{M} = \{x \mid -\tau/2 \leq \text{Re}(x) < \tau/2 \text{ and } -\tau/2 \leq \text{Im}(x) < \tau/2\}, \quad (\text{A.2})$$

where $x \in \mathbb{C}$, $\tau \in \mathbb{R}$, $\lfloor \cdot \rfloor$ represents the floor operator, and $\text{Re}(\cdot)$ and $\text{Im}(\cdot)$ correspond, respectively, to the real and imaginary parts of a complex number.

According to (3.41b) and (3.43b), it can be seen that the vector \mathbf{v} depends on the Cholesky decomposition \mathbf{L} of the channel matrix \mathbf{H} . For this reason, it is expected that the channel propagation model has a certain impact on how the elements of \mathbf{v} are distributed within region \mathbb{M} . This distribution determines the amount of energy that is required in order to transmit vector \mathbf{v} .

In [Joh04], a uniform area distribution is considered, which results in a variance σ_v^2 of

$$\begin{aligned} \sigma_v^2 &= \text{E}\{|v|^2\} - \text{E}\{v\}^2 = \\ &= \text{E}\{\text{Re}(v)^2\} + \text{E}\{\text{Im}(v)^2\} - (\text{E}\{\text{Re}(v)\} + j\text{E}\{\text{Im}(v)\})^2 = \frac{\tau^2}{6}, \end{aligned} \quad (\text{A.3})$$

where the individual terms were calculated based on the mean and variance of random uniform variables [Pap91], assuming that both the real and imaginary parts of v are uniformly distributed within $[-\tau/2, \tau/2]$:

$$\text{E}\{\text{Re}(v)\} = \text{E}\{\text{Im}(v)\} = (\tau/2 - \tau/2)/2 = 0, \quad (\text{A.4})$$

$$\text{E}\{\text{Re}(v)^2\} = \text{E}\{\text{Im}(v)^2\} = (\tau/2 + \tau/2)^2/12 = \tau^2/12. \quad (\text{A.5})$$

Fig. A.1 shows the distribution of v within the complex-plane for both the NLOS and LOS channel scenarios. These figures are the result of a simple simulation considering 1,000 channel realizations, 4 single-antenna users, 4 transmit antennas, QPSK modulation, and $\tau = 2\sqrt{2}$.

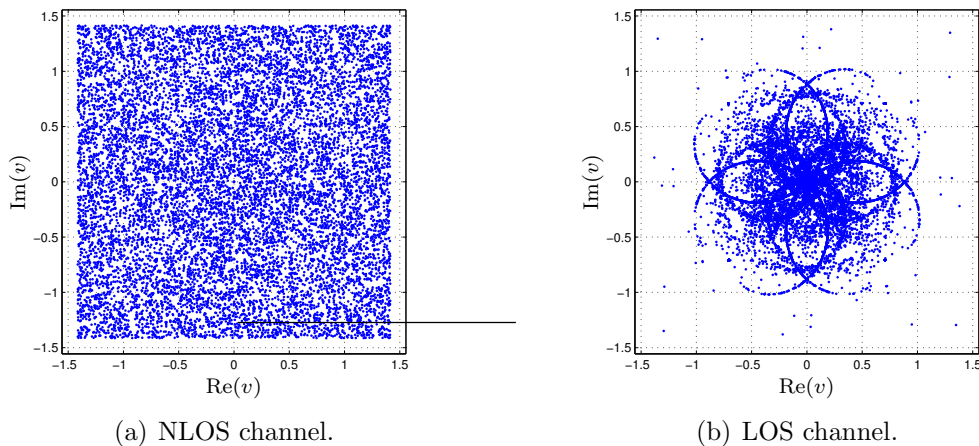


Figure A.1. Complex-plane distribution of the THP-precoded symbols.

It can be seen that the uniform assumption is in fact valid for the NLOS scenario. Nevertheless, for the LOS scenario, the symbols present a different distribution, with a larger concentration near the origin.

If the variance obtained by the uniform assumption is applied to the LOS channel, very pessimistic results are achieved. The reason for this poor performance is that the modulation matrix \mathbf{M} is normalized assuming that the symbols require more energy than they actually do. This false assumption leads to a waste of energy.

Since the calculation of σ_v^2 for the LOS scenario is not within the scope of this thesis, the LOS THP simulations in Section 3.5 take into account the actual value of the symbols, instead of their variance. This means that at each symbol time $\mathbf{R}_v = \mathbf{v}\mathbf{v}^H$ is calculated and the modulation matrix \mathbf{M} is normalized accordingly. Even though this methodology is not feasible in practice, it provides an upper bound on the THP performance that would be achievable by calculating σ_v^2 and \mathbf{R}_v appropriate to the LOS scenario.

A.2 Complexity of mathematical operations and decompositions

In this section, the computational complexity of some general mathematical operations and decompositions is presented, which are necessary for determining the complexity order of the beamforming algorithms of Sections 3.4, 4.4, and 4.5.

Table A.1 shows the computational complexity of several mathematical operations involving scalars, vectors, and matrices. The complexity is expressed in terms of the number of required complex multiplications, and the complexity order takes into account the big O notation [GL96]. Divisions and square roots have the same complexity as a multiplication, when they are efficiently implemented using Newton's method [BV04], and therefore are counted as such, whereas additions and subtractions are not considered. In [Hun07], a similar general complexity table is presented, which includes the summations as well.

For the multiplication of triangular matrices, it is assumed that both matrices are either lower-triangular or upper-triangular. The complexity of multiplying triangular matrices of dimension L is demonstrated in [Hun07]. Alternatively, this can also be demonstrated by showing that the number of required multiplications is numerically equal to the L^{th} element of a sequence of tetrahedral numbers, which is given by $C(L + 2, 3)$ [Slo07], where $C(n, k)$ is the number of k combinations from a set with n elements.

In addition to Table A.1, the complexity of certain matrix decompositions is shown in Table A.2. The algorithms applied for calculating the factorizations are described in [GL96]. The Cholesky decomposition can be found either through the Gaxpy [GL96] or the outer product [GL96] algorithms, which have both the same complexity order. The eigenvalue decomposition is assumed to be calculated by the QR algorithm [GL96] with Householder reductions [GL96]. The singular value decomposition takes the Golub-Reinsch algorithm into account, but assuming that only the singular values and the right singular vectors are calculated [Bjo96].

Table A.1. Computational complexity of mathematical operations.

Operation	Notation	Number of multiplications	Complexity order
Multiplication	ab	1	$\mathcal{O}(1)$
Division	a/b	1	$\mathcal{O}(1)$
Square root	\sqrt{a}	1	$\mathcal{O}(1)$
Multiplication of vectors (inner product)	$\mathbf{a}_{1 \times L} \mathbf{b}_{L \times 1}$	L	$\mathcal{O}(L)$
Multiplication of vectors (outer product)	$\mathbf{b}_{L \times 1} \mathbf{a}_{1 \times L}$	L^2	$\mathcal{O}(L^2)$
Multiplication of vector and matrix	$\mathbf{A}_{L \times M} \mathbf{b}_{M \times 1}$	LM	$\mathcal{O}(LM)$
Multiplication of matrices	$\mathbf{A}_{L \times M} \mathbf{B}_{M \times N}$	LMN	$\mathcal{O}(LMN)$
Multiplication of diagonal matrices	$\mathbf{A}_{L \times L} \mathbf{B}_{L \times L}$	L	$\mathcal{O}(L)$
Multiplication of either lower or upper triangular matrices	$\mathbf{A}_{L \times L} \mathbf{B}_{L \times L}$	$\frac{1}{6}L^3 + \frac{1}{2}L^2 + \frac{1}{3}L$	$\mathcal{O}(\frac{1}{6}L^3)$
Gram matrix generation	$\mathbf{A}_{L \times M} \mathbf{A}_{M \times L}^H$	$\frac{1}{2}L^2M + \frac{1}{2}LM$	$\mathcal{O}(\frac{1}{2}L^2M)$
Inversion of a matrix	$\mathbf{A}_{L \times L}^{-1}$	L^3	$\mathcal{O}(L^3)$
Inversion of a diagonal matrix	$\mathbf{A}_{L \times L}^{-1}$	L	$\mathcal{O}(L)$
Inversion of a triangular matrix	$\mathbf{A}_{L \times L}^{-1}$	$\frac{1}{6}L^3 + \frac{1}{2}L^2 + \frac{1}{3}L$	$\mathcal{O}(\frac{1}{6}L^3)$
Pseudoinverse of a full row rank matrix	$(\mathbf{A}_{L \times M})^+ = \mathbf{A}^H (\mathbf{A} \mathbf{A}^H)^{-1}$	$\frac{3}{2}L^2M + L^3 + \frac{1}{2}LM$	$\mathcal{O}(\frac{3}{2}L^2M + L^3)$
Pseudoinverse of a full column rank matrix	$(\mathbf{A}_{L \times M})^+ = (\mathbf{A}^H \mathbf{A})^{-1} \mathbf{A}^H$	$\frac{3}{2}LM^2 + M^3 + \frac{1}{2}LM$	$\mathcal{O}(\frac{3}{2}LM^2 + M^3)$

Table A.2. Computational complexity of matrix decompositions.

Operation	Notation	Complexity order
Cholesky decomposition	$\mathbf{A}_{L \times L} = \mathbf{L} \mathbf{L}^H$	$\mathcal{O}(\frac{1}{3}L^3)$
Eigenvalue decomposition of a matrix	$\mathbf{A}_{L \times L} = \mathbf{Q} \mathbf{\Lambda} \mathbf{Q}^{-1}$	$\mathcal{O}(\frac{5}{3}L^3)$
Eigenvalue decomposition of a symmetric matrix	$\mathbf{A}_{L \times L} = \mathbf{Q} \mathbf{\Lambda} \mathbf{Q}^{-1}$	$\mathcal{O}(\frac{2}{3}L^3)$
Singular value decomposition	$\mathbf{A}_{L \times M} = \mathbf{U} \mathbf{\Sigma} \mathbf{V}^H$	$\mathcal{O}(2LM^2 + 4M^3)$

List of Acronyms

ARQ	Automatic Repeat Request
BD	Block Diagonalization
BER	Bit Error Rate
CDMA	Code Division Multiple Access
CP	Cyclic Prefix
DPC	Dirty Paper Coding
FEC	Forward Error Correction
FPA	Fair Power Allocation
GCTM	Group Criterion for Throughput Maximization
GSM	Global System for Mobile communications
HLNP	Hybrid Linear and Non-linear Precoding
IFFT	Inverse Fast Fourier Transform
ILDLP	Iterative Least Distance Programming
ILS	Integer Least Squares
ISD	Iterative Spatial Diagonalization
KKT	Karush-Kuhn-Tucker
LLL	Lenstra-Lenstra-Lovász
LOS	Line-Of-Sight
LP	Linear Programming
LSI	Least Squares with Inequality constraint
MA	Multicast-Aware
MaxAvg	Maximization of the Average SNR
MBMS	Multimedia Broadcast/Multicast Service
MC	Multicast

MF	Matched Filter
MIMO	Multiple Input Multiple Output
MIMO-MU	MIMO Multi User
MMSE	Minimum Mean Square Error
MSE	Mean Square Error
NLOS	Non-Line-Of-Sight
NP	Non-Polynomial time
NP-hard	Nondeterministic Polynomial time hard
OFDM	Orthogonal Frequency Division Multiplexing
P2M	Point-to-Multipoint
P2P	Point-to-Point
PSK	Phase Shift Keying
QAM	Quadrature Amplitude Modulation
SB	SINR Balancing
SDMA	Spatial Division Multiple Access
SDP	Semi-Definite Programming
SDR	Semi-Definite Relaxation
SFB	Switched Fixed Beams
SINR	Signal-to-Interference plus Noise Ratio
SNR	Signal-to-Noise Ratio
SQP	Sequential Quadratic Programming
SSA	Simple Subchannel Allocation
STM	Sum Throughput Maximization
SVD	Singular Value Decomposition
THP	Tomlinson-Harashima Precoding

UC	Unicast
UMTS	Universal Mobile Telecommunications System
USMF	User-Selective Matched Filter
UTRAN	UMTS Terrestrial Radio Access Network
VP	Vector Precoding
WiMAX	Worldwide interoperability for Microwave Access
WLAN	Wireless Local Area Network
ZF	Zero-Forcing

List of Symbols

$\mathbf{1}$	Vector of ones
$\operatorname{argmax}_x y$	Returns the value of x that maximizes y
a_f	Maximum μ achieved for $p_f = 0$
\mathbf{a}	Auxiliary symbol vector at the transmitter or perturbation vector
\mathbf{a}'	Auxiliary symbol vector at the transmitter or perturbation vector in the reduced form
$\hat{\mathbf{a}}$	Auxiliary symbol vector at the receiver
A_k	Auxiliary dimension of null-space algorithms
$A_{i,j}$	Element of \mathbf{A}
\mathbf{A}	Subchannel allocation matrix
b_n	Index of group to which user n belongs
\mathbf{b}	Vector that associates which users belong to which group
\overline{BER}_i	Average bit error rate for the i^{th} channel realization
c_f	f^{th} element of vector \mathbf{c}
$c_{i,i}$	i^{th} element of the main diagonal of \mathbf{C}
\mathbf{c}	Inverse equivalent channel gain vector for the multicast group
\mathbf{C}	Non-zero diagonal matrix of the USMF algorithm
$\operatorname{diag}(\cdot)$	Returns a diagonal matrix when the argument is a vector, or returns a vector containing the elements of the main diagonal when the argument is a matrix
$\operatorname{diag}_b(\cdot)$	Returns a block diagonal matrix from another matrix based on the definition of multicast groups
d	Receive filter coefficient for the single-user unicast case
d_n	Receive filter coefficient associated to user n
\mathbf{d}_n	Receive filter coefficients associated to user n for the MIMO case
\mathbf{D}	Receive filter matrix
e	Base of the natural logarithm, also called Napier's constant
$\operatorname{eigv}(\cdot)$	Returns the unit-norm principal eigenvector of a matrix
$E\{\cdot\}$	Expectation operator
\mathbf{e}_i	Vector corresponding to the i^{th} column of the identity matrix
E	Number of errors
E_s/N_0	Ratio of the symbol power to the spectral noise density
f	Subcarrier index
\tilde{f}	Subcarrier iteration index

F	Number of subcarriers
\mathbf{F}	Feedback filter matrix of THP
\mathbf{F}'	Feedback filter matrix of THP in the reduced form
\mathbf{F}'_{uc}	Feedback filter matrix of THP for all multicast users in the reduced form
g_f	Group quality indicator of subchannel f
g'_f	Equivalent channel gain for the multicast group in subchannel f
g_k	Size of multicast group k
$G_{n,f}$	Element of \mathbf{G}
\mathbf{g}	Vector of group sizes
\mathbf{G}	Normalized channel gain conditioned to the channel allocation
\mathbf{G}_f	f^{th} column of matrix \mathbf{G}
\mathbf{G}_n	Normalized Gram matrix of the channel of user n
\mathbf{G}'_k	Normalized Gram matrix of the equivalent channel of group k in the reduced form
\mathbf{h}	Vector of channel coefficients for the single-user unicast case
\mathbf{h}_n	Vector corresponding to the n^{th} row of matrix \mathbf{H}
$\bar{\mathbf{h}}_n$	n^{th} row of matrix $\bar{\mathbf{H}}$
$\mathbf{h}_{(k,i)}$	Vector of channel coefficients of the i^{th} user within group k
$H_{n,l}$	Channel coefficient between transmit antenna element l and user n
$H_{n,l}(\nu)$	Transfer function of the radio link between transmit antenna element l and user n in the frequency domain
$H_{n,l,f}$	Channel coefficient between transmit antenna element l and user n on subcarrier f
\mathbf{H}	Matrix of channel coefficients
\mathbf{H}_k	Matrix of channel coefficients of group k
\mathbf{H}_n	Matrix of channel coefficients of user n
\mathbf{H}_{PL}	Matrix of channel coefficients with included path-loss components
$\mathbf{H}^{(R)}$	Regularized matrix of channel coefficients
$\mathbf{H}_k^{(R)}$	Regularized matrix of channel coefficients of group k
$\mathbf{H}_k^{(eq)}$	Equivalent matrix of channel coefficients of group k
$\mathbf{H}_{(uc)}$	Matrix of channel coefficients of all unicast users
$\bar{\mathbf{H}}$	Matrix of channel coefficients with only LOS components
$\check{\mathbf{H}}$	Matrix of channel coefficients with only NLOS components
$\tilde{\mathbf{H}}_k$	Matrix of channel coefficients of all groups except k
\mathbf{I}	Identity matrix

j	$\sqrt{-1}$
\mathbf{J}	Matrix of ones
k	Multicast group index
K	Number of multicast groups
K_{uc}	Number of unicast groups
K_{mc}	Number of multicast groups
l	Antenna element index
$L(\cdot)$	Lagrangian function
L	Number of antenna elements at the base station
L_t	Number of transmit antennas for the MIMO case
L_r	Number of receive antennas for the MIMO case
$L_r^{(n)}$	Number of receive antennas of user n for the MIMO case
\mathbf{L}	Lower triangular matrix that comes from the Cholesky factorization of the channel
\mathbf{L}_d	Diagonal matrix containing the elements of the main diagonal of \mathbf{L}
$\min_i x_i$	Returns the minimum x_i for all possible indices i
$\min_+ x_i$	Returns the minimum non-zero x_i for all possible indices i
m_l	Transmit filter coefficient associated to transmit antenna element l for the single-group multicast case
$m_{l,n}$	Transmit filter coefficient associated to transmit antenna element l and user n
\mathbf{m}	Transmit filter vector for the single-group multicast or single-user unicast cases
\mathbf{m}_n	Vector corresponding to the n^{th} column of matrix \mathbf{M}
\mathbf{m}'_k	Vector corresponding to the k^{th} column of matrix \mathbf{M}'
$\mathbf{m}_k^{(\text{eq})}$	Equivalent beamforming vector obtained after applying single-group beamforming to $\mathbf{H}_k^{(\text{eq})}$
M_o	Modulation order
\mathbf{M}	Transmit filter matrix (also called beamforming matrix or modulation matrix)
\mathbf{M}'	Transmit filter matrix in the reduced form
\mathbf{M}'_{uc}	Transmit filter matrix of all unicast users in the reduced form
n	User index
N	Number of users
N_f	Number of users within subcarrier f
N_s	Number of symbol intervals

N_{uc}	Number of unicast users
N_{mc}	Number of users within multicast group
p_f	Power allocated to subcarrier f
p_n	n^{th} element of power allocation vector
p'_k	k^{th} element of power allocation vector in the reduced form
\mathbf{p}	Power allocation vector
\mathbf{p}'	Power allocation vector in the reduced form
\mathbf{p}'_{PR}	Power re-allocation vector in the reduced form
\mathbf{p}_{ext}	Extended power allocation vector
P	Total transmission power
P_{req}	Required amount of power
$P'_{i,j}$	Element of \mathbf{P}'
\mathbf{P}'	Alternative feedback filter representation in the reduced form
q_n	n^{th} element of vector \mathbf{q}
\mathbf{q}	Uplink power allocation vector
\mathbf{Q}_n	Uplink sum interference matrix of user n
$\text{rank}(\cdot)$	Rank of a matrix
r_b	Distance between base station and cell border
r_n	Distance between user n and the base station
\tilde{r}_k	Rank of matrix $\tilde{\mathbf{H}}_k$
R	Throughput
$R_{n,f}$	Throughput of user n in subcarrier f
\mathbf{r}	Vector with distance of all users to the base station
\mathbf{r}_k	Received power vector of group k
\mathbf{R}_s	Signal covariance matrix
\mathbf{R}'_s	Signal covariance matrix in the reduced form
\mathbf{R}_v	Covariance matrix of the precoded data vector \mathbf{v} for THP
s	Data symbol for the single-group multicast or single-user unicast cases
\hat{s}	Estimate of data symbol s for the single-user unicast case
s_n	Data symbol intended for user n
s'_k	Data symbol intended for group k in the reduced form
\hat{s}_n	Estimate of data symbol s_n
$s_{n,f}$	Data symbol intended for user n and mapped to subcarrier f
\mathbf{s}	Data symbol vector
\mathbf{s}_{eq}	Equivalent data symbol vector

\mathbf{s}'_{eq}	Equivalent data symbol vector in the reduced form
\mathbf{s}'	Data symbol vector in the reduced form
$\hat{\mathbf{s}}$	Estimated data symbol vector
$\hat{\mathbf{s}}_{\text{eq}}$	Equivalent estimated data symbol vector
$\hat{\mathbf{s}}'_{\text{eq}}$	Equivalent estimated data symbol vector in the reduced form
S	Number of symbols
$S_{i,j}$	Element of matrix \mathbf{S}
$S'_{i,j}$	Element of matrix \mathbf{S}'
\mathbf{S}	Signal part matrix (SB algorithm)
\mathbf{S}'	Signal part matrix in the reduced form (SB algorithm)
$\tilde{\mathbf{S}}_k$	Diagonal matrix resulting from the SVD of $\tilde{\mathbf{H}}_k$
$\text{tr}(\cdot)$	Trace of a matrix
\mathbf{t}	Transformation vector for the single-group multicast case
\mathbf{t}^+	Pseudoinverse of \mathbf{t} for the single-group multicast case
\mathbf{t}_n^+	Vector corresponding to the n^{th} row of matrix \mathbf{T}^+
T_f	Frame duration
T_s	Symbol time
\mathbf{T}	Transformation matrix that relates the reduced and complete forms
\mathbf{T}^+	Right pseudoinverse of matrix \mathbf{T}
\mathbf{u}_n	n^{th} column of matrix \mathbf{U}
\mathbf{u}'_k	k^{th} column of matrix \mathbf{U}'
\mathbf{U}	Unit-norm beamforming matrix
\mathbf{U}'	Unit-norm beamforming matrix in the reduced form
$\tilde{\mathbf{U}}_k$	Unitary matrix resulting from the SVD of $\tilde{\mathbf{H}}_k$
$\tilde{\mathbf{V}}_k^{(0)}$	Matrix of right singular vectors resulting from the SVD of $\tilde{\mathbf{H}}_k$
$\tilde{\mathbf{V}}_k^{(1)}$	Matrix of left singular vectors resulting from the SVD of $\tilde{\mathbf{H}}_k$
\mathbf{v}	Data vector after the feedback filter for THP
\mathbf{w}_i	i^{th} beamforming vector of the set of fixed beamformers
x_l	Signal transmitted by antenna element l
$x_l(\nu)$	Signal transmitted by antenna element l in the frequency domain
$x_{l,f}$	Signal transmitted by antenna element l on subcarrier f
\mathbf{x}	Data symbol vector after transmit processing
\mathbf{X}	Matrix to be optimized by the single-group multicast SDR algorithm
y_n	Signal received by user terminal n
$y_n(\nu)$	Signal received by user terminal n in the frequency domain

$y_{n,f}$	Signal received by user terminal n on subcarrier f
\mathbf{y}	Estimate of data symbol vector before receive processing
z	Additive white Gaussian noise for the single-user unicast case
z_n	Additive white Gaussian noise of user n
$z_n(\nu)$	Additive white Gaussian noise of user n in the frequency domain
$z_{n,f}$	Additive white Gaussian noise of user n on subcarrier f
\mathbf{z}	Additive white Gaussian noise vector
\mathbf{z}_n	Additive white Gaussian noise vector of user n for the MIMO case
α	Path-loss exponent
β	Energy normalization factor
γ	SNR value
γ_n	SNR or SINR of user n
γ_{eq}	Equivalent SNR or SINR
γ_{tgt}	SNR or SINR target
γ_{max}	Maximal SNR or SINR value
$\gamma_{\text{min}}(\mathbf{C})$	Worst-user SNR given a certain matrix \mathbf{C} for the USMF algorithms
δ	Antenna spacing in wavelengths
θ	Angular direction of the user
κ	Rician factor
λ_{max}	Dominant eigenvalue of the power allocation problem (SB algorithm)
μ	Lagrange multiplier
ν	Frequency
ν_f	Lagrange multiplier
$\boldsymbol{\nu}$	Vector of Lagrange multipliers
$\rho_{i,j}$	Correlation between the vector channels of users i and j
σ_s^2	Average symbol power
σ_v^2	Average power of the THP precoded symbols
σ_z^2	Average noise power
τ	THP parameter for delimiting the complex plane
$\mathbf{\Gamma}$	Power loading matrix
$\mathbf{\Lambda}$	Matrix of Lagrange multipliers
$\mathbf{\Upsilon}$	Extended coupling matrix
$\mathbf{\Upsilon}'$	Extended coupling matrix in the reduced form
$\mathbf{\Upsilon}^{(\text{ul})}$	Extended uplink coupling matrix
$\Psi_{i,j}$	Element of matrix $\mathbf{\Psi}$

$\Psi'_{i,j}$	Element of matrix Ψ'
Ψ	Interference part matrix (SB algorithm)
Ψ'	Interference part matrix in the reduced form (SB algorithm)
\mathcal{B}	Set of indices of available switched fixed beams
\mathcal{B}_g	Set of beam indices requested by the group of users
\mathcal{F}	Set of all subchannel indices
\mathcal{N}_k	Set that contains the indices of users belonging to group k
$\mathcal{O}(\cdot)$	Complexity order of the argument
\mathbb{C}	Set of complex numbers
\mathbb{R}	Set of real numbers
\mathbb{Z}	Set of integer numbers
$(\cdot)^T$	Transpose of a vector or matrix
$(\cdot)^H$	Conjugate transpose of a vector or matrix
$(\cdot)^*$	Conjugate of a scalar, vector, or matrix
$(\cdot)^+$	Pseudoinverse of a vector or matrix
$(\cdot)^{-1}$	Inverse of a square matrix
$ \cdot $	Absolute value of a scalar
$\ \cdot\ $	Euclidean norm or 2-norm of a vector
$\ \cdot\ _1$	1-norm of a vector

Bibliography

- [3GP06a] 3GPP, “Multimedia Broadcast/Multicast service (MBMS); architecture and functional description,” Technical Specification Group Services and System Aspects, Tech. Rep. TS 23.246 v6.10.0, June 2006.
- [3GP06b] 3GPP, “Physical layer aspects for evolved Universal Terrestrial Radio Access (UTRA),” Technical Specification Group Radio Access Network, Tech. Rep. TR 25.814 v7.1.0, Sep. 2006.
- [AEVZ02] E. Agrell, T. Eriksson, A. Vardy, and K. Zeger, “Closest point search in lattices,” *IEEE Transactions on Information Theory*, vol. 48, pp. 2201–2214, Aug. 2002.
- [AH04] A. Alexiou and M. Haardt, “Smart antenna technologies for future wireless systems: trends and challenges,” *IEEE Communications Magazine*, pp. 90–97, Sep. 2004.
- [ANS03] ANSI/IEEE, “Wireless LAN Medium Access Control (MAC) and Physical Layer (PHY) specifications,” ANSI/IEEE, Tech. Rep. Std 802.11, 1999 Edition (R2003), June 2003.
- [BB99] M. Bossert and M. Breitbach, *Digitale Netze*, 1st ed. Teubner, 1999.
- [BF99] A. N. Barreto and G. Fettweis, “On the downlink capacity of TDD CDMA systems using a pre-Rake,” in *Proc. IEEE Global Telecommunications Conference (GLOBECOM)*, vol. 1a, pp. 117–121, Dec. 1999.
- [BF03] ———, “Joint signal precoding in the downlink of spread-spectrum systems,” *IEEE Transactions on Wireless Communications*, vol. 2, pp. 511–518, May 2003.
- [BGWM07] M. Bohge, J. Gross, A. Wolisz, and M. Meyer, “Dynamic resource allocation in OFDM systems: an overview of cross-layer optimization principles and techniques,” *IEEE Network*, pp. 53–59, Jan./Feb. 2007.
- [BH05] M. Bakhuizen and U. Horn, “Mobile broadcast/multicast in mobile networks,” *Ericsson Review*, issue no. 01/2005, May 2005.
- [Bjo96] A. Bjorck, *Numerical methods for least squares problems*, 1st ed. SIAM: Society for Industrial and Applied Mathematics, 1996.
- [BL61] J. Butler and R. Lowe, “Beam-forming matrix simplifies design of electronically scanned antennas,” *Electronic Design*, pp. 170–173, Apr. 1961.
- [BO99] M. Bengtsson and B. Ottersten, “Optimal downlink beamforming using semidefinite optimization,” in *Proc. Annual Allerton Conference on Communication, Control, and Computing*, pp. 987–996, Sep. 1999.

- [BPD00] M. Brandt-Pearce and A. Dharap, "Transmitter-based multiuser interference rejection for the down-link of a wireless CDMA system in a multipath environment," *IEEE Journal on Selected Areas of Communication*, vol. 18, pp. 407–417, Mar. 2000.
- [BV04] S. Boyd and L. Vandenberghe, *Convex optimization*, 1st ed. Cambridge University Press, 2004.
- [Cal04] D. B. Calvo, "Fairness analysis of wireless beamforming schedulers," Ph.D. dissertation, Technical University of Catalonia, 2004.
- [CLM01] R. L. Choi, K. B. Letaief, and R. D. Murch, "MISO CDMA transmission with simplified receiver for wireless communications handsets," *IEEE Transactions on Communications*, vol. 49, pp. 888–898, May 2001.
- [Cos83] M. H. M. Costa, "Writing on dirty paper," *IEEE Transactions on Information Theory*, vol. IT-29, no. 3, pp. 439–441, May 1983.
- [CZ06] X.-W. Chang and T. Zhou, "MILES: MATLAB package for solving Mixed Integer LEast Squares problems – Theory and Algorithms," McGill University, Tech. Rep., Oct. 2006. [Online]. Available: <http://www.cs.mcgill.ca/~chang>
- [EN93] R. Esmailzadeh and M. Nakagawa, "Pre-RAKE diversity combination for direct sequence spread spectrum mobile communication systems," *IEICE Transactions on Communications*, vol. E76-B, pp. 1008–1015, Aug. 1993.
- [FGH05] M. Fuchs, G. D. Galdo, and M. Haardt, "A novel tree-based scheduling algorithm for the downlink of multi-user MIMO systems with ZF beamforming," in *Proc. IEEE International Conference on Acoustics, Speech, and Signal Processing (ICASSP)*, vol. 3, pp. 1121–1124, Mar. 2005.
- [FLFV00] F. R. Farrokhi, A. Lozano, G. J. Foschini, and R. A. Valenzuela, "Spectral efficiency of wireless systems with multiple transmit and receive antennas," in *Proc. IEEE International Symposium on Personal, Indoor and Mobile Radio Communications (PIMRC)*, vol. 1, pp. 18–21, Sep. 2000.
- [FN96] C. Farsakh and J. A. Nossek, "A real time downlink channel allocation scheme for an SDMA mobile radio system," in *Proc. IEEE International Symposium on Personal, Indoor and Mobile Radio Communications (PIMRC)*, vol. 3, pp. 1216–1220, Oct. 1996.
- [FWLH02] R. F. H. Fischer, C. Windpassinger, A. Lampe, and J. B. Huber, "Space-time transmission using Tomlinson-Harashima precoding," in *Proc. ITG Conference on Source and Channel Coding (SCC)*, pp. 139–147, Jan. 2002.
- [GJ79] M. R. Garey and D. S. Johnson, *Computers and intractability: A guide to the theory of NP-completeness*. W. H. Freeman, 1979.
- [GL96] G. H. Golub and C. F. V. Loan, *Matrix computations*, 3rd ed. Johns Hopkins University Press, 1996.

- [GS05a] Y. Gao and M. Schubert, "Group-oriented beamforming for multi-stream multicasting based on quality-of-service requirements," in *Proc. IEEE International Workshop on Computational Advances in Multi-Sensor Adaptive Processing (CAMSAP)*, pp. 193–196, Dec. 2005.
- [GS05b] A. Gershman and N. Sidiropoulos, Eds., *Space-Time Processing for MIMO Communications*. John Wiley & Sons, Apr. 2005.
- [GS06] Y. Gao and M. Schubert, "Power allocation for multi-group multicasting with beamforming," in *Proc. ITG/IEEE Workshop on Smart Antennas (WSA)*, Mar. 2006.
- [HM72] H. Harashima and H. Miyakawa, "Matched-transmission technique for channels with intersymbol interference," *IEEE Transactions on Communications*, vol. 20, pp. 774–780, Aug. 1972.
- [HP03] S. Hara and R. Prasad, *Multicarrier techniques for 4G mobile communications*, 1st ed., ser. Universal Personal Communications Series. Artech House, 2003.
- [HPS05] B. M. Hochwald, C. B. Peel, and A. L. Swindlehurst, "A vector-perturbation technique for near-capacity multiantenna multiuser communication - Part II: Perturbation," *IEEE Transactions on Communications*, vol. 53, pp. 537–544, Mar. 2005.
- [HSJ+07] R. Hunger, D. A. Schmidt, M. Joham, A. Schwing, and W. Utschick, "Design of single-group multicasting-beamformers," in *Proc. IEEE International Conference on Communications (ICC)*, June 2007.
- [Hun07] R. Hunger, "Floating point operations in matrix-vector calculus," Technische Universität München, Tech. Rep., Sep. 2007. [Online]. Available: <http://www.msv.ei.tum.de/MSV/people/rahu/index.html>
- [IEE04] IEEE, "Air interface for fixed broadband wireless access systems," IEEE, Tech. Rep. IEEE 802.16-2004, Oct. 2004.
- [IGAG05] R. Ibrahim, M. Gharavi-Alkhansari, and A. B. Gershman, "Exact error probability analysis of multimedia multicast transmission in MIMO wireless networks using orthogonal space-time block codes," in *Proc. IEEE International Conference on Acoustics, Speech, and Signal Processing (ICASSP)*, vol. 4, pp. 889–892, Mar. 2005.
- [JBS00] M. C. Jeruchim, P. Balaban, and K. S. Shanmugan, *Simulation of Communication Systems - Modeling, Methodology, and Techniques*, 2nd ed. Springer, 2000.
- [JBU04] M. Joham, J. Brehmer, and W. Utschick, "MMSE approaches to multiuser spatio-temporal Tomlinson-Harashima precoding," in *Proc. ITG Conference on Source and Channel Coding (SCC)*, pp. 387–394, Jan. 2004.

- [JLSX05] H. Jenkac, G. Liebl, T. Stockhammer, and W. Xu, “Retransmission strategies for MBMS over GERAN,” in *Proc. IEEE Wireless Communications and Networking Conference (WCNC)*, vol. 3, pp. 1773–1779, Mar. 2005.
- [Joh04] M. Joham, “Optimization of linear and nonlinear transmit signal processing,” Ph.D. dissertation, Technische Universität München, 2004.
- [JSBU07] M. Joham, D. A. Schmidt, H. Brunner, and W. Utschick, “A symbol-wise order optimization for successive precoding,” in *Proc. ITG/IEEE Workshop on Smart Antennas (WSA)*, Feb. 2007.
- [JUN01] M. Joham, W. Utschick, and J. A. Nossek, “On the equivalence of prerake and transmit matched filter,” in *Proc. Aachen Symposium on Signal Theory*, pp. 313–318, Sep. 2001.
- [JUN05] —, “Linear transmit processing in MIMO communications systems,” *IEEE Transactions on Signal Processing*, vol. 53, pp. 2700–2712, Aug. 2005.
- [JXCN07] T. Jiang, W. Xiang, H.-H. Chen, and Q. Ni, “Multicast broadcast services support in OFDMA-based WiMAX systems,” *IEEE Communications Magazine*, vol. 45, no. 8, pp. 78–86, Aug. 2007.
- [KBB⁺05] T. Kaiser, A. Bourdoux, H. Boche, J. R. Fonollosa, J. B. Andersen, and W. Utschick, Eds., *Smart antennas - State of the Art*, 1st ed., ser. EURASIP Book Series on Signal Processing and Communications. Hindawi, 2005.
- [Kes07] F. Keskin, “Precoding for MIMO multi-user mobile radio downlinks,” Ph.D. dissertation, TU Kaiserslautern, 2007.
- [Khi04] A. Khisti, “Coding techniques for multicasting,” Master’s thesis, Massachusetts Institute of Technology, 2004.
- [KSL05] E. Karipidis, N. D. Sidiropoulos, and Z.-Q. Luo, “Transmit beamforming to multiple co-channel multicast groups,” in *Proc. IEEE International Workshop on Computational Advances in Multi-Sensor Adaptive Processing (CAMSAP)*, pp. 109–112, Dec. 2005.
- [KSL06] —, “Convex transmit beamforming for downlink multicasting to multiple co-channel groups,” in *Proc. IEEE International Conference on Acoustics, Speech, and Signal Processing (ICASSP)*, vol. 5, pp. 973–976, May 2006.
- [KSL07] —, “Far-field multicast beamforming for uniform linear antenna arrays,” *IEEE Transactions on Signal Processing*, vol. 55, no. 10, pp. 4916–4927, Oct. 2007.
- [Lar03] E. G. Larsson, “Unitary nonuniform space-time constellations for the broadcast channel,” *IEEE Communications Letters*, vol. 7, no. 1, pp. 21–23, Jan. 2003.
- [LK05] J. Liu and W. A. Krzymień, “A null space constraint based block Tomlinson-Harashima precoding technique for the multi-user MIMO downlink,” in *Proc. IEEE Pacific Rim Conference on Communications, Computers and Signal Processing*, pp. 61–64, Aug. 2005.

- [LLJL82] A. K. Lenstra, H. W. Lenstra-Jr., and L. Lovász, “Factoring polynomials with rational coefficients,” *Mathematische Annalen*, vol. 261, no. 4, pp. 515–534, Dec. 1982.
- [Löf98a] C.-G. Löf, “Distributed power control in cellular radio systems with downlink multicast traffic,” in *Proc. International Workshop on Mobile Multimedia Communication (MoMuC)*, Oct. 1998.
- [Löf98b] —, “Power control in cellular radio systems with multicast traffic,” in *Proc. IEEE International Symposium on Personal, Indoor and Mobile Radio Communications (PIMRC)*, vol. 2, pp. 910–914, Sep. 1998.
- [Lop02] M. J. Lopez, “Multiplexing, scheduling, and multicasting strategies for antenna arrays in wireless networks,” Ph.D. dissertation, Massachusetts Institute of Technology, 2002.
- [Mic01] D. Micciancio, “The hardness of the closest vector problem with preprocessing,” *IEEE Transactions on Information Theory*, vol. 47, pp. 1212–1215, Mar. 2001.
- [Mir01] N. F. Mir, “A survey of data multicast techniques, architectures, and algorithms,” *IEEE Communications Magazine*, vol. 39, no. 9, pp. 164–170, Sep. 2001.
- [MK06] T. F. Maciel and A. Klein, “A low-complexity SDMA grouping strategy for the downlink of multi-user MIMO systems,” in *Proc. IEEE International Symposium on Personal, Indoor and Mobile Radio Communications (PIMRC)*, Sep. 2006.
- [NLTW98] A. Narula, M. J. Lopez, M. D. Trott, and G. W. Wornell, “Efficient use of side information in multiple-antenna data transmission over fading channels,” *IEEE Journal on Selected Areas in Communications*, vol. 16, pp. 1423–1436, Oct. 1998.
- [OKKK05] H. Oh, S. Kim, S.-H. Kim, and M.-G. Kim, “Novel transmit diversity techniques for broadcast services in cellular networks,” in *Proc. IEEE Vehicular Technology Conference (VTC)*, vol. 2, pp. 896–900, May 2005.
- [OM03] J. Ogunbekun and A. Mendjeli, “MBMS service provision and its challenges,” in *Proc. International Conference on 3G Mobile Communication Technologies*, pp. 128–133, June 2003.
- [Osn05] S. M. Osnaga, “On rank one matrices and invariant subspaces,” *Balkan Journal of Geometry and its Applications*, vol. 10, pp. 145–148, 2005.
- [Pap91] A. Papoulis, *Probability, random variables, and stochastic processes*, 3rd ed., ser. McGraw-Hill Series in Electrical Engineering. McGraw-Hill, 1991.
- [PF05] D. P. Palomar and J. R. Fonollosa, “Practical algorithms for a family of waterfilling solutions,” *IEEE Transactions on Signal Processing*, vol. 53, pp. 686–695, Feb. 2005.

- [PHS05] C. B. Peel, B. M. Hochwald, and A. L. Swindlehurst, "A vector-perturbation technique for near-capacity multiantenna multiuser communication - Part I: Channel inversion and regularization," *IEEE Transactions on Communications*, vol. 53, pp. 195–202, Jan. 2005.
- [PJU06] G. K. Psaltopoulos, M. Joham, and W. Utschick, "Comparison of lattice search techniques for nonlinear precoding," in *Proc. ITG/IEEE Workshop on Smart Antennas (WSA)*, Mar. 2006.
- [PNG03] A. Paulraj, R. Nabar, and D. Gore, *Introduction to space-time wireless communications*, 1st ed. Cambridge University Press, 2003.
- [Pro95] J. G. Proakis, *Digital Communications*, 3rd ed., ser. Electrical Engineering Series. McGraw-Hill, 1995.
- [PS99] M. B. Pursley and J. M. Shea, "Nonuniform phase-shift-key modulation for multimedia multicast transmission in mobile wireless networks," *IEEE Journal on Selected Areas in Communications*, vol. 17, pp. 774–783, May 1999.
- [Qiu05] W. Qiu, "Transmit power reduction in MIMO multi-user mobile radio downlinks by the rationale receiver orientation," Ph.D. dissertation, TU Kaiserslautern, 2005.
- [RZF04] M. Rossi, M. Zorzi, and F. H. P. Fitzek, "Investigation of link layer algorithms and play-out buffer requirements for efficient multicast services in 3G cellular systems," in *Proc. IEEE International Symposium on Personal, Indoor and Mobile Radio Communications (PIMRC)*, vol. 3, pp. 2256–2261, Sep. 2004.
- [SB04] M. Schubert and H. Boche, "Solution of the multiuser downlink beamforming problem with individual SINR constraints," *IEEE Transactions on Vehicular Technology*, vol. 53, pp. 18–28, Jan. 2004.
- [SBM⁺04] G. L. Stüber, J. R. Barry, S. W. McLaughlin, Y. G. Li, M. A. Ingram, and T. G. Pratt, "Broadband MIMO-OFDM wireless communications," *Proceedings of the IEEE*, vol. 92, pp. 271–294, Feb. 2004.
- [SD04] N. D. Sidiropoulos and T. N. Davidson, "Broadcasting with channel state information," in *Proc. IEEE Sensor Array and Multichannel Signal Processing Workshop (SAM)*, pp. 489–493, July 2004.
- [SDL06] N. D. Sidiropoulos, T. N. Davidson, and Z.-Q. Luo, "Transmit beamforming for physical-layer multicasting," *IEEE Transactions on Signal Processing*, vol. 54, pp. 2239–2251, June 2006.
- [SE94] C. P. Schnorr and M. Euchner, "Lattice basis reduction: Improved practical algorithms and solving subset sum problems," *Mathematical Programming*, vol. 66, pp. 181–199, 1994.

- [SH02] Q. H. Spencer and M. Haardt, "Capacity and downlink transmission algorithms for a multi-user MIMO channel," in *Proc. Asilomar Conference on Signals, Systems and Computers*, vol. 2, pp. 1384–1388, Nov. 2002.
- [SH04] C. Suh and C.-S. Hwang, "Dynamic subchannel and bit allocation for multicast OFDM systems," in *Proc. IEEE International Symposium on Personal, Indoor and Mobile Radio Communications (PIMRC)*, vol. 3, pp. 2102–2106, Sep. 2004.
- [Sha48] C. E. Shannon, "A mathematical theory of communication," *Bell System Technical Journal*, vol. 27, pp. 379–423 and 623–656, Jul. and Oct. 1948.
- [SK06a] Y. C. B. Silva and A. Klein, "Adaptive antenna techniques applied to multicast services in wireless networks," *Frequenz - Journal of RF-Engineering and Telecommunications*, vol. 60, pp. 199–202, Sep./Oct. 2006.
- [SK06b] —, "Adaptive beamforming and spatial multiplexing of unicast and multicast services," in *Proc. IEEE International Symposium on Personal, Indoor and Mobile Radio Communications (PIMRC)*, Sep. 2006.
- [SK06c] —, "Multicast transmission performance improvement through adaptive antenna arrays," in *Proc. Karlsruhe Workshop on Software Radios (WSR)*, vol. 1, pp. 177–182, Mar. 2006.
- [SK07a] —, "Analysis of linear and non-linear precoding techniques for the spatial separation of unicast and multicast users," in *Proc. IEEE International Symposium on Personal, Indoor and Mobile Radio Communications (PIMRC)*, Sep. 2007.
- [SK07b] —, "Downlink beamforming and SINR balancing for the simultaneous provision of unicast/multicast services," in *Proc. IST Mobile and Wireless Communications Summit*, July 2007.
- [SK07c] —, "Power allocation in multi-carrier networks with unicast and multicast services," in *Proc. IEEE International Conference on Communications (ICC)*, pp. 5433–5438, June 2007.
- [Sk197] B. Sklar, "Rayleigh fading channels in mobile digital communication systems - part 1: Characterization," *IEEE Communications Magazine*, vol. 35, pp. 90–100, July 1997.
- [SL04] Y. Sun and K. J. R. Liu, "Transmit diversity techniques for multicasting over wireless networks," in *Proc. IEEE Wireless Communications and Networking Conference (WCNC)*, vol. 1, pp. 593–598, Mar. 2004.
- [Slo07] N. J. A. Sloane, "Sequence A000292 - Tetrahedral (or pyramidal) numbers," *The On-Line Encyclopedia of Integer Sequences*, 2007. [Online]. Available: <http://www.research.att.com/~njas/sequences/A000292>
- [SPC05] C. Suh, S. Park, and Y. Cho, "Efficient algorithm for proportional fairness scheduling in multicast OFDM systems," in *Proc. IEEE Vehicular Technology Conference (VTC)*, vol. 3, pp. 1880–1884, June 2005.

- [SS04] Q. H. Spencer and A. L. Swindlehurst, "Channel allocation in multi-user MIMO wireless communications systems," in *Proc. IEEE International Conference on Communications (ICC)*, vol. 5, pp. 3035–3039, Jun. 2004.
- [SSH04] Q. H. Spencer, A. L. Swindlehurst, and M. Haardt, "Zero-forcing methods for downlink spatial multiplexing in multiuser MIMO channels," *IEEE Transactions on Signal Processing*, vol. 52, pp. 461–471, Feb. 2004.
- [STKL01] F. Shad, T. D. Todd, V. Kezys, and J. Litva, "Dynamic slot allocation (DSA) in indoor SDMA/TDMA using a smart antenna basestation," *IEEE/ACM Transactions on Networking*, vol. 9, no. 1, pp. 69–81, Feb. 2001.
- [Stu99] J. F. Sturm, "Using SeDuMi 1.02, a MATLAB toolbox for optimization over symmetric cones," *Optimization Methods and Software*, vol. 11-12, pp. 625–653, 1999.
- [Tom71] M. Tomlinson, "New automatic equaliser employing modulo arithmetic," *Electronics Letters*, vol. 7, pp. 138–139, Mar. 1971.
- [TZ01] W. Tan and A. Zakhor, "Video multicast using layered FEC and scalable compression," *IEEE Transactions on circuits and systems for video technology*, vol. 11, pp. 373–386, Mar. 2001.
- [Var02] U. Varshney, "Multicast over wireless networks," *Communications of the ACM*, vol. 45, no. 12, pp. 31–37, Dec. 2002.
- [VJ98] B. R. Vojčić and W. M. Jang, "Transmitter precoding in synchronous multiuser communications," *IEEE Transactions on Communications*, vol. 46, pp. 1346–1355, Oct. 1998.
- [WCLM99] C. Y. Wong, R. S. Cheng, K. B. Letaief, and R. D. Murch, "Multiuser OFDM with adaptive subcarrier, bit, and power allocation," *IEEE Journal on Selected Areas in Communications*, vol. 17, pp. 1747–1758, Oct. 1999.
- [WFH04] C. Windpassinger, R. F. H. Fischer, and J. B. Huber, "Lattice-reduction-aided broadcast precoding," *IEEE Transactions on Communications*, vol. 52, pp. 2057–2060, Dec. 2004.
- [WFVH04] C. Windpassinger, R. F. H. Fischer, T. Vencel, and J. B. Huber, "Precoding in multiantenna and multiuser communications," *IEEE Transactions on Wireless Communications*, vol. 3, pp. 1305–1316, July 2004.
- [YG05] T. Yoo and A. Goldsmith, "Optimality of zero-forcing beamforming with multiuser diversity," in *Proc. IEEE International Conference on Communications (ICC)*, vol. 1, pp. 542–546, May 2005.
- [Zan92] J. Zander, "Performance of optimum transmitter power control in cellular radio systems," *IEEE Transactions on Vehicular Technology*, vol. 41, pp. 57–62, Feb. 1992.

-
- [ZSV02] J. Zhang, A. M. Sayeed, and B. D. V. Veen, “Optimal transceiver design for selective wireless broadcast with channel state information,” in *Proc. IEEE International Conference on Acoustics, Speech, and Signal Processing (ICASSP)*, vol. 3, pp. 2153–2156, May 2002.
- [ZSV04] ———, “Optimal space-time transceiver design for selective wireless broadcast with channel state information,” *IEEE Transactions on Wireless Communications*, vol. 3, pp. 2040–2050, Nov. 2004.

Lebenslauf

Name: Yuri Carvalho Barbosa Silva
Anschrift: Von-der-Au-Straße 15, 64297 Darmstadt
Geburtsdatum: 15. September 1978
Geburtsort: Fortaleza, Brasilien
Familienstand: verheiratet, eine Tochter

Schulausbildung

1984-1988 Grundschole in Fortaleza, Brasilien
1989-1995 Gymnasium in Fortaleza, Brasilien

Studium

1996-2001 Studium der Elektrotechnik an der
Federal University of Ceará, Fortaleza, Brasilien,
Studienabschluß: Bachelor of Engineering
2002-2003 Studium der Elektrotechnik an der
Federal University of Ceará, Fortaleza, Brasilien,
Studienabschluß: Master of Science

Berufstätigkeit

2001-2004 Forschungstätigkeit als Mitarbeiter am
Wireless Telecommunications Research Group (GTEL),
Federal University of Ceará, Fortaleza, Brasilien
seit 2005 wissenschaftlicher Mitarbeiter am
Fachgebiet Kommunikationstechnik,
Institut für Nachrichtentechnik,
Technische Universität Darmstadt

